MARTIN MARIETTA ENERGY SYSTEMS LIBRARIES

3 4456 0268460 0

ornl

ORNL/TM-10579

OAK RIDGE NATIONAL LABORATORY

MARTIN MARIETTA

ORNL Contributions to the Advanced Neutron Source (ANS) Project for October 1986–March 1987

OAK RIDGE NATIONAL LABORATORY
CENTRAL RESEARCH LIBRARY
CIRCULATION SECTION
4500N ROOM 175
LIBRARY LOAN COPY
DO NOT TRANSFER TO ANOTHER PERSON
If you wish someone else to see this report, send in name with report and this library will arrange a loan.

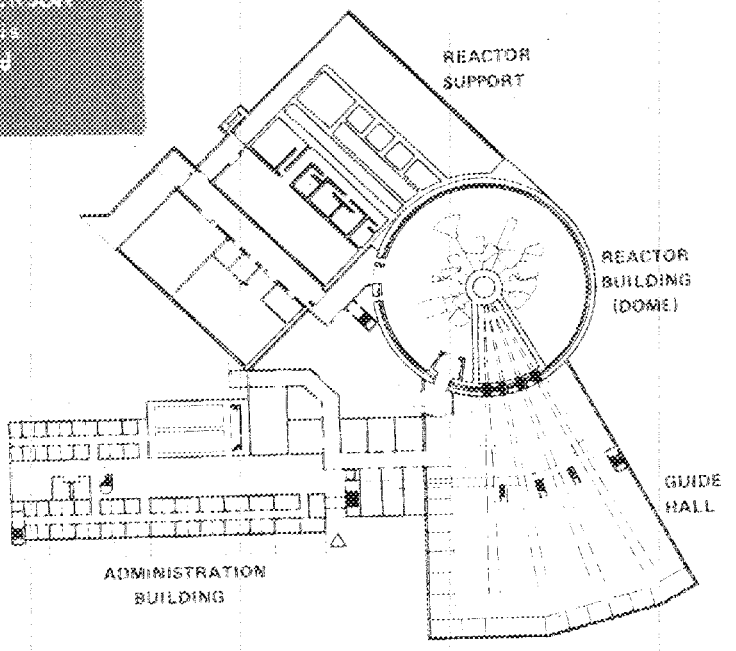

OPERATED BY
MARTIN MARIETTA ENERGY SYSTEMS, INC.
FOR THE UNITED STATES
DEPARTMENT OF ENERGY

Printed in the United States of America. Available from
National Technical Information Service
U.S. Department of Commerce
5285 Port Royal Road, Springfield, Virginia 22161
NTIS price codes—Printed Copy: A09; Microfiche: A01

This report was prepared as an account of work sponsored by an agency of the United States Government. Neither the United States Government nor any agency thereof, nor any of their employees, makes any warranty, express or implied, or assumes any legal liability or responsibility for the accuracy, completeness, or usefulness of any information, apparatus, product, or process disclosed, or represents that its use would not infringe privately owned rights. Reference herein to any specific commercial product, process, or service by trade name, trademark, manufacturer, or otherwise, does not necessarily constitute or imply its endorsement, recommendation, or favoring by the United States Government or any agency thereof. The views and opinions of authors expressed herein do not necessarily state or reflect those of the United States Government or any agency thereof.

ORNL/TM-10579

ORNL CONTRIBUTIONS TO THE ADVANCED NEUTRON SOURCE (ANS) PROJECT FOR OCTOBER 1986–MARCH 1987

Principal Authors

D. L. Selby R. M. Harrington
Oak Ridge National Laboratory

F. J. Peretz
Martin Marietta Engineering

Contributing Authors

R. G. Alsmiller, Jr. B. H. Montgomery
Y. Y. Azmy R. E. Pawel
G. L. Copeland R. T. Primm, III
F. C. Difilippo C. D. West
W. R. Gambill
Oak Ridge National Laboratory

D. C. Lousteau P. B. Thompson
Martin Marietta Engineering

S. S. Kalsi
Grumman Corporation

Report Staff

C. A. Chance K. F. Rosenbalm
Oak Ridge National Laboratory

Date Published - November 1987

Prepared by the
OAK RIDGE NATIONAL LABORATORY
Oak Ridge, Tennessee 37831
operated by
MARTIN MARIETTA ENERGY SYSTEMS, INC.
for the
U.S. DEPARTMENT OF ENERGY
under Contract No. DE-AC05-84OR21400

MARTIN MARIETTA ENERGY SYSTEMS LIBRARIES

3 4456 0268460 0

CONTENTS

Page

ABSTRACT 1

1. INTRODUCTION 2

2. RESEARCH AND DEVELOPMENT TASKS 3

2.1 Reactor Core Design 3

2.1.1 Relationship of power, core volume, and peak thermal flux for the single-core concept . . 5
2.1.2 D_2O vs H_2O primary cooling 8
2.1.3 Reactor pressure vessel design 11
2.1.4 ANS core plate geometry 13
2.1.5 Neutron transport models 16
2.1.6 Cross sections 16

2.2 Fuel Element Specifications and Manufacturing . . . 22

2.3 Corrosion/Erosion Tests on Aluminum Alloy-Clad-Material. 23

2.3.1 Design of corrosion/erosion test loop . . . 23
2.3.2 Preanalysis of corrosion/erosion test loop experiments 27

2.4 Core Flow and Heat Transfer Tests 28

2.5 Control Element Design, Tests, and Manufacturing Procedures 29

2.6 Validation of Neutronics Performance Predictions Through Critical Experiments 30

2.7 Structural Analysis and Tests 30

2.8 Cold Neutron Source Development 30

2.8.1 Number of cold neutron sources 31
2.8.2 Cold neutron source location 32
2.8.3 Cold neutron source shape and size 33
2.8.4 Cold neutron source moderator 34
2.8.5 Cold neutron source structural materials . . 35
2.8.6 Cold neutron source cooling options 35

2.9 Beam Tube and Instrument Development 40

2.10 Hot Neutron Source Development 40

2.11 Shielding Concepts and Validation 40

2.12 Plant Instrumentation and Controls 40

2.13 BOP Concepts 40

2.13.1 Core and facility configurations 41
2.13.2 Containment and ventilation 44
2.13.3 Tritium and deuterium control 47
2.13.4 Refueling and vessel replacement 49

3. SAFETY TASKS 51

3.1 Development and Specification of Design Criteria for Safety-Related Systems 52

3.2 Probabilistic Risk Assessment Task 53

3.3 Development of Computer Codes and Analytical Methods for Safety Analysis 53

3.4 Containment Functional Requirements 54

3.4.1 Containment functional objectives 55
3.4.2 Calculation model 57
3.4.3 Analysis results 64
3.4.4 Implications for design 72
3.4.5 Implications for emergency planning 73
3.4.6 Containment analysis conclusions 74
3.4.7 Recommendations 75

4. CONCEPTUAL DESIGN TASKS 77

4.1 Main Construction Contracts 77

4.2 ORNL Retained Reactor 77

4.3 ORNL Retained Experiments 77

4.4 Systems Integration 77

5. PROJECT SUPPORT 79

5.1 Work Breakdown Structure 79

5.2 Schedule 81

5.3 Costs 83

REFERENCES 85

APPENDIX A: GROUND RULES FOR CORE DESIGN STUDIES 87

APPENDIX B: FURTHER DEFINITION OF WORK BREAKDOWN STRUCTURE 95

APPENDIX C: DETAILED SCHEDULE FOR THE ANS PROJECT . . . 103

ORNL Contributions to the Advanced Neutron Source (ANS) Project for October 1986 - March 1987

Abstract

The Advanced Neutron Source (ANS) Facility -- formerly called the Center for Neutron Research -- will provide the world's best facilities for the study of neutron scattering. The ANS high power density reactor will be fueled with uranium silicide and cooled, moderated, and reflected by D_2O. Peak neutron fluxes in the reflector are expected to be 5 to 10 x 10^{19} neutrons per square meter with a power level between 270 MW and 300 MW.

This report describes the status of technical work at ORNL on the ANS Project during the first half of FY 1987. Earlier work is described in a previous report, Center for Neutron Research Project Status Report, ORNL/TM-10065[1].

The scope of this report includes Research and Development Tasks; Safety Tasks; Conceptual Design Tasks; and Project Support. The last two areas were only initiated as separate activities during this reporting period.

Technical highlights include a better understanding of the relationship among neutron flux, core power, and core volume; preconceptual design work on a cold source for use in a very high gamma and neutron flux environment; identification of the major applicable safety rules and guidelines; and establishment of initial functional objectives for the containment structure.

1. INTRODUCTION

This report describes the status of technical work at ORNL on the Advanced Neutron Source (ANS) Project -- formerly called the Center for Neutron Research -- during the first half of FY 1987. Earlier work is described in a previous report, Center for Neutron Research Project Status Report, ORNL/TM-10065[1]. This report does not include work that was begun during this period by subcontractors.

The scope of this report includes Research and Development Tasks; Safety Tasks; Conceptual Design Tasks; and Project Support. The last two areas were only initiated as separate activities during this reporting period.

This period has also seen some important nontechnical events for the ANS Project: the U.S. Congress placed funding for "the Advanced Steady State Research Reactor at Oak Ridge" in the FY 1987 budget; the Department of Energy's (DOE's) Office of Basic Energy Sciences nominated Oak Ridge National Laboratory (ORNL) as the lead laboratory for this project; a National Steering Committee for an Advanced Neutron Source was formed and has become active; and arrangements were initiated for certain tasks to be undertaken at other laboratories and universities with appropriate experience and expertise.

Technical highlights include a better understanding of the relationship among neutron flux, core power, and core volume; preconceptual design work on a cold source for use in a very high gamma and neutron flux environment; identification of the major applicable safety rules and guidelines; and establishment of initial functional objectives for the containment structure. These, and many other topics, are discussed below.

2. RESEARCH AND DEVELOPMENT TASKS

The research and development activities during the first half of FY 1987 focused on the continuation of the core design optimization studies and the initiation of certain tasks considered crucial for fulfillment of the design objectives. This chapter summarizes tasks performed in-house at ORNL as well as tasks performed under subcontract at universities and other laboratories.

2.1 Reactor Core Design

The reactor core design studies continued to be a focus of the R&D activities. Two core design concepts are being considered: a single-core similar to that of the High Flux Isotope Reactor (HFIR) and a twin-core with an axial heavy-water plenum proposed by Idaho National Engineering Laboratory (INEL); both are illustrated in Fig. 1. In the first half of FY 1987, more detailed neutronics studies were carried out to advance the core design and to develop initial conceptual design specifications for the two alternatives. Initial comparison of the designs proposed by INEL and ORNL indicated that most of the reported performance differences were actually due to differences in basic design assumptions: maximum allowable fuel temperature, oxide film buildup rate, fraction of fission energy deposited in the fuel, minimum practical coolant gap, minimum acceptable fuel plate thickness, and maximum fuel density (see Table 1). The establishment of a set of consistent ground rules for both design efforts was initiated and is now complete (see Appendix A). These ground rules will be used by INEL to perform a comparison of the two designs in the second half of FY 1987 and in future design work, pending the completion of experimental tests on fuel and oxide behavior.

Present plans are to make a choice between the single- and twin-core design concepts early next year; the dilution and duplication of effort that results from carrying two designs is seriously delaying programs in other project areas.

ORNL-DWG 87-4202 ETD

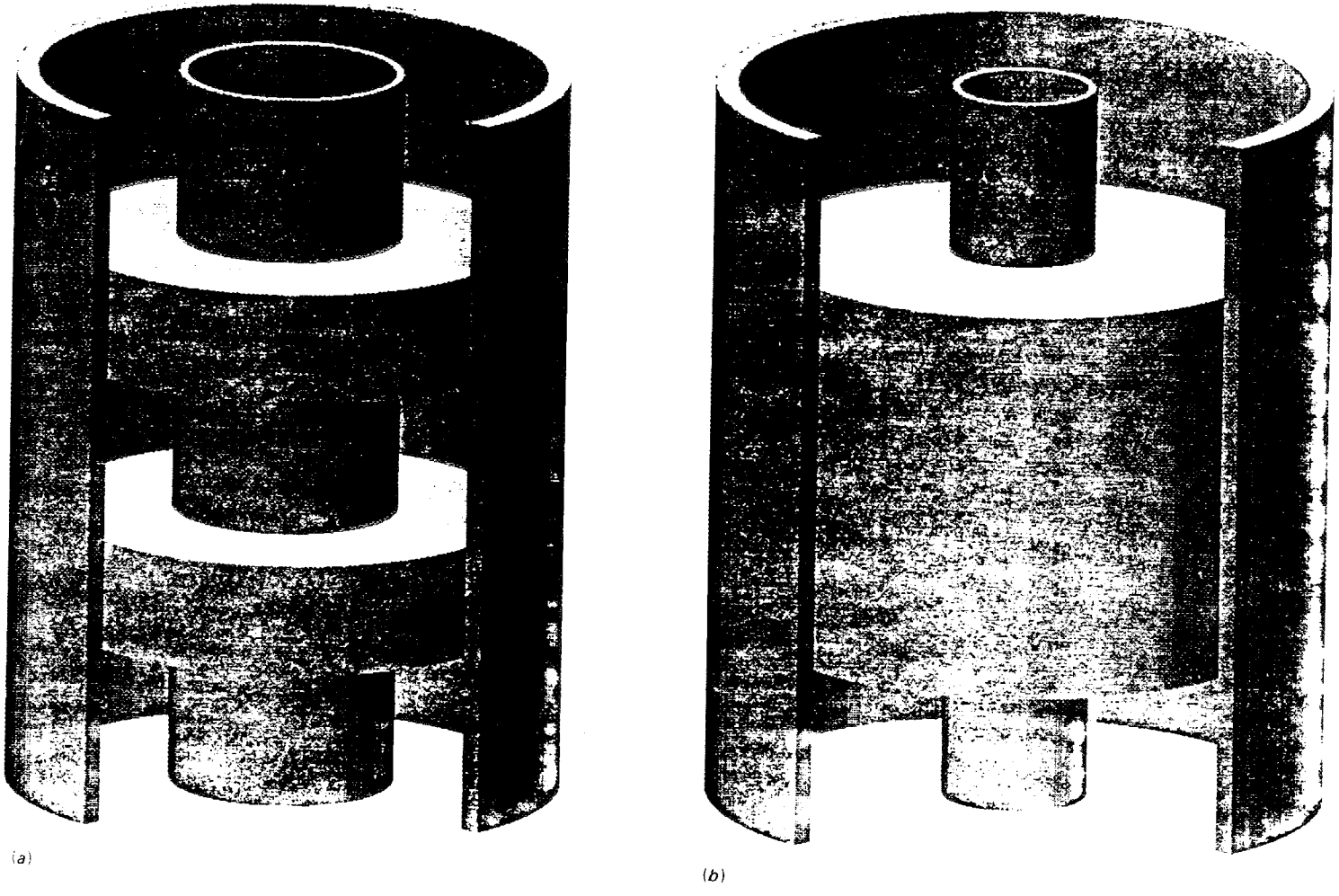

Fig. 1. Cut-away views of (a) twin-core and (b) single-core models

Table 1. Some design assumptions

Parameters	INEL[a]	ORNL[a]	Ground Rules
Maximum permissible fuel temperature[b], °C	450	350	385
Oxide film formation	0.5 x Griess[c]	1.0 x Griess[c]	0.5 x Griess[c]
Fraction of fission energy deposited in fuel, %	91	98	91
Coolant inlet temperature, °C	38	49	49
Minimum coolant gap, mm	0.76	1.27	ND[d]
Minimum acceptable fuel plate thickness, mm	1.02	1.27	ND[d]
Heat transfer correlation	Dittus Boelter	Petukhov	Petukhov
Fuel burnup limit, fissions/mL of meat	2.0×10^{21}	2.6×10^{21}	2.6×10^{21}

[a]Data represent design parameters prior to May 1987. New ground rules, to be followed by both laboratories, were agreed upon in May 1987 and are shown in column 3: a more complete list of the current assumptions may be found in Appendix A.

[b]U_3Si_2 fuel dispersed in an aluminum matrix.

[c]"Griess" is the growth rate predicted by the correlation based on out-of-pile measurements by J. Griess. The reduction factor of 0.5 adopted by INEL is based on measurements of irradiated Advanced Test Reactor (ATR) fuel plates that have a lower heat flux than any of the ANS designs.

[d]Not defined in ground rules.

2.1.1 Relationship of power, core volume, and peak thermal flux for the single-core concept

It has long been known that a relationship exists between the core volume and the power necessary to achieve a given peak reflector flux. This relationship has now been more closely

examined, and the results are summarized by Fig. 2. The top curve presented in Fig. 2 is based on data from a series of calculations performed by the ORNL Engineering Physics and Mathematics Division: the additional curves follow from the fact that for any given core the flux at the end of core life is approximately proportional to the reactor power. All the curves calculated have a central hole of 128-mm diameter, the same as the HFIR, and a height-to-diameter ratio of 0.8 in the fueled region. The results were used to develop an understanding of the relationship between peak flux in the reflector and reactor core parameters such as power density. One interesting aspect of this work is illustrated in Fig. 3 where the peak flux is plotted as a function of average power density for various power levels. As can be seen, we are designing for a region where further increases in power density, for a constant power level, bring little further increase in peak

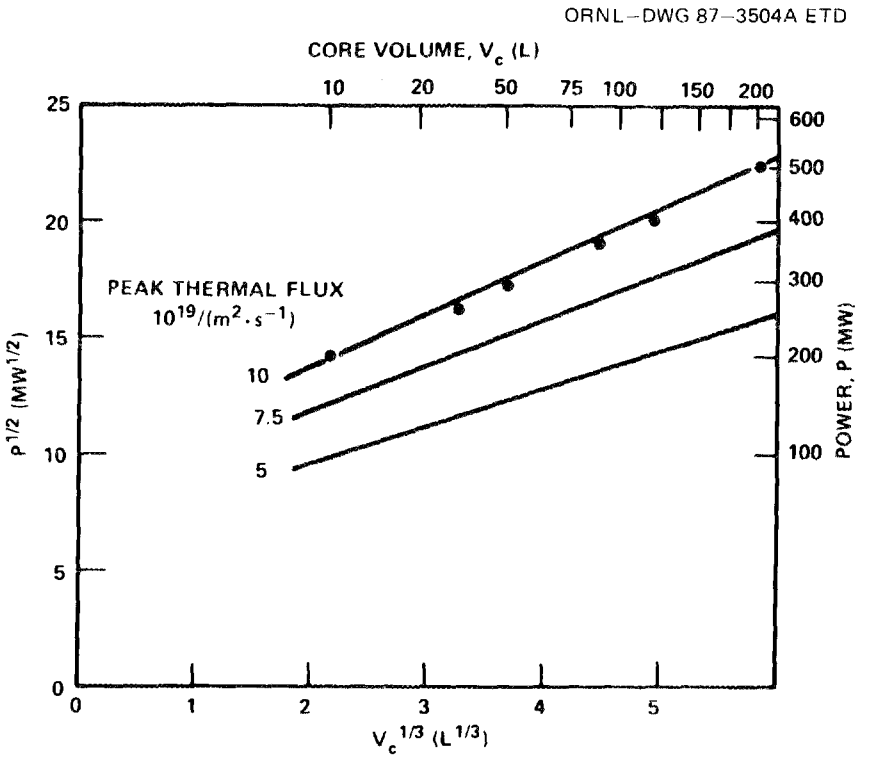

Fig. 2. Power, core volume, and peak thermal flux relationships for 14-d cores

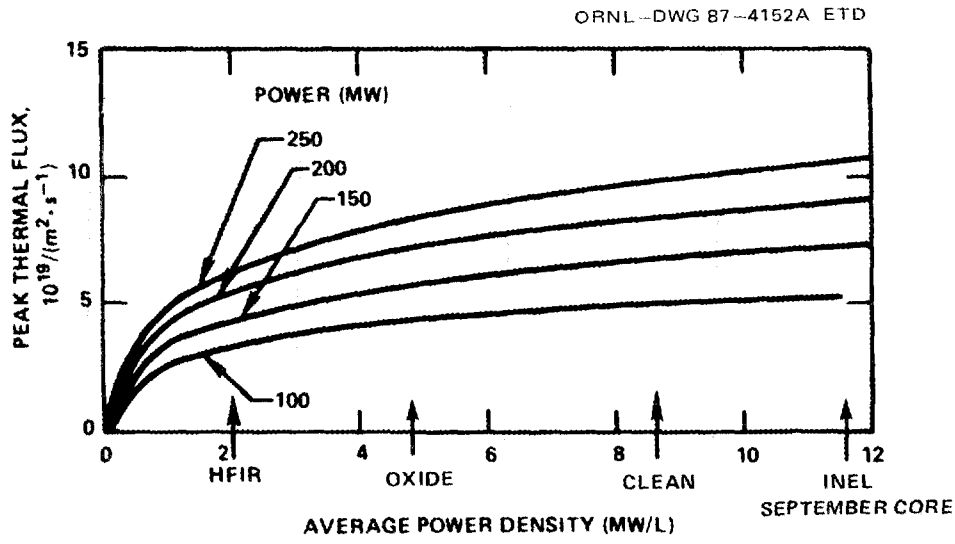

Fig. 3. Power, power density, and flux relationships

thermal flux. The physical reason for this is that the thermal flux peak lies some 180-mm outside the core: in other words, for very small (i.e., high power density) cores, the surface area of the high flux region is determined primarily by the thermalization distance in the heavy-water (D_2O) and not by the core dimensions.

The flatness of the curves in Fig. 3 provided the motive for the development of a new optimized, oxided, single-core concept. Instead of lowering the power level of the 35-L core until the power density dropped below the limitation imposed by the oxide buildup, one could maintain the same power level and simply increase the core size until the desired power density is obtained. This led to a 55-L core design which, although not optimized, produced a higher peak reflector flux than our previous approach of lowering the power level for the smaller core. The 55-L oxided core produced a peak reflector flux that was only 13% lower than that produced by the 35-L core under the oxide-free condition. The unperturbed radial thermal flux profiles in the reflector are given for both the 35-L non-oxided core and 55-L oxided core designs in Fig. 4. (The configurations of these two cores are discussed in Section 2.12.1). Further optimization may

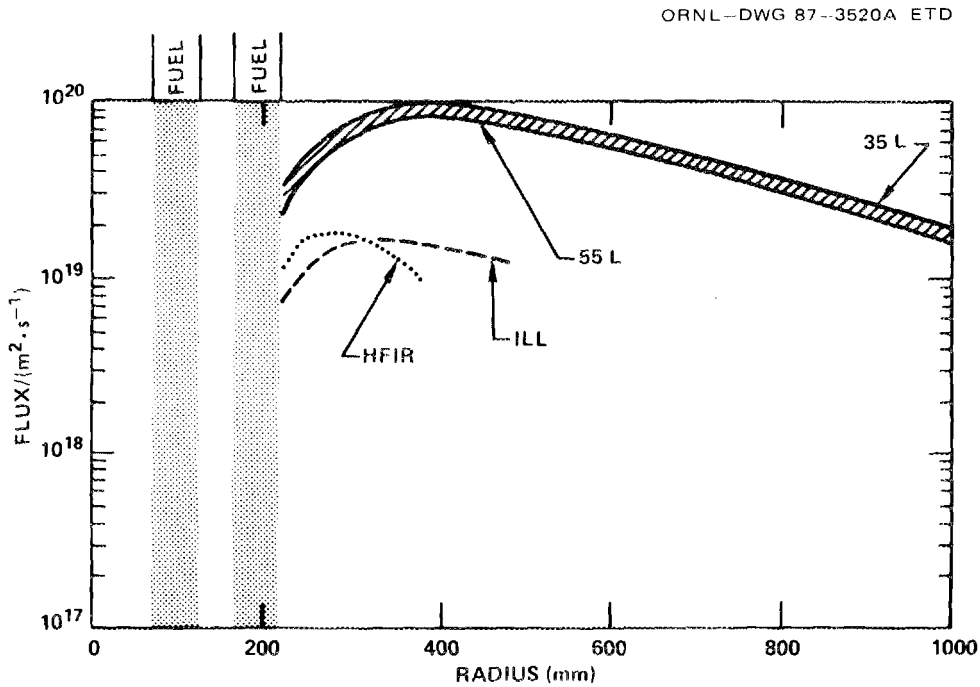

Fig. 4. Unperturbed thermal fluxes

lead to a still smaller difference between the oxide and non-oxide core performance predictions.

2.1.2 D_2O vs H_2O primary cooling

In 1984 a decision had been made to use D_2O rather than H_2O as the primary coolant. That decision was based on a U_3O_8 fuel design that produced a peak reflector flux of only about 3 x 10^{19} neutrons/(m^2s). At that flux level, the flux penalty associated with using H_2O was not acceptable. Subsequently, the change to the U_3Si_2 fuel form and other improvements in the core design have led to a significantly higher peak flux. A re-evaluation of the choice of coolant was initiated and the following potential advantages of H_2O cooling have been identified:

1. smaller D_2O inventory,
2. reduction of construction costs,
3. operational simplifications,
4. no tritiated D_2O outside the reactor containment dome,
5. increased worth at locations within the core for excess reactivity control due to the softer spectrum of the H_2O system, and
6. resolution of some engineering technical issues relating to D_2O/H_2O interfaces.

As a result, a decision was made to reexamine, in detail, the H_2O coolant option.

A significant effort was expended during this period to review the performance penalties and the economics of using light water rather than heavy water for the primary coolant. Several major facility simplifications resulting from use of a light-water coolant were identified. The problem of transferring spent fuel and in-core irradiation experiments from heavy to light water would be avoided. A direct cost saving associated with the heavy-water inventory would be realized. In addition, a variety of facility simplifications in the reactor support building would result from eliminating the presence of tritium and heavy water in that building. These advantages range from the design of primary system equipment and elimination of a helium buffer gas over the D_2O coolant to simplifications of the waste and ventilation systems. Potential capital cost savings in the range of $30M to $80M were identified, as shown in Table 2. Operation and maintenance of the facility would also be simpler, which could have a significant impact on the plant availability factor. A simpler refueling operation could also reduce downtime during refueling with a further increase in availability.

Not all of the above benefits would necessarily be fully realized, however. For example, decay heat considerations may dominate in the refueling sequence, negating potential gains in reactor availability. In addition, most of the tritium could also be kept out of the primary loop by maintaining separate coolant and reflector circuits, if mechanical considerations in the core region allow such a separation. Thus, there are large uncertainties in the actual capital cost savings associated with using light-water coolant. The minimum saving would be at least the direct cost of the heavy-water coolant inventory.

The initial neutronics calculation of a 35-L core with H_2O primary cooling indicated that the peak reflector flux would be decreased by ~35% from the 35-L D_2O reference core. This decrease in flux in the reflector is attributable to two factors: (1) an

Table 2. Breakdown of potential cost savings for H_2O coolant

Item	Cost saving range ($ M)	Comment
Heavy-water inventory	25	A relatively certain saving
Heavy-water drains in support building	0.5 - 5	Including drains and tanks as contingency
Helium cover-gas system for coolant	0.5 - 5	A relatively certain saving
Dry ventilation system in support building	1 - 10	Gastight containment may be similar in cost
Coolant detritiation and upgrade system	15	Reflector circuit may require these systems anyway
Pump and valve seals	0.5 - 5	Low-leakage equipment needed in any case
Tritium monitoring and control in support building	0.5 - 5	Some system required in any case
Simplification of refueling procedure	1 - 10	Difference may be small if refueling schedule is dominated by decay heat loads (as anticipated)

increase in the thermalization of neutrons within the core region and (2) an increase in absorption of neutrons in the coolant. A series of calculations was then initiated to identify design changes that would enhance the peak flux level for the H_2O-cooled design. The initial results indicate that by using some beryllium components and some complex geometries, the flux penalty can be reduced to 22%. However, the increased complexity in geometry will lead to higher fuel cycle costs* and increased complexities in operation. Other unfavorable factors associated with H_2O coolant included the following:

1. vessel replacement becomes a more complicated process,
2. the number of H_2O - D_2O interfaces is increased,
3. a potential for positive void coefficient exists, and
4. oxide formation will have a bigger impact due to an increase in the H_2O flux penalty as the core is made larger.

In general, the conflict boils down to a simplification of balance-of-plant (BOP) and potential reduction in facility costs vs a 25 to 35% reduction in the peak flux level and a potentially complex core design. Although the decision was not clear cut, it was decided that the flux penalty was too large, the overall cost savings too uncertain, and complexities in BOP were preferable to a complex design for the core that must be replaced every 2 to 3 weeks. Therefore, the decision was made to remain with the heavy-water-cooled concept. Note that the use of H_2O coolant would have an even more deleterious effect on the twin-core design because of the amount of coolant in the plenum between the two core halves and in the necessarily large by-pass flow annulus.

2.1.3 Reactor pressure vessel design

In both of the present design concepts (single and twin-core), the primary coolant pressure boundary is located between the core and the D_2O reflector. The boundary is simply a tube or pipe, the Core Pressure Boundary Tube (CPBT), with no penetrations and an

*The actual increases in fuel assembly costs could not be evaluated without a detailed study. However, because we need a new fuel assembly every 17 days, even a small increase in the cost of the fuel assembly can lead to a very large expense over the life of the facility.

inside diameter of approximately 540 mm. The advantage of this arrangement is that the beam tubes, cold source and certain other experimental facilities do not penetrate the pressure boundary. This reduces the risk of pressure boundary failure and simplifies the design and operation of the beam tubes and other devices located in the D_2O reflector, and improves their performance since they do not have to be designed for a high-pressure environment. The in-close location of the pressure tube does however present three major problems:

1. the high fluence associated with this position causes intense damage to the tube material;

2. the presence of a wall between the core and the thermal flux peak in the reflector reduces the magnitude of the thermal flux peak; and

3. the high gamma heating rate in the vicinity of the tube makes it difficult to cool the tube.

It does appear that there are solutions to these problems.

Because the tube is of small diameter, only a relatively thin wall is necessary to provide the pressure boundary. In addition, the simplicity of its design (a single tube with no penetrations) makes it relatively easy to fabricate. The cost of the CPBT is therefore small enough to consider frequent replacement of the vessel. Thus, we propose to replace the CPBT frequently to deal with the high fluence problem. Initial indications are that the tube would be replaced every 6 months to a year depending on the material chosen.

The flux penalty is a little more difficult to resolve because there is very little we can do to reduce the flux loss imposed by the wall, ~15% when the wall is moved as far in from the thermal flux peak as practical. Increases in the fuel loading and a shift from our previously conservative estimates of thermal-to-fission*

*Thermal power as used in this context refers to the amount of fission energy deposited in the core and primary coolant region (i.e., it is the amount of heat energy that must be removed by the primary coolant system). For conservatism, all thermal power is assumed to be deposited into the fuel plates.

power ratio, offset the previously unaccounted for penalty due to the wall, and we believe there will be little change from previously reported flux values for the 35-L core.

Present estimates of gamma heating rates in the region where we propose to locate the pressure vessel range from 28 W/g to 100 W/g. As a result a significant amount of heat will be deposited in the vessel material. Wall temperature and stress limitations dictate that for successful single-side forced-flow cooling, the total neutronic and gamma heating would have to be <8 W/g for a Zircaloy vessel or <25 W/g for an aluminum alloy vessel. In the case of forced flow on both sides of the pressure tube, the limits appear to be 30 W/g for the Zircaloy vessel and 60 W/g for the aluminum one; consequently an aluminum pressure vessel with forced flow on both sides will be proposed by ORNL. The INEL designs presently favor a Zircaloy tube because the larger diameter of the twin-core pressure tube (to accommodate the larger coolant bypass annulus) places the wall closer to the thermal flux peak in the reflector where the flux penalty associated with the pressure tube is much higher; the use of Zircaloy with a lower thermal absorption cross section than aluminum reduces this flux penalty.

2.1.4 <u>ANS core plate geometry</u>

The ANS core is based on the use of curved fuel plates spanning, in a primarily radial direction, the annular gaps between concentric support cylinders. As in the HFIR, two concentric fuel zones will be utilized. To maintain a constant gap between the fuel plates over their radial expanse, the plates are formed into a geometric shape defined as an "involute of a circle". A routine that allows rapid calculation of basic geometric parameters of the core has been written for TK Solver[2], a personal computer based application program for solving a system of simultaneous equations.

The basic sections of the core are shown in Fig. 5. Progressing radially outward from the centerline, the cross section consists of the following regions: an inner D_2O cavity,

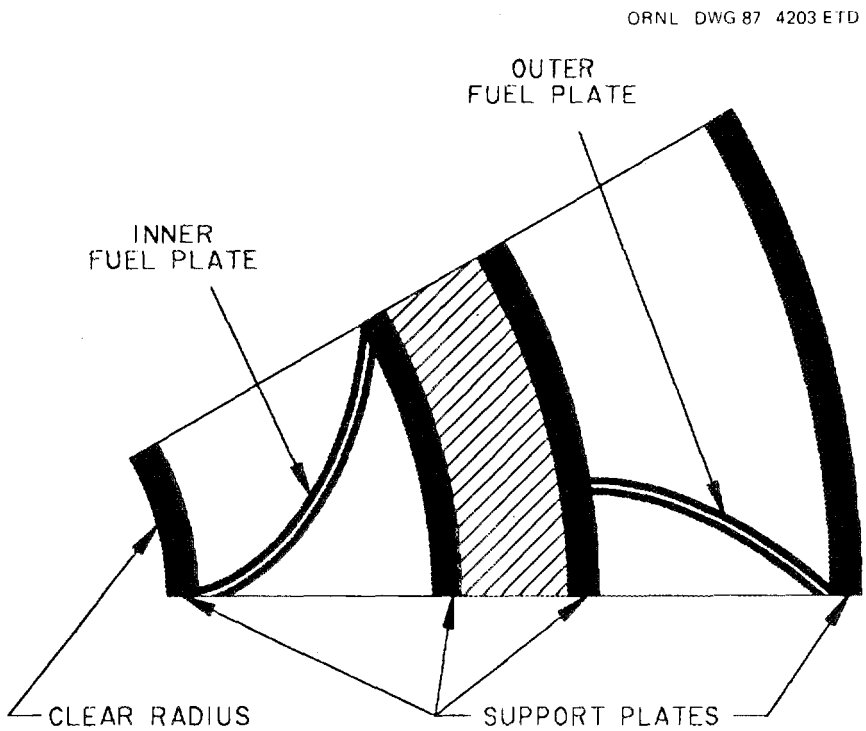

Fig. 5. Fuel core elements

the inner element inner-side plate, the inner element plate annulus, the inner element outer-side plate, the interfuel zone irradiation target basket, the outer element inner-side plate, the outer element plate annulus, and the outer element outer-side plate. The arcs used to generate the fuel-plate curvature are not shown in Fig. 5. These arcs, referred to as the inner and outer generating circles, represent the theoretical inner limit of the respective fuel zones. If extended inward to this limit the fuel plate would be normal to the generating circle.

Using the routine developed, the affect of different input variables or boundary conditions can be rapidly evaluated and since there are six unknowns (i.e., the radii of the two generating circles, and the inner and outer limiting radii of the two respective involute shaped fuel zones), six constraints can be specified. Input can be either a desired numerical value for one of the variables or a required relationship between variables.

The baseline case was established by (1) fixing the radius of the inner edge of the inner fuel plates, the desired core volume, minimum bend radius for the fuel plates, and fuel-plate nominal thickness; and (2) requiring that the arc length of the inner and outer fuel plates be equal.* The resulting geometry for the base case is shown in Fig. 6 with the major parameters for the

*The inner and outer fuel-plates are made equal to minimize the maximum fuel-plate radial length. This maximized the critical velocity for the system.

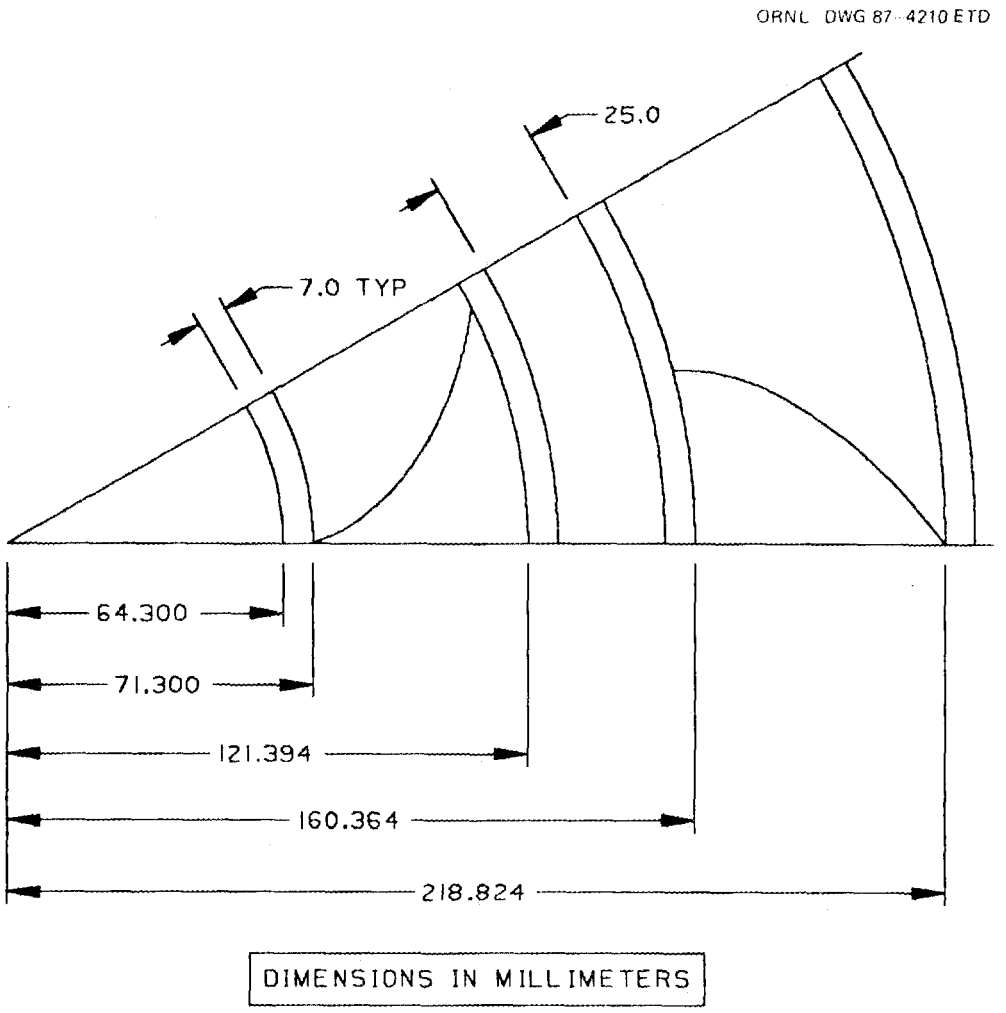

Fig. 6. Basic dimensions for reference 35-L core

reference 35-L core as follows:

1. Core volume, 35-L
2. Core length, 350-mm
3. Length along arc of fuel plate
   Inner 83.5, 69.5 fueled
   Outer 83.5, 69.5 fueled
4. Number of fuel plates
   Inner 172
   Outer 395
5. Fuel plate thickness, 1.27-mm
6. Coolant gap thickness, 1.27-mm
7. Minimum fuel plate bend radius, 16-mm

2.1.5 Neutron transport models

For some time we have been concerned about the adequacy of using neutron diffusion theory models in light of the steep flux gradients in the core and the deep penetration problems associated with the D_2O reflector. One-dimensional comparisons between diffusion and transport models have now been made, and the results are illustrated in Fig. 7. The results indicate that although diffusion theory methods are adequate for core calculations, a transport or transport-correction approach may indeed be necessary to study neutron transport through the D_2O reflector.

A two-dimensional (2-D) R-Z transport model is also now available. Comparisons of the 2-D transport calculations and 2-D diffusion calculations will be made as soon as a convergence problem in the transport model is resolved.

2.1.6 Cross sections

The cross-section development effort for ANS can be divided into two categories: (1) evaluation of cross-section point data and (2) generation of few group cross-section libraries (both diffusion and transport) which are specific to the ANS model. As an individual project there was little that could be done in the way of measurement and evaluation of point data; therefore, the effort associated with item (1) was limited. However, as discussed below, an evaluation of the potential weaknesses of the point data was performed.

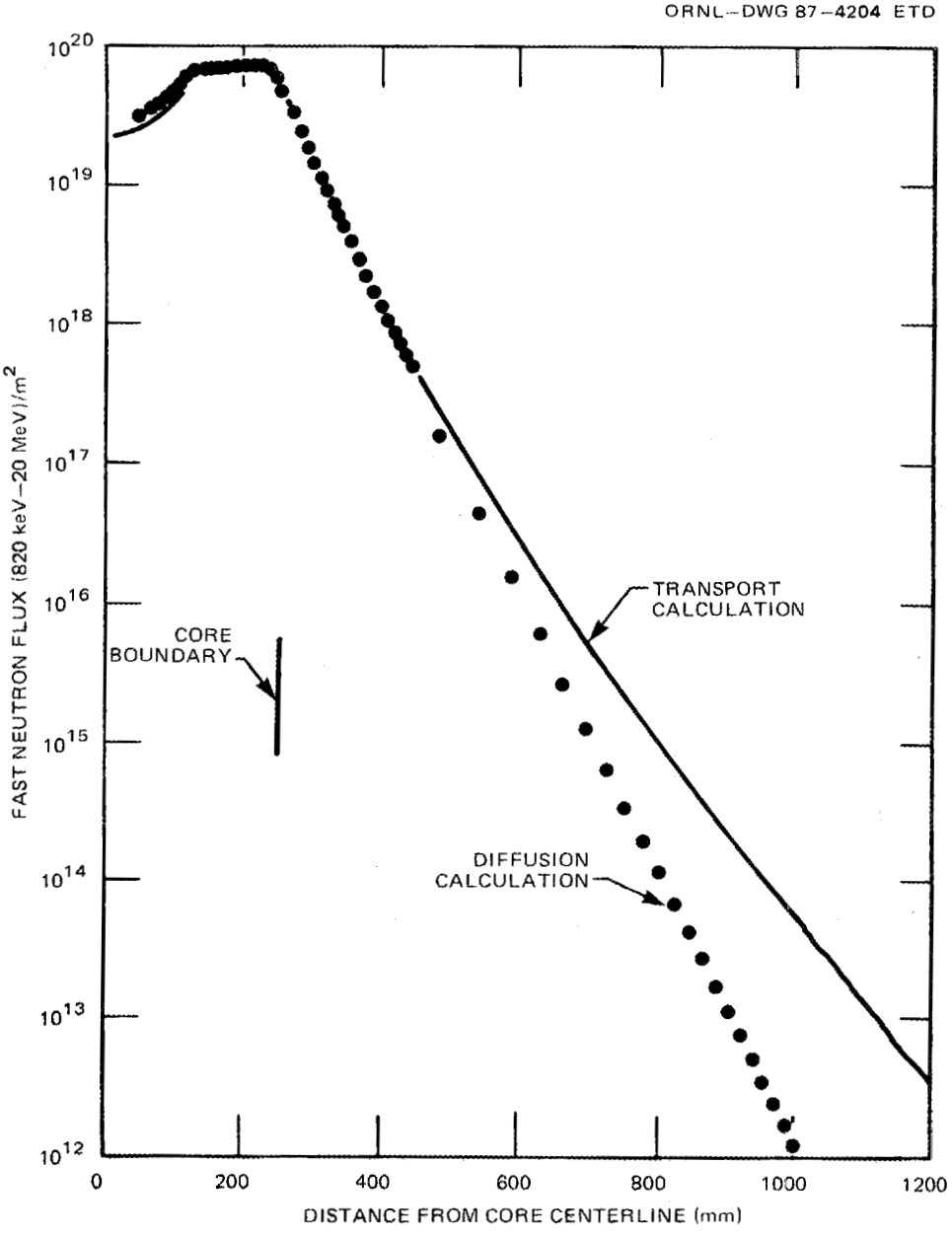

Fig. 7. Comparison of transport and diffusion calculations of fast flux (800 KeV - 20 MeV) in the ANS core and reflector regions

2.1.6.1 Cross-section point data. The ANS neutronics analysis is presently using cross-section data files from the ENDF/B-V data base. According to a brief study by D. C. Larson of the Engineering Physics and Mathematics Division, some ENDF/B-V

data base files, important to the ANS analysis, are not professionally sound. The silicon evaluation was done under Defense Nuclear Agency sponsorship, with particular emphasis on reactions at energies around 14 MeV and on charged particle production. As a result, there are no resonance parameters for silicon; only point data are given, and of 11 resonances now known below 500 keV, only one is included in the ENDF/B-V data base. Similarly, the resonance regions in ^{235}U and aluminum are inadequately treated. Because these three materials are important to the ANS design, some concerns were raised.

The major concern appears to be with the ^{235}U and aluminum data, because the silicon resonances would have to be very severe to have a significant impact on the analysis efforts. A new resonance parameter evaluation is now available for ^{235}U. The goal is to incorporate this new evaluation into the ANS cross-section library by the end of this year.

The solution to the aluminum problem may not be as easy. Present ENDF/B aluminum data are the result of an evaluation performed in 1973. In 1975 an evaluation containing resolved resonance parameters for aluminum was made (JENDL-2). A comparison of the broad group cross sections for the two evaluations reveals rather large differences for both the elastic and capture cross sections. In particular, in the energy range between 550 eV and 17 keV -- a very important energy range for ANS-- the contribution of a 5.9-keV resonance in the JENDL-2 evaluation results in a significant increase in the capture cross section over the present ENDF/B-V value. It has been recommended that the impact of this difference in capture cross section be examined. One possible solution is to incorporate the resolved resonance parameters from the JENDL-2 evaluation into the ANS cross section libraries.

2.1.6.2 ANS cross section libraries. The Computing and Telecommunications Nuclear Engineering Applications Department (NEAD) is generating pseudo-problem-independent multigroup cross-section libraries to support general design work with special

efforts to develop cross sections for use in analyzing the ANS cold- and hot-neutron sources and their interaction with the reactor core. The collection of libraries are designated ANSL-V (Advanced Neutron Source Cross-section Libraries derived from Evaluated Nuclear Data File-B, Version V).

The following broad-group libraries are being generated for ANSL-V:

1. a 123-material General-Purpose Neutron (GPN) Library,
2. a 44-material Secondary Gamma-Ray Production (SGRP) Library, and
3. a 34-material Gamma-Ray Interaction (GRI) Library.

The GPN library is to include appropriate data for core and shield analyses, activation analyses after irradiation of certain elements in the ANS reactor environment, and safety analyses. The SGRP library will include data, where available, for the generation of gamma-rays resulting from neutron-induced reactions in the ANS core, structural, and shielding regions. The GRI library is to include data for use in calculating the transport of photons throughout the ANS.

In further support of the ANS project, NEAD is completing development and testing of the XLACS-III module and a new version of the NITAWL module. Both modules are components of the AMPX System. XLACS-III is needed to generate multigroup data for the CNRXS GPN library; and the new version of NITAWL is needed to process resolved resonance data when pseudo-problem-independent data from the GPN library are converted into problem-independent data. Approximately one-third of the nuclides to be included in the GPN have been processed. Specifically, data sets for hydrogen, deuterium, oxygen, aluminum, uranium-235, and uranium-238 have been completed so that some benchmarking with the library could be attempted. Comparisons of experimentally measured values to calculated values are shown in Table 3. Agreement is generally good.

Cold neutron cross section data for hydrogen and deuterium have been generated and are shown in Figs 8, 9, and 10 along with data obtained from the Institute-Laue Langevin (ILL) facility.

Table 3. Benchmark lattice results using ANSL-V cross sections

Experiment/ parameter	Measured Value	Calculated Value	C/E
BAPL-1[a]			
k-effective	1.0	0.9988	0.998
U238 cap./ U235 fis.	0.078	0.0754	0.967
TRX-1[a]			
k-effective	1.0	0.9936	0.994
U238 fis./ U235 fis.	0.0946	0.0985	1.041
U238 cap./ U235 cap.	0.797	0.8070	1.013
ZEEP-1[b]			
k-effective	1.0	0.9991	0.999
U238 fis./ U235 fis.	0.0675	0.0681	1.009
RCR[c]	1.260	1.2867	1.021

[a]Documented in "Cross Section Evaluation Working Group Benchmark Specifications," BNL-19302 (ENDF-202), 1974 (Rev. 1981).

[b]Documented in "Testing ENDF/B-V Data for Thermal Reactors," AECL-7690 (Rev. 1), June 1964.

[c]RCR = U238 captures/ U235 fissions (in the cell) divided by the same ratio in a Maxwellian at the temperature of the moderator.

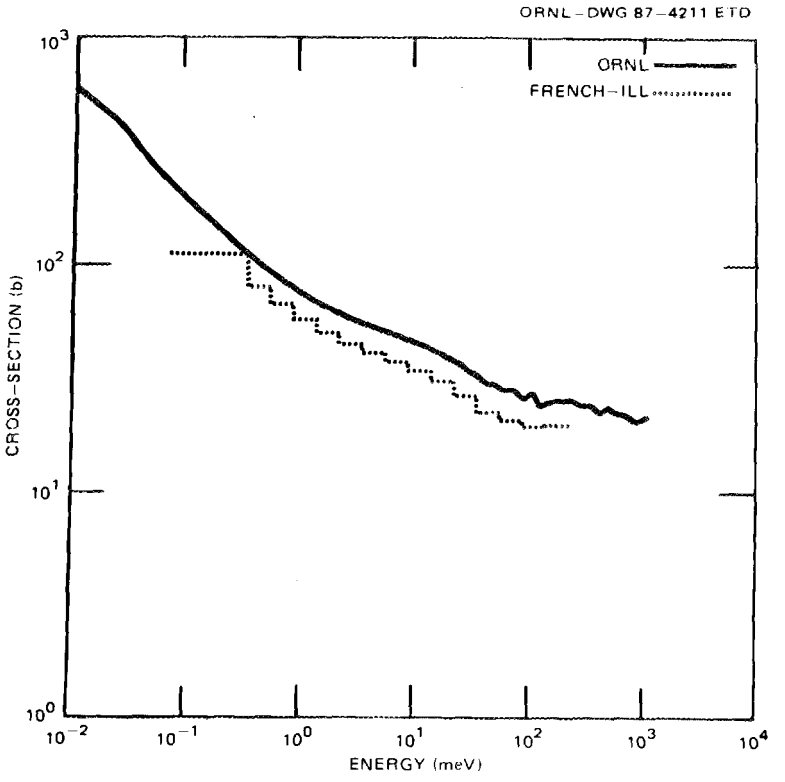

Fig. 8. Microscopic-scattering cross section for orthohydrogen

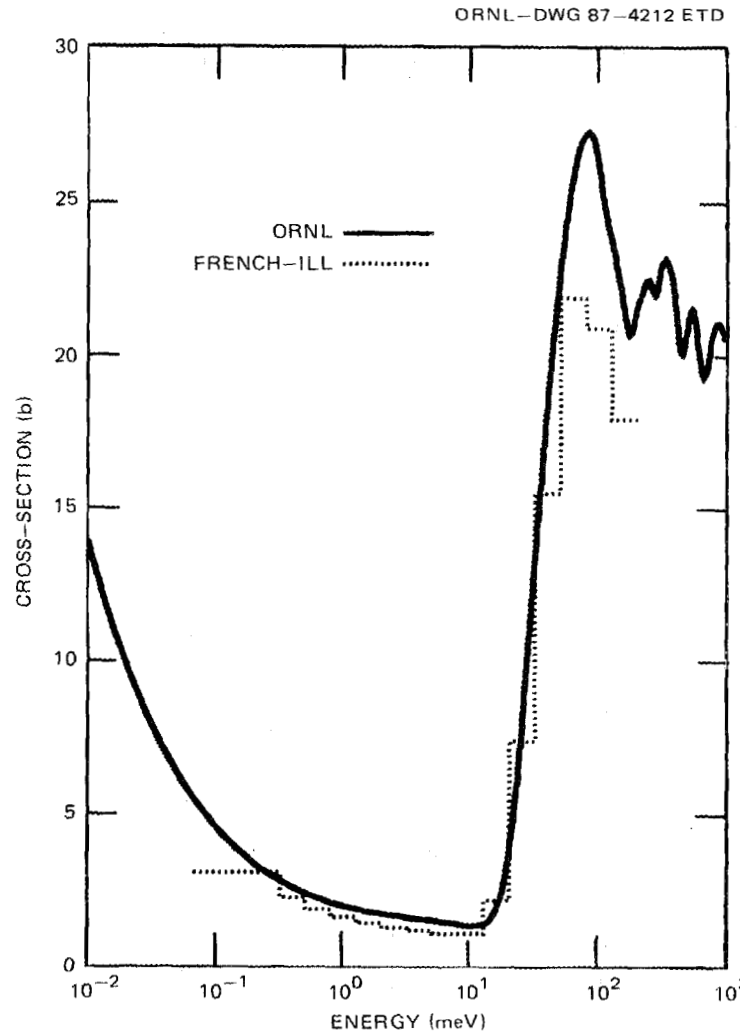

Fig. 9. Microscopic-scattering cross section for parahydrogen

The lower French values reflect the inclusion of a void fraction into the cross section representation. The deviation at low energies of the French deuterium data from the ORNL data reflects ILL's experimental correction to the Young and Koppel theoretical model. A new neutron scattering model is under investigation at ORNL for use at energies less than 7 meV. This new model attempts to account for chemical binding effects by treating liquid hydrogen to be of a quasicrystalline nature. It is anticipated that this model modification will resolve the differences.

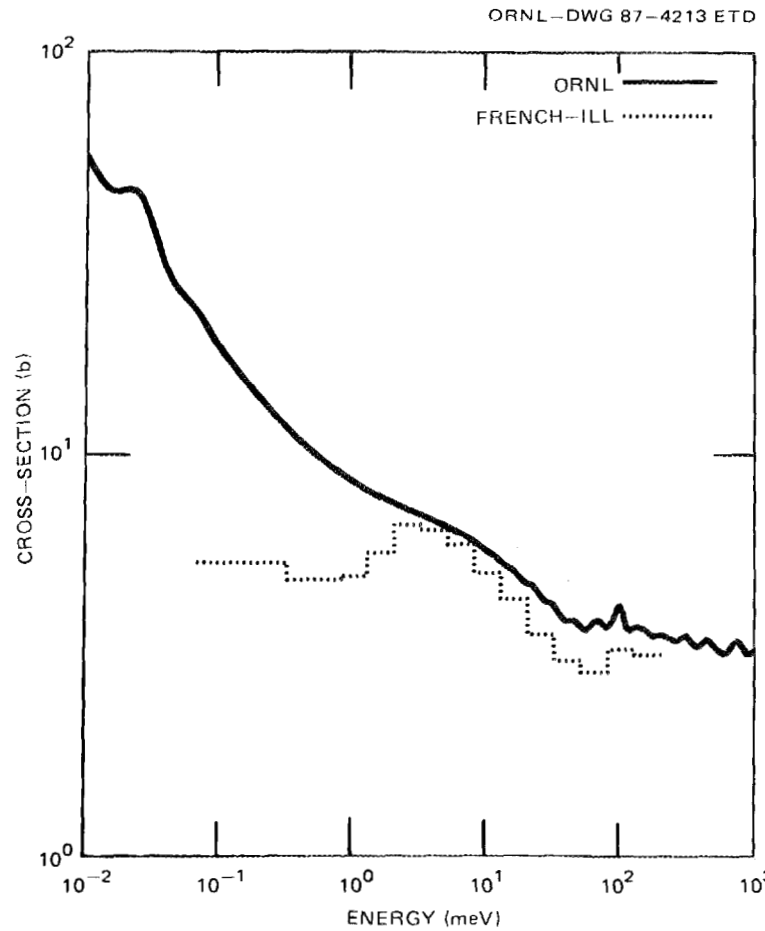

Fig. 10. Microscopic-scattering cross section for deuterium

The SGRP library has been completed and documented in an informal, internal memorandum. Likewise, the GRI library has been completed and documented. Benchmarking of these libraries will not be attempted until FY 1988.

2.2 Fuel Element Specifications and Manufacturing

To achieve acceptable core lifetimes at the desired performance level, a different fuel form from the U_3O_8/Al dispersion used in the HFIR or the UAl_x used in other research reactors is required. The major modification is the use of a uranium silicide rather than a uranium oxide or aluminide. The higher density uranium silicide fuel allows the achievement of a

high specific loading for ^{235}U with a low volume fraction of fuel in the dispersion, thus retaining high thermal conductivity. During the first half of FY 1987, work agreements between ORNL and Argonne National Laboratory (ANL) as well as ORNL and Babcock & Wilcox (B&W) have been developed to qualify, over the next three and a half years, the performance capability and feasibility of fabrication of the fuel element materials. Existing facilities at ANL and B&W are being modified to fabricate miniature and full-size fuel plates with radial and axial fuel-loading gradients. Present plans call for the delivery of initial plates for testing purposes by the end of FY 1987. In addition, B&W has been asked to provide engineering assessments of the feasibility and relative cost impacts of

1. twin-core vs single-core fuel elements,
2. thinner plates,
3. narrower coolant channels, and
4. ATR-type plate vs involute plate cores.

2.3 Corrosion/Erosion Tests on Aluminum-Alloy-Clad Material

The ANS reference cores have a configuration very similar to those of the HFIR: simply, an array of aluminum-alloy-clad fuel plates immersed in rapidly flowing water. The high thermal conductivity of the aluminum combined with the high heat transfer coefficient governing heat flow from the plate to the water keeps the fuel plates at a reasonable temperature. Unfortunately, the exposure of aluminum under these conditions leads to the formation of a thin layer of an oxide (boehmite), which separates the fuel plates from the coolant water. The boehmite film has a very low thermal conductivity, and the high heat flux through the film can cause excessive heating of the plates during the lifetime of the core. Experimental verification of acceptable corrosion behavior is therefore a critical consideration for the ANS.

2.3.1 Design of corrosion/erosion test loop

In the late 1950s and early 1960s, the HFIR Project supported a corrosion test program that examined the behavior of aluminum under conditions relevant to the operation of that reactor. This

test program did not extend beyond the HFIR conditions of heat flux and coolant velocity. As a result of the higher heat fluxes and coolant flow velocities in the ANS design, it is only possible to apply the HFIR experience directly to the present project by unsubstantiated extrapolation from existing experimental data. Therefore, a test loop is being built to determine experimentally the rate of corrosion product formation on the aluminum cladding at the higher heat fluxes and flow rates.

The test facility, shown in the flow diagram in Fig. 11, is a two-loop system. The high-pressure portion will operate with a loop pressure of up to 6.9-MPa (1000-psig) pump discharge pressure and a flow rate of 1.9 L/s (30 gal/min). Only 0.5 L/s (8 gal/min) will be supplied to the test section with the remainder flowing through the by-pass. The test section power is supplied by a 30,000 A, 20-V dc Transrex Power Supply. Heat is removed by a water-cooled heat exchanger, and the test section flow will be measured and controlled by an orifice-type flowmeter and a flow control valve. Loop pressure will be maintained using a metering pump. The low-pressure portion of the facility contains the loop water chemistry conditioning equipment. A flow of 4 to 8 L/h (1 to 2 gal/h) will be maintained by the letdown valve and cooled as it passes through a heat exchanger. The water then passes through an ion exchange column, a conductivity cell, a pH meter, and a dissolved oxygen meter before returning to an open 114-L (30-gal) sump tank. Nitric acid will be added to the water to control the pH.

The test section assembly is shown in Fig. 12. The first test specimens will be 6061 aluminum, the same material as the HFIR fuel-plate cladding. The heated length of each specimen is 165 mm (6.5 in.) with a coolant flow channel cross section of 12.7 mm X 1.27 mm (0.5 in X 0.05 in). Tests are scheduled to be conducted with heat fluxes from 5 to 20 MW/m^2 and coolant velocities from 9 to 33 m/s. Currently, the design is for light-water testing. Heavy-water tests will be conducted in the future and will require some additional modifications.

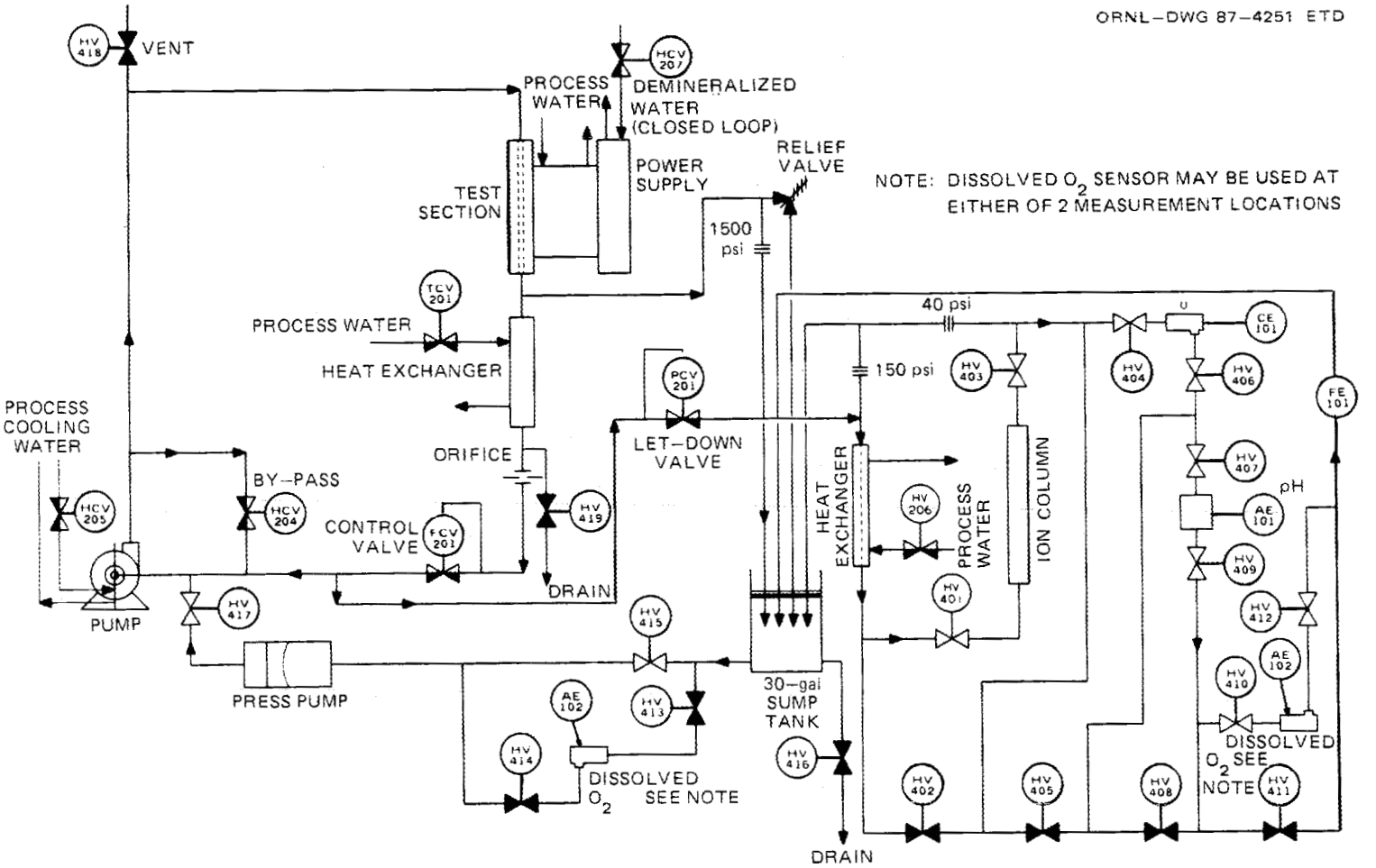

Fig. 11. ANS corrosion loop flow diagram

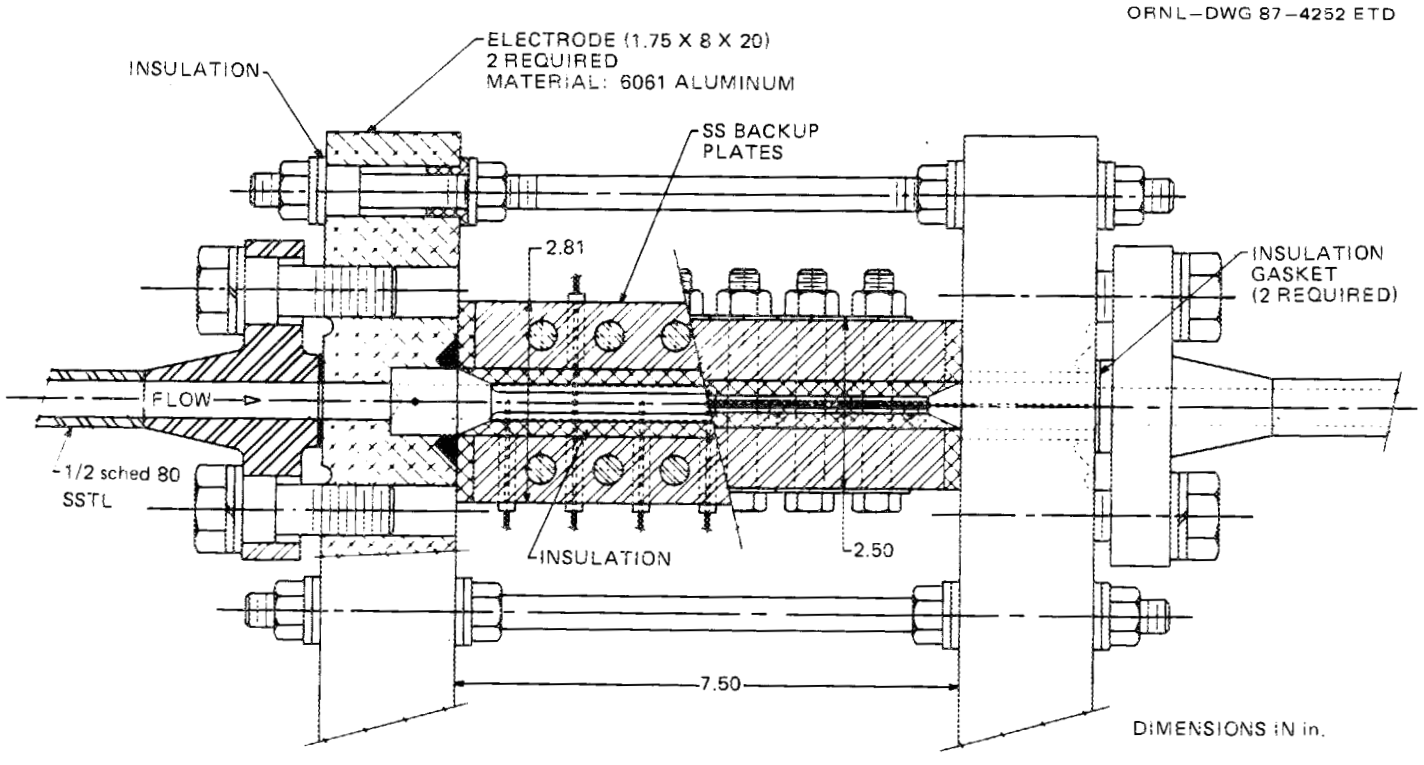

Fig. 12. ANS corrosion loop test section assembly

This same facility will later be used for thermal-hydraulic testing. However, modifications will be necessary due to higher heat fluxes, temperatures, and pressures.

The engineering design of the test facility has been completed. The corrosion test specimen design is currently awaiting verification of the development of a welding technique for the longitudinal seam welds and a trial specimen assembly. Purchase orders have been awarded for the circulating pump, the metering pump, the heat exchanger, and the loop package.

2.3.2 Preanalysis of corrosion/erosion test loop experiments

The basic information to be extracted from the first experiments in the ANS corrosion test loop will be an estimate of the temperature drop across the growing corrosion product layer as a result of the local heat flux. Because the experimental data will generally involve only measurements of average heat flux (or total power) in the specimen and temperature measured along the axis on the outer surface of the specimen, the required information on local heat flux and various temperatures across the heat flow path must be calculated. This calculation is normally performed with commonly used simplified equations. Because it is unlikely that a practical precise analytical solution to this problem exists, the use of the simplified equations could introduce unacceptable uncertainties. As a result, an analysis was performed during this report period using a more sophisticated finite difference solution to the heat transfer problem to evaluate the accuracy of the simplified analytical equations.

The HEATING5 computer code was used to perform a 2-D heat flow analysis of an appropriate segment geometry defining the active part of the specimen (a strip that is 7.6 mm wide, 2.5 mm thick, and 165 mm long). To account for the temperature variation of the physical properties, the specimen segment was divided into nine zones: three axial by three lateral. The corrosion product layer was divided into 12 axial zones because the temperature and therefore the oxide thickness will vary significantly along that

direction. Properties were assigned according to the temperature at the center of each zone, and the steady-state heat transfer solutions were iterated until satisfactory agreement was reached between the assigned and the computed temperatures.

After each solution, the calculated temperature at the oxide film-water interface at the midpoint of each of the 12 axial zones was used to assign a thickness to the corrosion product at that zone. In addition, the thermal conductivity, electrical resistivity, and heat generation rate were reassigned to the nine zones, representing the aluminum alloy, on the basis of the new temperature distributions. This procedure was followed until a reasonable convergence was apparent.

The temperature distributions computed by HEATING5 were then used to obtain estimates of the accuracy of calculated temperatures or parameters based on assumptions made to simplify either the data gathering or data treatment processes. The comparisons indicated that when temperature variations are large along the axis of the specimen, the variation in local heat flux should not be overlooked when using the approximate equations. The approximate equations were determined to be most accurate at some point near the center of the specimen, where the heat flux remains closest to the average value.

2.4 Core Flow and Heat Transfer Tests

To characterize the thermal-hydraulic performance of the ANS, the following parameters and/or the accuracy of their prediction have to be known:

1. pressure drop across the core,
2. heat transfer coefficient,
3. thermal conductance of clad with and without oxide layer,
4. incipient boiling heat flux,
5. minimum burnout heat flux, and
6. the pump coastdown characteristic.

Measurements of these parameters will be used to validate computer codes that, in turn, will be used to assess hot channel conditions and capability for natural convection cooldown. The accuracy required of the measurements must be determined.

The same experimental facility described in the previous section will be used for the thermal-hydraulic testing; however, modifications will be necessary due to higher heat fluxes, temperatures, and pressures. Under the present schedule, the modifications to the loop would be performed in early summer of FY 1988. It is anticipated that it will take approximately 3 months to modify the loop and an additional 3 months to perform the required thermal-hydraulics tests. Upon completion of the thermal-hydraulics tests, the loop will be reconfigured to continue corrosion tests.

2.5 Control Element Design, Tests, and Manufacturing Procedures

The design of the control elements is an integral part of the ANS core design. The present plans call for two separate control element systems: (1) an excess reactivity control system and (2) a safety shutdown control system. By separating the two systems, the excess reactivity control system can be designed to minimize impact on the peak reflector flux, and the safety shutdown system can be located for maximum shutdown worth because impacts on the peak reflector flux are not a consideration.

No assessments have been made concerning the actual design of these control systems, but some ideas have been generated. It has been estimated that as much as 20% excess reactivity may be required at the beginning of life to ensure a 14-d core life. This excess reactivity is expected to be controlled by two methods: (1) fixed burnable poison probably in the fuel plates and (2) movable control rods of reflective or absorptive material.

The most likely choice for the burnable poison is boron. Boron has been used in other reactors, including the HFIR, as a reasonably efficient burnable poison. The primary limitation of boron is associated with production of helium from the boron decay following neutron absorption. The distribution of the poison within the fuel plates could also be used as a means for further flattening of the power distribution.

At this time, only absorptive (i.e., not reflective) materials have been examined for the movable control rods. Hafnium rods are

used in Advanced Test Reactor (ATR) and have been proposed by INEL. Hafnium has good capturing power in the epithermal ranges, fair resistance to radiation damage, and good corrosion resistance. Neutron absorption is by means of five successive (n,gamma) reactions. The major disadvantages of hafnium are that heavy pieces of hafnium are required for long-life usage and it is quite expensive to obtain and fabricate. Europium is another material that could be used in the movable control rods. With respect to neutron absorptive capabilities, it is very similar to hafnium. The major disadvantage of the europium is its expense. Other rod compositions such as the silver/cadmium rods used in ILL will also be considered.

2.6 Validation of Neutronics Performance Predictions Through Critical Experiments

This activity is not scheduled to begin until late FY 1988.

2.7 Structural Analysis and Tests

Due to funding limitations, no work in this area was undertaken in this reporting period.

2.8 Cold Neutron Source Development

The major capability to be provided by the ANS is that of a source of low-energy neutrons for neutron physics experiments. Thus, R&D activities to optimize the cold-source design are important. Four design goals have now been identified:

1. The cold source(s) should provide a high flux of cold neutrons (at least five times the ILL level). A preferred neutron energy distribution will be defined by the National Steering Committee.

2. The design of the cold source(s) should provide a total of at least 8 cold neutron guide tubes for the ANS Facility.

3. The cold source(s) should have minimal effects on safety. This implies that the cold source should not be a major contributor to the overall risk associated with the facility.

4. The cold source(s) should have minimal effects on normal reactor operation. This implies that the status of the cold source has either no impact on the normal operation

of the reactor or that cold source conditions that could have an impact on normal operation have acceptably low probabilities of occurrence.

The major design factors for the cold source include number, location, shape., size, moderator type, structural materials and cooling concept. During this report period, several of these factors have been examined on a preconceptual design basis.

2.8.1 Number of cold neutron sources

The decision has been made initially to approach the cold-source goals with two cold sources of basically identical design located on opposite sides of the core. This decision was made for three major reasons:

1. The requirement for eight guide tubes can be met by either a single cold source or two cold sources. However, in the case of a single cold source, the tubes would be concentrated in a small area or separated axially to the point where some tubes would be in a less than optimal flux field. In either case, the cold neutron source integrated over all eight tubes would be reduced for the single cold-source vs the two cold-source option.

2. One of the design objectives identified for the cold source was to minimize the reactor core flux or power tilting effects caused by the presence of the cold source. With two cold sources located 180° apart, the impact of the cold source on the core is more balanced with respect to localized positions in the core; thus, the flux or power tilting effects are reduced.

3. Because the cold source is such an important component of the ANS Facility, it is important that the availability of a cold neutron source capability be as high as possible. The use of two cold sources will enhance the probability that at least some cold neutrons are available at all times even though the two cold sources are not expected to be totally separate systems.

The major disadvantage associated with the choice of two cold sources is that in all likelihood it is somewhat more expensive to build two smaller cold sources than it is to build one large one. In making the decision to provide two cold sources it was determined that the advantages outweighed the probable increase in system cost. It should be noted, however, that we are still in

the preconceptual design phase and that other factors not yet identified could result in a reversal of this decision.

2.8.2 Cold neutron source location

The choice of location for the cold source is influenced by several factors. For maximum cold neutron production, the source should be located as close to the thermal peak in the reflector as possible. This factor encourages locating the cold source close to the reactor core. On the other hand, we do not wish to be so close to the core that significant reactivity and flux tilting effects result. In addition, the nuclear heating rates increase very rapidly as the cold source is moved closer to the core, and thus the amount of heat that must be removed at cryogenic temperatures is increased.

The nuclear heat deposited in the cold source was estimated in a first step toward resolution of the location issue. The estimation was made by scaling and extrapolating available data on heat deposited in the ILL cold source. These values were subsequently reviewed by ILL staff and determined to be reasonable. Table 4 summarizes the amount of heat deposited by

Table 4: Sources and magnitudes of heat deposited in the cold source

Heat source	ILL (kW)	ANS at 10 x ILL (kW)	ANS at 80% peak (kW)
Core gammas	1.3	8.4	31
Fast neutrons	0.1	1.4	4
Betas in aluminum	1.1	11.3	17
Capture gammas			
From LD_2	0.8	8.4	13
From structure	1.3	10.3	16
Heat in-leakage	1.2	1.2	1
TOTAL	5.8	41.0	82

various sources in the ILL cold source as well as our estimated values for two locations in the D_2O reflector tank of the ANS Facility, assuming the same cold-source shape and size. The high heat deposition levels indicated by these estimates indicate that unless improvements in the thermal design of the cold source can be made, the nuclear heat would limit us to a minimum distance from the center of the core to the center of the cold source of ~700 mm.

2.8.3 Cold neutron source shape and size

The principle cold source at the ILL facility has a spherical external shape.[3] In recent years, a chamber has been added inside the cold source that allows the formation of a cavity region extending from the center to the back inner wall of the cold source. The cavity region effectively removes material which: (1) has a diminishing returns impact on the cold neutron population and (2) provides a target for additional neutronic heating. This design offers a reference configuration to start our analysis but may not be optimized for the ANS conditions. Because many of the heat sources identified in Table 4 appear as so many watts per gram, we need to maximize the cold neutron flux while minimizing the amount of moderator and structural material. Some possible shapes for the ANS cold source are shown in Fig. 13. Each shape offers advantages as well as disadvantages over the more conventional sphere. However, a direct evaluation of each shape, as well as other potential shapes, to perform a tradeoff analysis would be both time-consuming and expensive.

An analytic method that could make an optimization effort practical is under consideration. This method would involve adapting transport adjoint methodologies, developed in shielding analysis to trace streaming paths, for the purpose of determining the origin of cold neutrons entering a guide tube. This approach could provide information on the importance of various moderator regions around the guide-tube entrance and thus some insights into the shape and size that would be most effective. Adjustments to

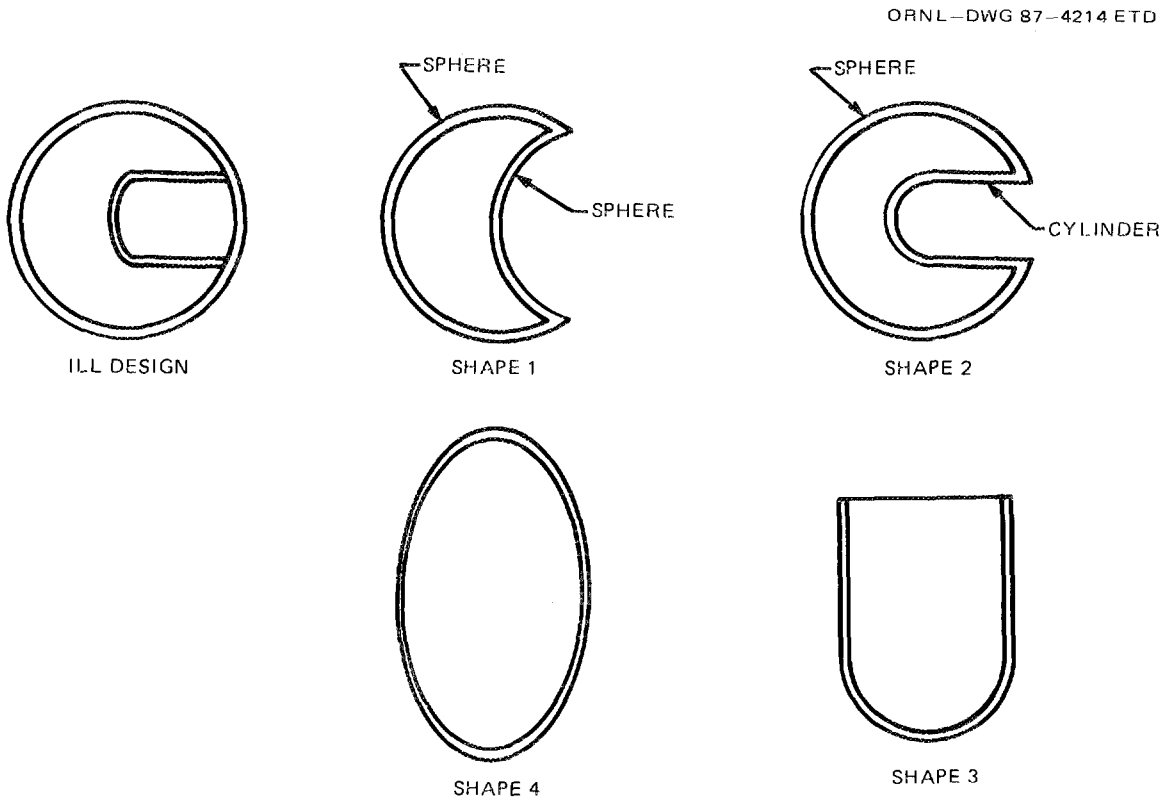

Fig. 13. Some shape considerations for ANS cold source

the shape to accommodate engineering design considerations could then be performed using direct evaluation techniques.

2.8.4 Cold neutron source moderator

Liquid hydrogen and liquid deuterium are the usual choices for the moderator of a cold source of the kind envisioned for ANS. Both have been used in previous high-flux-reactor cold-source designs. The major difference is that for liquid hydrogen cold sources the optimal flux is reached as the cold-source volume approaches 1000 cm^3. Beyond this volume, the hydrogen absorption cross section dominates and there is a net decrease in the number of cold neutrons available.[3] The smaller absorption cross section associated with liquid deuterium permits the design of larger cold sources with a greater number of cold neutrons.

One of the design goals for the ANS cold source(s) is to provide a total of at least eight cold neutron guide tubes.

Coupled with the decision to use two cold sources this implies that the volume for each cold source will be larger than the 1000-cm^3 value, if sufficient area is to be available to feed four large guides. As a result, the decision was made to consider liquid deuterium as the moderator material for the cold source.

2.8.5 Cold neutron source structural materials

Our present calculations for the cold source are based on the ILL design and therefore use aluminum as the primary cryostat structural material. Aluminum is certainly appropriate for the environment. However, the (n,β) reaction in the aluminum is a source of heat that is deposited by the β-particle in both the aluminum and the liquid deuterium. The elimination of this heat source could reduce the amount of heat that must be removed from the cold source at cryogenic temperatures by as much as 28%. Therefore, during this report period we have examined, in a preliminary manner, other materials for potential use as the cold neutron source structural material. The most promising material appears to be magnesium or at least some form of a magnesium-aluminum alloy. A search for material properties, irradiation, and cryogenic data for the magnesium-aluminum alloys will be performed during the coming months.

2.8.6 Cold neutron source cooling options

Four options were considered for cooling the cold source moderator: (1) single-phase thermal siphon, (2) forced flow, (3) direct helium gas cooling of subcooled liquid deuterium and (4) natural convection. Option 1 is identical to the ILL design and is capable of handling a total heat load of at least 5 kW. At this heat load, bubble fraction in the liquid moderator region is about 25%. At the preferred cold source location, the heat loads are nearly 10 times larger than the ILL heat load, and at such heat loads it would be impossible to create/maintain any substantial liquid deuterium inventory in the cold source. Therefore, this option can be ruled out for the ANS cold source.

Option 2 is based on forced flowing liquid deuterium with an external pump. The warm liquid deuterium would be transported to a helium-cooled heat exchanger. Although this system can handle the heat load of the ANS cold source, its main disadvantage is a much larger volume of liquid deuterium. Moreover, reliable pumps are not presently available for operation at very low temperatures (~20 K). For these reasons, this option is also not considered favorably at this time.

The most promising option appears to be No. 3. A schematic of this concept is shown in Fig. 14. An inner vessel contains deuterium under moderate pressure [~0.4 MPa (60 psig)]. An outer vessel provides the primary structural support, including the pressure boundary. In between the two vessels, helium gas flows at an inlet temperature of 6 K. One of the advantages of this concept is that the majority of the heat deposited in the structural material is removed directly by the helium gas rather than indirectly through transfer to the liquid deuterium. Although the conceptual design is <u>by no means complete</u> because neither the shape nor size of the cold source have been optimized, the present preconceptual design will provide for the removal of a significant amount of heat from the cold source structure and moderator. This capability should allow us to place the cold sources in positions that will provide a cold neutron flux level that is at least 10 times that of ILL. The major limitation appears to be the ability to transfer heat from the LD_2 to the inner wall. With natural circulation in the LD^2 pool, a heat flux value at the wall of only 1 W/cm^2 can be handled with an acceptable temperature difference between the cooled vessel wall and the liquid deuterium.

This limitation can be overcome by incorporating conductive fins along the inside surface of the inner deuterium vessel. This increases the surface area to handle the required heat load. Any heating generated into the fins is directly passed to the inner vessel wall where it is removed by the cold helium gas. A

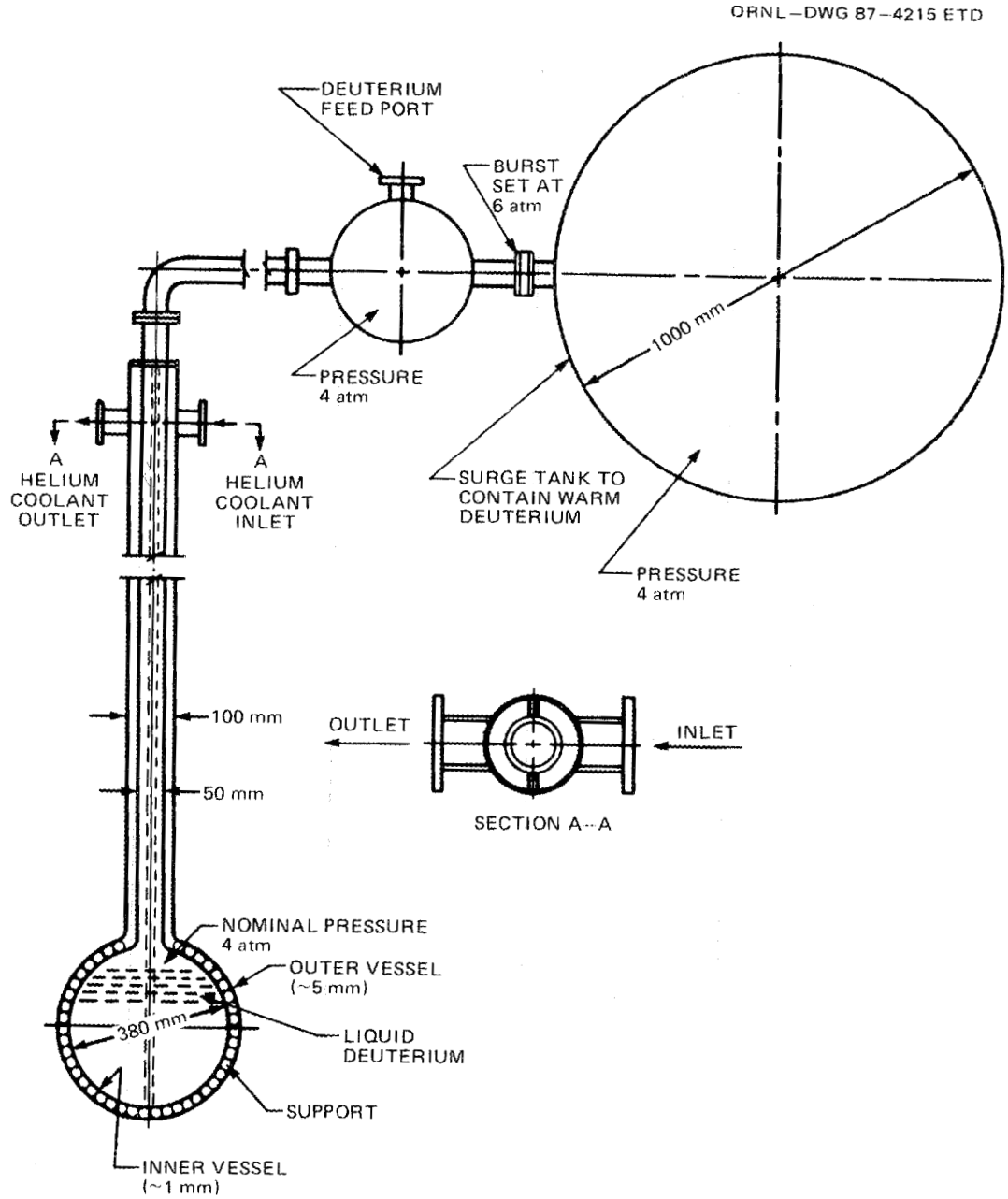

Fig. 14. Cold-source concept with liquid deuterium pool subcooled by gaseous helium

preliminary arrangement of the cold source vessel is shown in Fig. 15. The key feature of this concept is a stagnant pool of liquid deuterium.

Finally, Option 4 utilizes natural convection which is driven by gravity due to liquid deuterium density differences between the

ORNL–DWG 87–4216 ETD

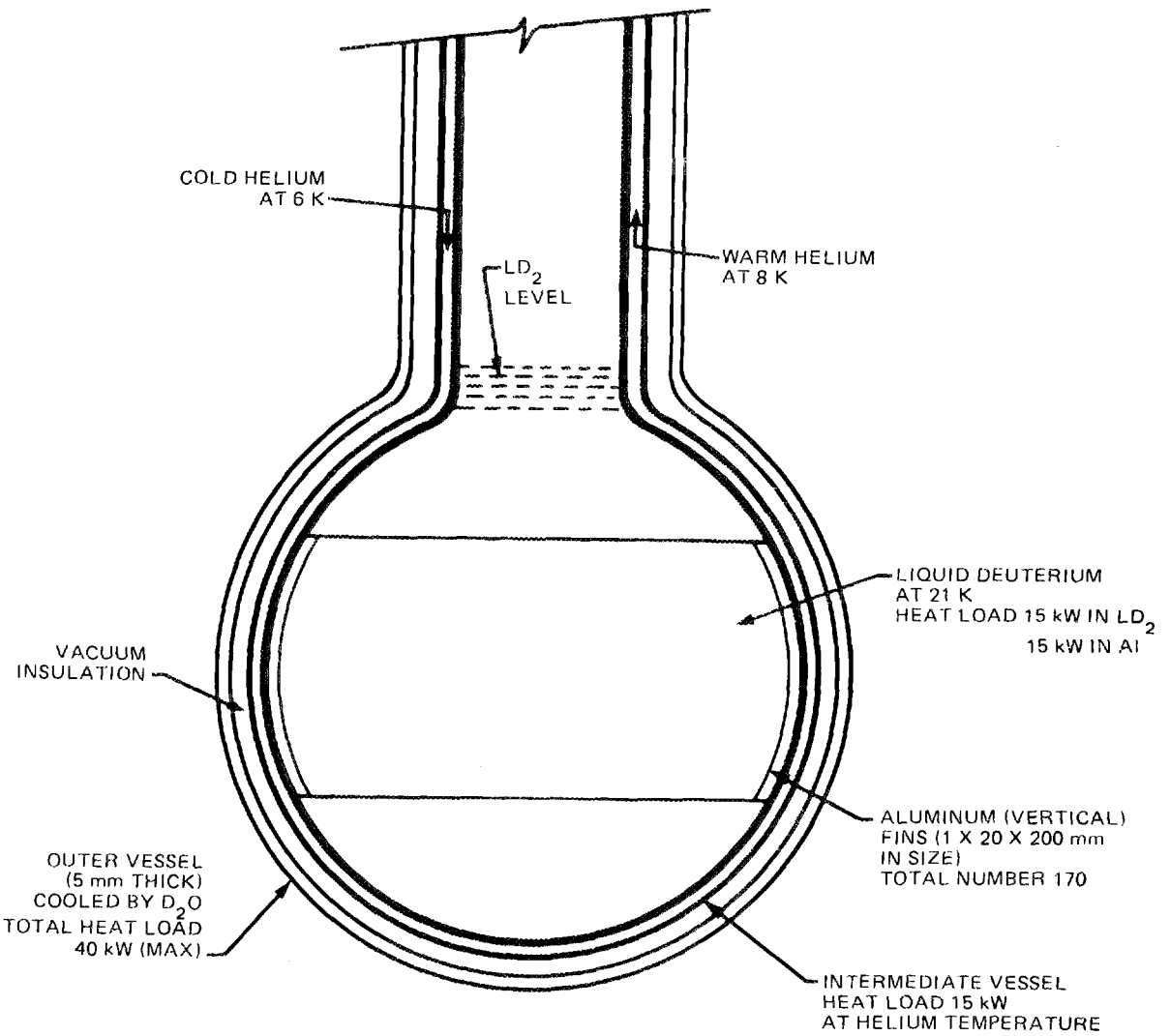

Fig. 15. Cold-source concept with aluminum fins inside inner vessel

warm and cold regions of the liquid deuterium. A cold source concept based on this approach is shown in Fig. 16. This design is similar to the concept of Fig. 15 with the following exception. The design of Fig. 16 does not have cooling fins, and the maximum heat load that can be handled by such a system would be limited to 5 kW. To remove an additional 10 kW heat load from the liquid deuterium, the system of Fig. 16 employs a helium gas-cooled heat exchanger and a liquid deuterium flow guide. The heat exchanger

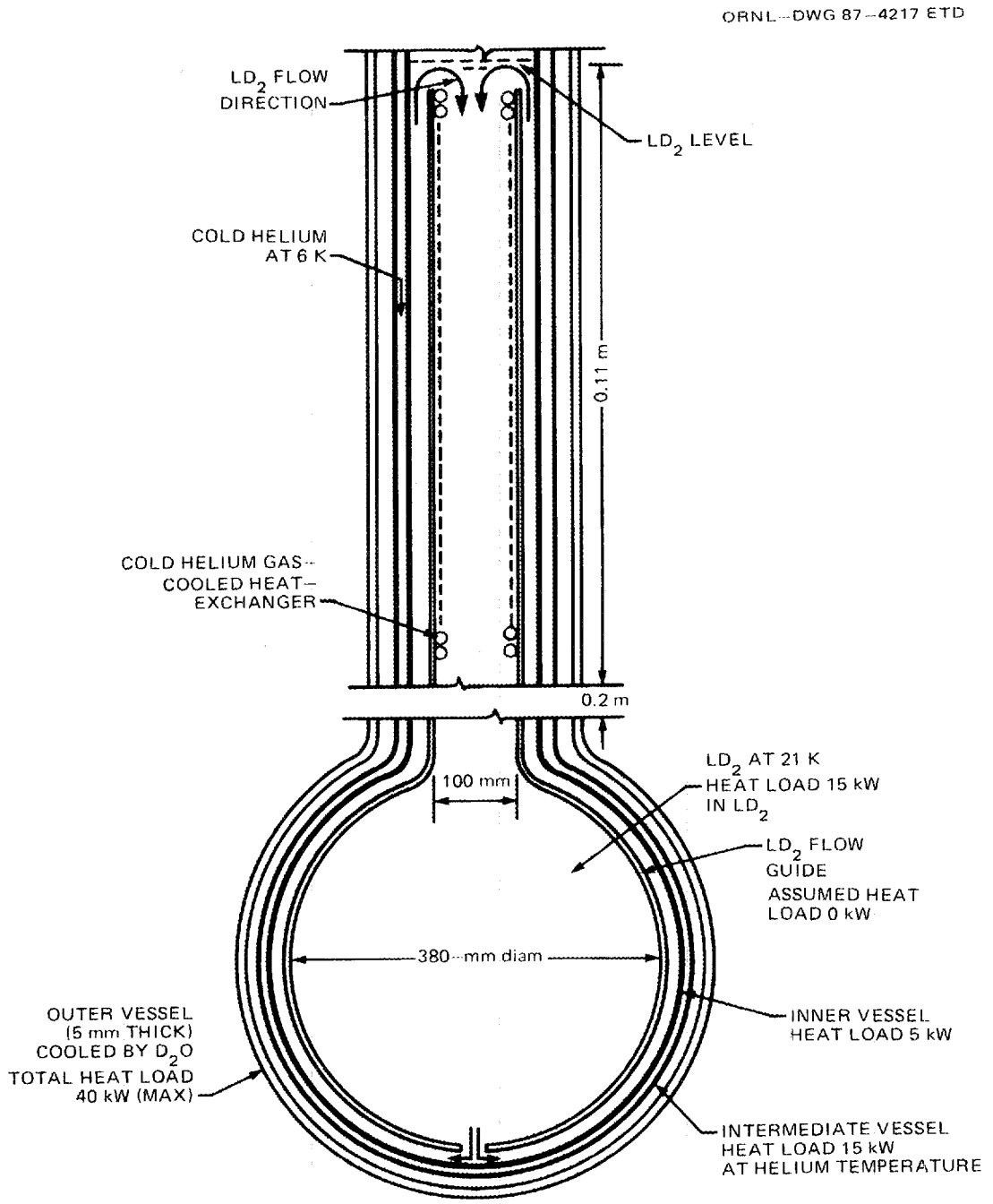

Fig. 16. Cold-source concept employing forced convection induced by cold helium-gas heat exchanger in neck tube

is located inside the neck tube of the inner vessel. Total length of this heat exchanger is 110 cm. For ease of maintenance, this heat exchanger will be located outside the D_2O moderator pool. This requirement will force the heat exchanger to be placed at least 200 cm above the cold source vessel. In this concept, sufficient liquid deuterium will be needed to fill the inner cold source vessel as well as up to 300 cm length of the neck tube. This requirement results in two times more liquid deuterium than the Option 3 cold-source concept. Moreover, the heat exchanger in the neck tube is a second active system with potential maintenance and reliability problems. This concept is also being considered as an option.

The above discussion is based on preliminary analyses which in turn are based on what may be inadequate material property data. More detailed analysis and model testing would be required to further differentiate among the various concepts discussed here.

2.9 Beam Tube and Instrument Development

This activity is not scheduled to begin until FY 1988.

2.10 Hot Neutron Source Development

This activity is not scheduled to begin until FY 1988.

2.11 Shielding Concepts and Validation

This activity is not scheduled to begin until FY 1988.

2.12 Plant Instrumentation and Controls

This activity is not scheduled to begin until FY 1988.

2.13 BOP Concepts

In addition to the 12 R&D tasks previously mentioned, numerous issues arise regarding integration of the ANS systems into a total plant concept. Many of these issues require R&D efforts to evaluate alternatives and provide feedback to the component design and safety evaluation efforts. During this report period, four R&D efforts fell into this category: (1) core and facility configuration evaluations, (2) containment and ventilation issues,

(3) tritium and deuterium control, and (4) refueling and vessel replacement.

2.13.1 Core and facility configuration

The major effort toward establishing the interface between core design activities and concepts for the BOP was the generation of a series of core and facility configuration sketches. Figure 17 shows a sketch of the 35-L reference core configuration, and Fig. 18 shows a similar sketch of a 55-L oxide core. These sketches do not, in general, reflect mechanical designs but rather show key dimensions and layouts of the core, CPBT and cold neutron source components as currently envisioned. This effort not only provides a point of reference from which general facility configurations can be established, but also serves to identify the

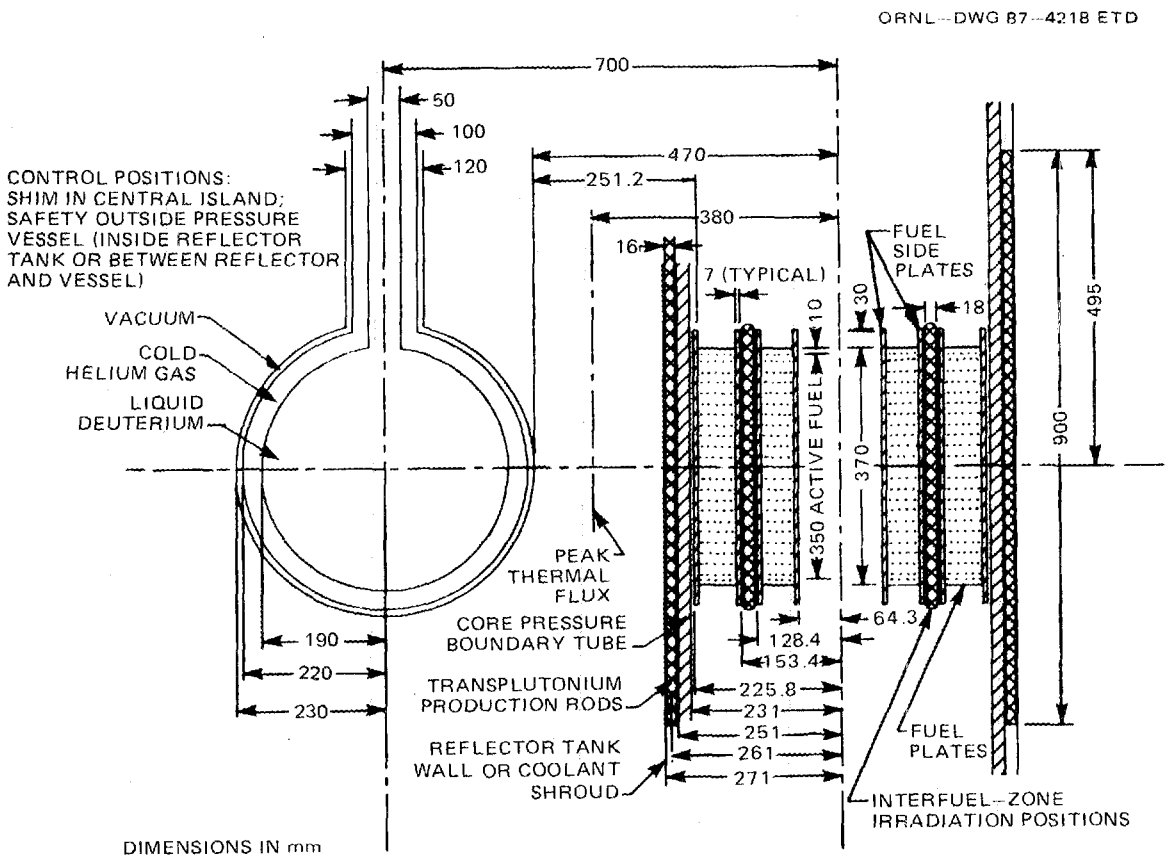

Fig. 17. Sketch of 35-L non-oxide base core and cold-source dimensions

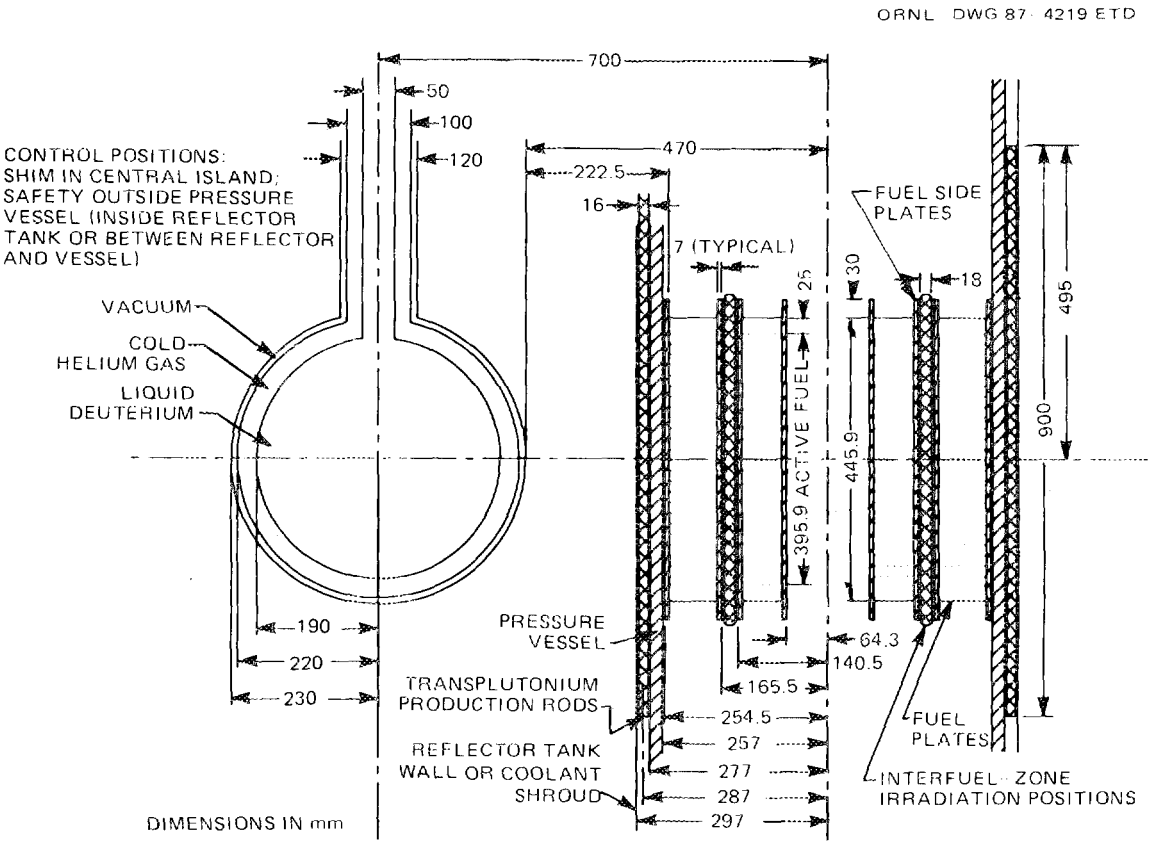

Fig. 18. Sketch of 55-L base core and cold-source dimensions

base dimensions under which all core calculations should be carried out.

Figures 19-21 extend the core configuration into the facility. Figure 19 shows the core and cold source set in a reflector tank extending ~1.5m from the active core and centered in a light-water pool. Figure 20 uses the standard beam tubes and typical shield thicknesses to set floor elevations for the ground floor beam room. Headroom requirements for the beam room and a typical reactor pool depth are used to establish floor elevations for the operating high bay and for the equipment and experiment areas on the first floor level. Possible layouts are also shown for 24-in. primary piping into a pipe chase and, for deuterium, piping to a fill station and safety relief tanks. It is interesting to note that the CPBT is smaller in diameter than the primary coolant

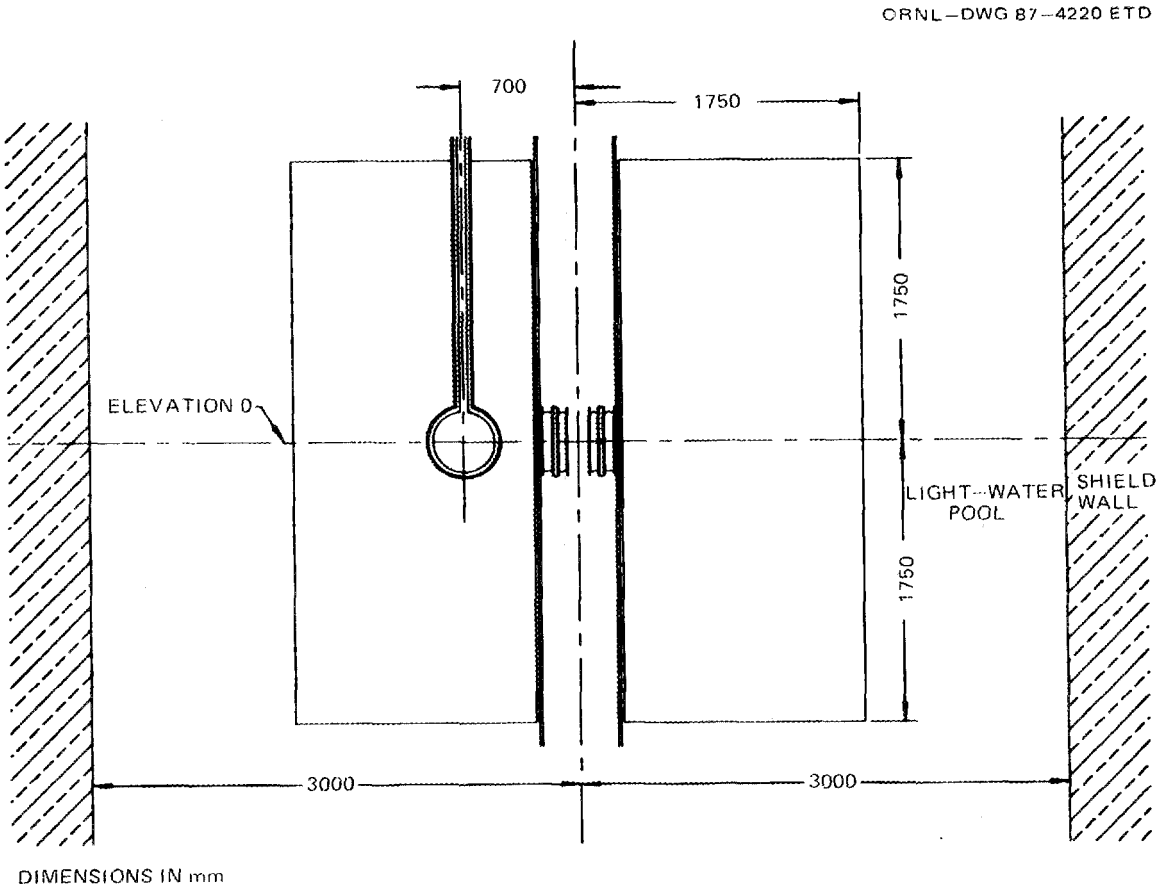

Fig. 19. Sketch of core, cold source, and reflector tank

piping. Figure 21 extends this configuration to a possible overall elevation section of the central reactor building. This configuration is based on the four-building concept of the FY 1984 feasibility study,[4] in which the central reactor building, adjoining reactor support (including primary pumps and heat exchangers) and guide hall buildings, and an administration building are all distinct structures. Figure 22 shows a section rotated 90 deg from Fig. 21, with the cold neutron beam guides passing through a flooded casement into the guide hall building. Spent-fuel pools are shown above the beam guide casement. Again, all of these sketches are only meant to reflect the general orientation of the facility as currently conceived and do not represent an actual design.

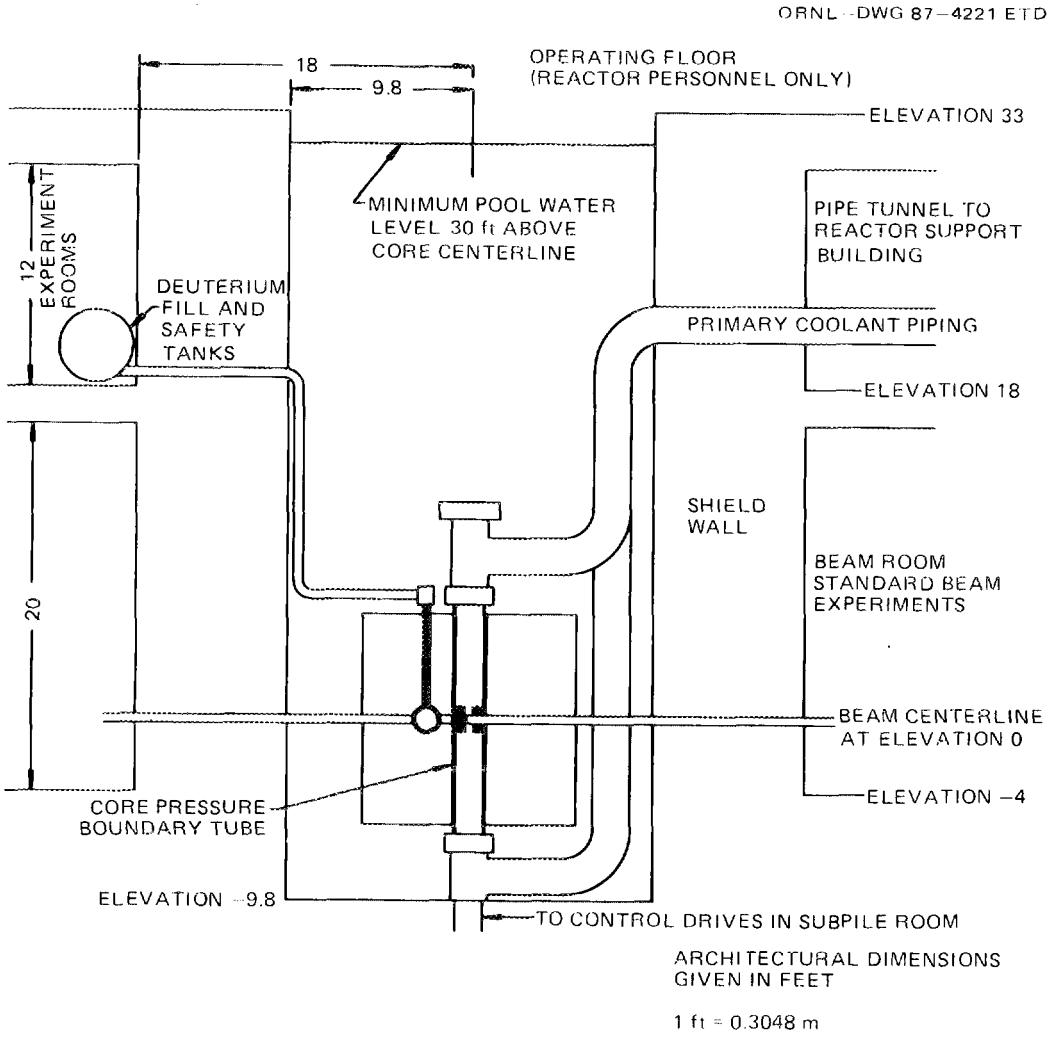

Fig. 20. Sketch of reactor pool, shield walls, and beam interface

2.13.2 Containment and ventilation

In the four-structure concept developed during the FY 1984 feasibility study, the primary coolant loop spans the central reactor building and the reactor support building. Thus, the primary reactor containment must also span the two structures. Figures 23 and 24 show the primary and secondary ventilation zones and the hardened protection boundary surrounding the primary system. In the reactor building, a steel structure inside the concrete dome forms the primary containment and will be designed to meet specified leak rates for all conceivable accident

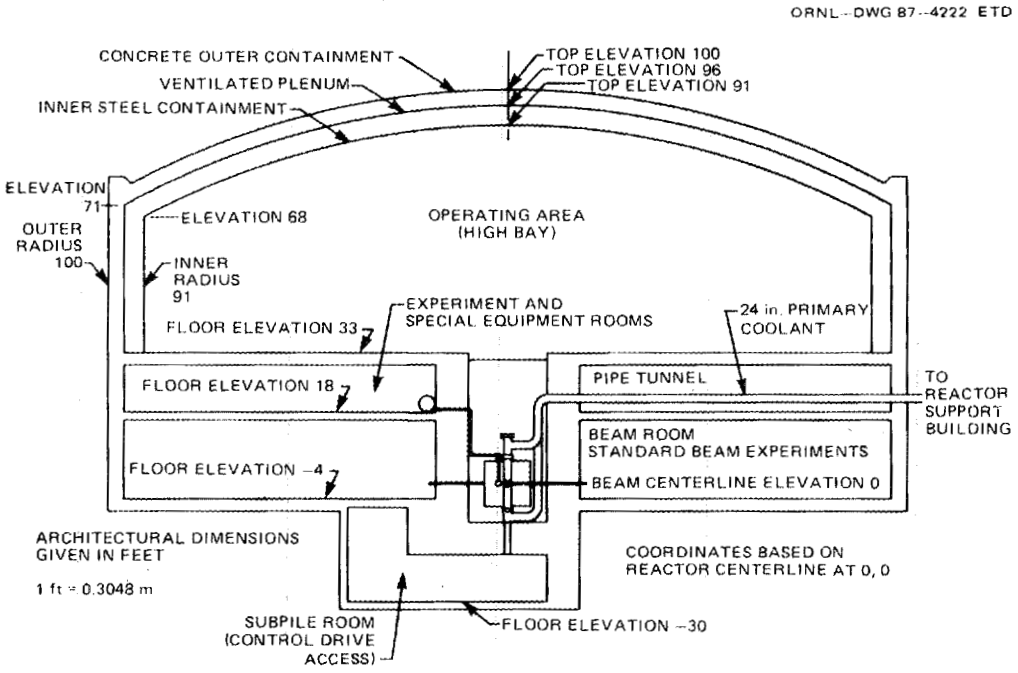

Fig. 21. Section of reactor building, showing pipe tunnel for primary coolant

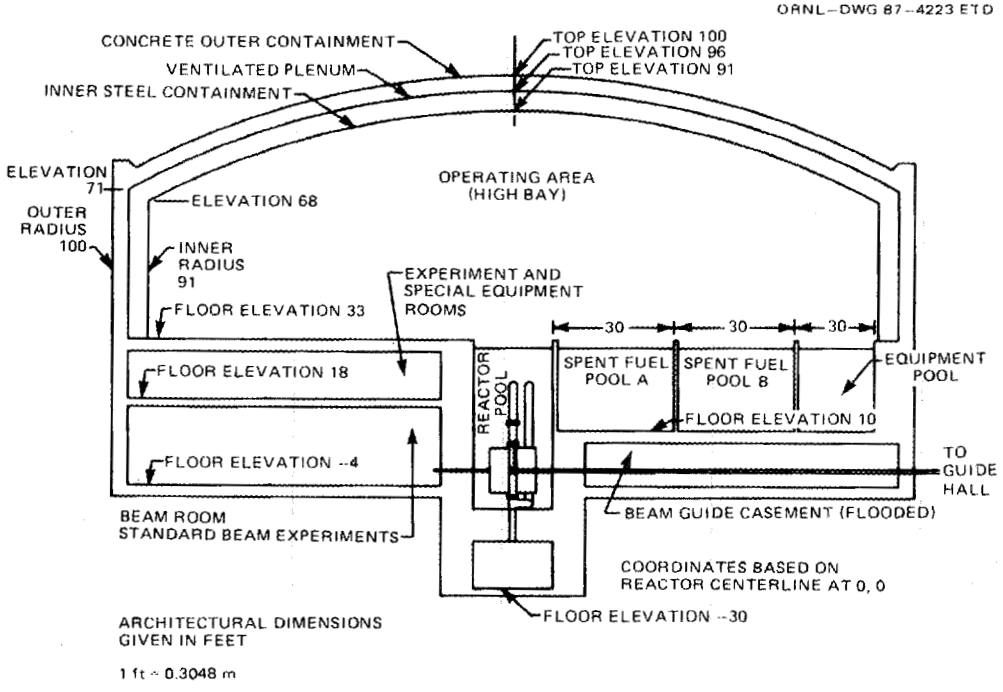

Fig. 22. Section of reactor building, showing beam guide passage and storage pools

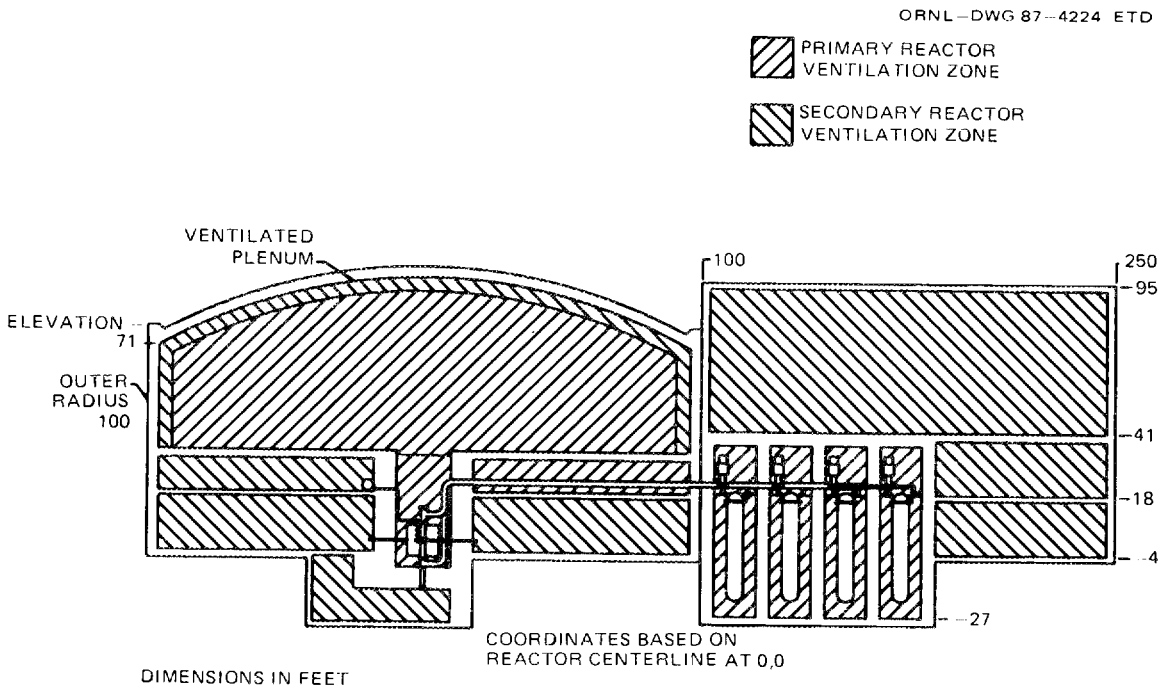

Fig. 23. Primary and secondary reactor ventilation zones in reactor and reactor support buildings

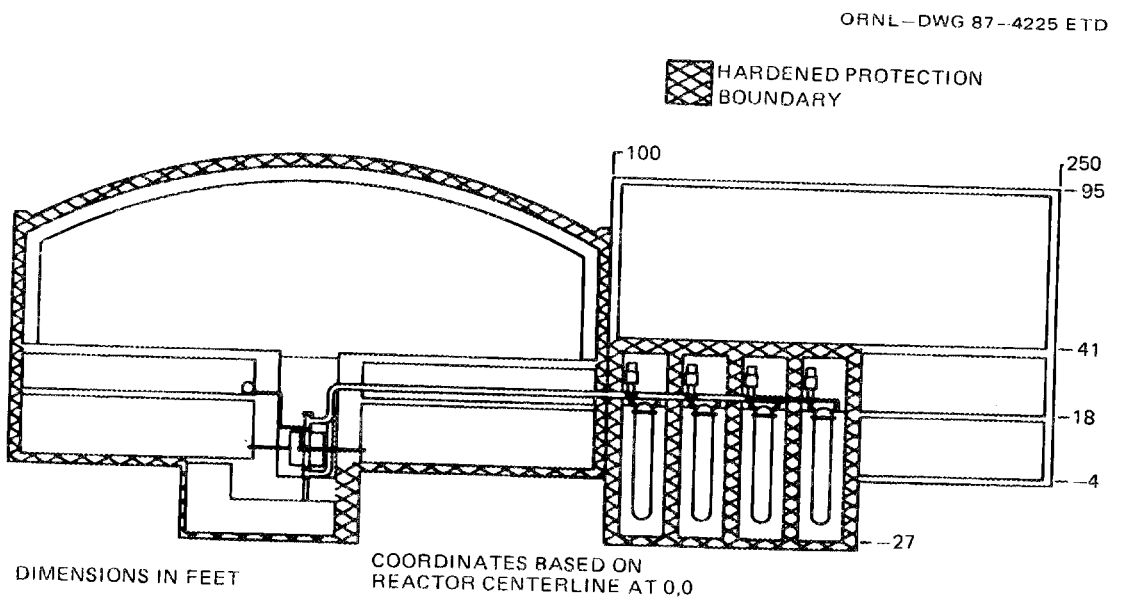

Fig. 24. Hardened structure perimeter around reactor and primary coolant systems

scenarios. Early safety studies have shown that a ventilated space between the primary containment and the outside environment may be useful in keeping the site boundary and low-population zones (LPZs) entirely on the DOE reservation. Such a ventilated space between the steel and concrete dome structures is shown on Fig. 23. In the reactor support building, the four primary heat exchanger cells form the primary containment structure, with the high bay and surrounding areas serving as the secondary ventilation zone. The pipe tunnel between the reactor pool and the heat exchanger cells is also a part of the primary containment structure. The passage of the primary piping from the reactor building into the reactor support building will require special care to ensure effective containment and seismic resistance.

During the second half of FY 1987, alternative configurations that keep the primary loop entirely inside the central reactor building will be examined. The motivation for placing the primary pumps and heat exchangers in a separate building was to maximize the accessible area around the reactor for experimental purposes and to provide distinct zones for personnel and contamination control. Further evaluation will be conducted to determine whether these goals can be achieved in a plant configuration in which primary containment does not span two structures.

2.13.3 Tritium and deuterium control

Tritium is produced in heavy-water reactors by absorption of neutrons in deuterium; it decays with a 12.3-year half life. Using a time-averaged constant rate of production during the life of the reactor and assuming no turnover of heavy water and no tritium removal system, an equilibrium concentration of tritium in coolant or reflector water can be calculated. Because it takes several half lives to reach this equilibrium (about 40 years to reach 90% of equilibrium), this value is more useful for providing common comparisons than as an actual projection. In practice, values of no more than about one third the equilibrium would likely be encountered during operation.

Table 5 shows assumptions for tritium production rates and the resulting equilibrium concentrations for separate coolant and reflector loops and for a common loop serving coolant and reflector. A range of 1 to 2 Ci/L is often considered the threshold for operational concern. For example, the detritiation system at ILL is used to hold tritium concentrations in their combined reflector-coolant system to 2 Ci/L. Conversations with Canadian engineers associated with the CANDU reactors have indicated that concentrations below 1 Ci/L do not cause operational difficulties. The value calculated for a separate coolant loop in the ANS is well below this threshold, although the

Table 5. Tritium concentration parameters and results[a]

	Coolant only (fuel+island)[b]	Reflector only (reflector)	Combined coolant and reflector
Tritium produced per cycle[c], grams	0.0059	4.05	4.056
Average tritium production rate, Ci/year	1,140	783,000	785,000
Volume of loop, liters	114,000	19,000	133,000
Calculated equilibrium tritium concentration, Ci/L	0.177	733	105

[a]Calculations for equilibrium concentrations assume no removal of tritium by mechanisms other than decay, such as leakage, diffusion, replacement of coolant or reflector water, or detritiation. Realistic conditions would result in lower equilibrium values.

[b]Concentrations are based on static calculations where the coolant flow outside of the fuel end caps is included in the reflector region. Therefore these numbers do not totally reflect the equilibrium tritium concentration in the primary coolant.

[c]Tritium production per cycle is based on a 270-MW reactor, with a 14-day operating cycle followed by a 3-day downtime for refueling.

calculation is based on an idealized coolant flow in the fuel and island regions only and a realistic value encompassing flow between the fuel element and reflector, and flow paths above and below the core would be several times higher. However, this value would still be relatively low because most of the tritium is produced in the reflector, where the highest thermal neutron fluxes encounter the largest volume of D_2O. These calculations point out the possibility of removing much of the tritium from the coolant system by keeping the coolant and reflector systems separate. However, a tritium removal system will be needed for the reflector system. The need for a system to remove light-water contamination applies to both the coolant and reflector.

Small, routine tritium and deuterium releases from the facility are unavoidable and acceptable. Monitored tritium releases occur at the existing ORNL reactors and at a variety of other ORNL facilities, consistent with current DOE guidelines for such emissions. Although deuterium is a naturally occurring isotope and is not radioactive, large releases may be harmful to aquatic life and the environment at ORNL. Existing ORNL waste systems are incapable of removing either tritium or deuterium from waste streams. Studies of anticipated release rates, environmental impacts, and waste handling alternatives will continue.

2.13.4 Refueling and vessel replacement

Removal of spent fuel from a heavy-water coolant into a light-water reactor and storage pool presents additional problems not encountered at other ORNL reactors. These problems are further complicated by the high decay heat rates expected for ANS fuel, for which forced-flow cooling may be required for as long as about 1 day after reactor shutdown.

Refueling approaches at several other heavy-water reactors were evaluated for applicability to the ANS reactor. Most heavy-water reactors discharge spent fuel directly from the heavy-water coolant into a light-water pool by lifting the elements into a dry discharge chute or canal. A flush water stream is often used to

wash heavy water off the fuel and provide some cooling during the transfer. Because of the high power density and high decay heat rates of the ANS fuel, these approaches may not be practical. The most promising system encountered is that used at the ILL. A dry "bell jar" transfer vessel is lowered into the reactor pool and attached to the top of the fuel element (which, at ILL, is also the reactor vessel i.e., the core pressure boundary tube is integral with the fuel element.) A valve is opened, allowing heavy-water coolant to flood the transfer vessel. A remote lifting device is then used to pull the fuel element into the transfer vessel, which is provided with a natural convection heat exchanger for transfer of decay heat to the pool. The fuel element and the transfer vessel are then sealed, and the transfer vessel containing the fuel, still immersed in heavy-water coolant, is moved to the spent-fuel pool. After about 45 days of cooling, an air transfer step is then used to move the fuel directly into the light-water pool environment.[5]

3. SAFETY TASKS

In general, safety goals and requirements for the ANS reactor are set by DOE orders, including DOE Order 5480.6[6] that mandates adherence to the NRC regulations of 10 CFR 100[7] (Reactor Site Criteria), to the General Design Criteria of Appendix A of 10 CFR 50,[8] and to the NRC standard format for safety analysis reports. This minimum set of applicable NRC requirements has been considerably widened by the general statement in DOE Order 5480.6 that DOE reactors must follow "...uniform standards, guides, and codes which are consistent with those applied to comparable licensed reactors."[6] Therefore, considerable effort was expended during this reporting period in the study of the safety goals and philosophies currently espoused by the NRC for new plants. Basically, it is our intent to anticipate the trend of NRC requirements for regulatory approval and to design the ANS reactor facility to meet those projected requirements. This should help ensure the acceptability of the ANS reactor design if review by the NRC or other outside agency should be required.

Major elements of the ANS reactor safety philosophy were developed and solid consensus reached among the ANS project staff; further review will be sought outside the project. Most basically, it was determined that a very high degree of protection should be provided for the public. To achieve this desired high degree of protection, it will be necessary to make the probability of a release very small and to provide containment of any radioactivity that could be released from the reactor as a result of an accident. ANS project management plan to use probabilistic risk assessment (PRA), starting early in the design of the reactor facility. This approach contrasts with the more common use of PRA only in the later stages of a reactor project i.e., after design and in many cases after construction. Greater assurance of safety and reliability will be provided by the ANS approach because even early decisions will be guided by the need to meet the requisite goals for limiting the probability of core damage or containment failure. This approach is inherently compatible with the USNRC

"Safety Goals for the Operations of Nuclear Power Plants" (51 FR 30028),[9] which states the desired safety characteristics of nuclear plants in terms of risk (probability x consequence). A contract has been placed with Brookhaven National Laboratory (BNL) to assist in the PRA effort, and work has begun. Progress in this area is discussed in Sect. 3.2.

To contain hypothetical accident releases, it is planned to house the ANS reactor and coolant system in a low leakage containment building. The expense of a tight containment, standard practice in U.S. power reactors, over a "confinement" concept is justified because it permits the achievement of very low risk consistent with the USNRC Safety Goals Policy. As discussed in Sect. 3.4, a sufficiently tight, but feasible, containment leakage specification will greatly reduce the territory covered by the reactor's LPZ. This reduction in the potential for radiation exposure to the population will be a major factor in showing that the ANS reactor complies with the regulatory requirements.

The process of defining functional requirements for safety-related systems was begun during this period and will continue throughout the entire design period. The first milestone is to contribute all needed safety requirements to the Conceptual Design Criteria to be issued prior to the beginning of the Conceptual Design (July 1988). This area is discussed in somewhat more detail in Sect. 3.1.

3.1 Development and Specification of Design Criteria for Safety-Related Systems

The progress realized during this period was the identification of applicable regulatory criteria that the reactor must meet; the selection of a means of choosing and categorizing anticipated events, design basis events, and emergency planning events; and an initial selection of candidate safety-related systems. The information comprises the document "ANS Functional Specifications for Safety-Related Systems",[10] a draft of which is currently (June 1987) undergoing internal review before a wider review. The document is intended to communicate essential safety

requirements and the safety philosophy to system designers during the design process.

3.2 Probabilistic Risk Assessment Task

A contract to perform PRA has been placed with BNL to use its experience and expertise in probabilistic risk analysis for the benefit of the ANS reactor facility. Initial meetings were held, and a plan for their work scope for the remainder of FY 1987 has been agreed upon. Because the ANS design is still in the pre-conceptual stage, the initial efforts will include a cursory macroscopic evaluation of potential initiating events, event sequences, etc., and a gathering of information that will be needed later in the PRA. Tasks for the remainder of FY 1987 will include:

1. review of the draft version of the functional requirements for safety-related systems document;

2. development of functional system models of ANS using failure modes and effects analysis, fault trees, or event trees;

3. development of a list of abnormal events and transients requiring special design consideration to achieve the risk and reliability goals;

4. development of prioritized lists of reactor systems based on each system's effect on safety and on reliability; and

5. initial review of system interaction and common mode potential.

3.3 Development of Computer Codes and Analytical Methods for Safety Analysis

The development and/or acquisition of calculational tools is essential for the ANS project because the safety analysis report must substantiate the ability of the plant to withstand a wide range of operational occurrences, accidents, and external events. Available industry-standard computer codes will be used where beneficial and feasible; however, it must be recognized that code development over the past 20 years has been largely directed toward power reactors. Some code development may be necessary because of the unique nature of a high-flux research reactor with

subcooled liquid coolant. Computer models are required for analysis of potentially severe accidents, including flow decrease, loss-of-coolant, and reactivity accidents. These models typically calculate the transient reactor response during the course of an accident.

The PARET computer code[11], developed at INEL for the analysis of reactivity accidents, has been obtained from ANL and made operational on the ORNL computer system. The test case with the code provided by ANL is a reactivity excursion for a small-core research reactor using thin plate-type fuel elements. This successful operation of the code with input for a thin plate-type fuel indicates that it should be feasible to apply the PARET code to the ANS reactor. The next step in the evaluation of the PARET code will be to prepare an input data set applicable to the HFIR reactor and to compare the results with previous HFIR calculations. The use of the existing PARET code for ANS analysis is desirable because PARET calculations have been compared successfully to the experimental results obtained in the SPERT reactor experiments and because considerable cost savings can be realized by using an existing code.

3.4 Containment Functional Requirements

The current plans for the 270-MW ANS reactor are to use, if acceptable, a site that is very close to the present HFIR location. A calculational study was undertaken during this reporting period to determine functional requirements that the containment would have to meet if the surrounding low-population zone (LPZ) were to be accommodated entirely on the DOE reservation at Oak Ridge.

The major conclusion of this study is that the containment for the ANS reactor should have a leak rate of 4%/d or less (well within the capabilities already demonstrated at other reactors) and that it should be provided with an effluent filtration system with an efficiency of at least 0.99 (which is well within the proven capabilities of the system now operating at the HFIR facility). The adoption of these functional performance

specifications would meet by more than a two-thirds margin the 10 CFR 100 limits for off-site radiation exposure, with the LPZ entirely on the DOE reservation, and should make it unnecessary for off-site personnel emergency planning to include evacuation even in the event of the maximum hypothetical accident.

3.4.1 Containment functional objectives

DOE Order 5480.6, dated September 23, 1986, requires that new DOE reactors meet the requirements of NRC regulation 10 CFR 100. This document requires that off-site radiation exposures must be acceptable for a hypothetical accident, postulated for analysis purposes, more severe than any credible accident. The maximum allowable exposures are defined as 25-rem whole-body dose and 300-rem thyroid dose over the first 2 h of the accident at any point along the Exclusion Area Boundary (EAB), or for the duration of the accident at any point on the outer boundary of the LPZ. The Exclusion Area is the zone surrounding the reactor that is under the physical control of the operator at all times. The LPZ, on the other hand, need not be controlled by the operator and may contain private property and residences. Plans for the ANS reactor are to design the containment such that even the LPZ can be located entirely within the DOE reservation at Oak Ridge and would therefore not involve any private property or residences.

Figure 25 illustrates the site presently considered for the ANS reactor. The EAB and the LPZ are both drawn as a circle of radius equal to 2.2 km, with center at the HFIR/TRU stack. The radius of 2.2 km was chosen as the distance to the nearest inlet of Melton Hill lake. The LPZ is chosen to be the same size as the Exclusion Area because of the design objective of keeping the LPZ entirely on the DOE reservation. Larger off-site releases would be allowed (e.g., at the 2.2-km EAB) if the LPZ were extended outward (e.g. the HFIR LPZ is 5.72 km), but to do so would include within the LPZ public segments of Anderson, Loudon, and Knox counties and possibly some residential sections of Roane County, which would sacrifice the safety licensing and emergency planning advantages of the smaller site.

ORNL-DWG 87-4205 ETD

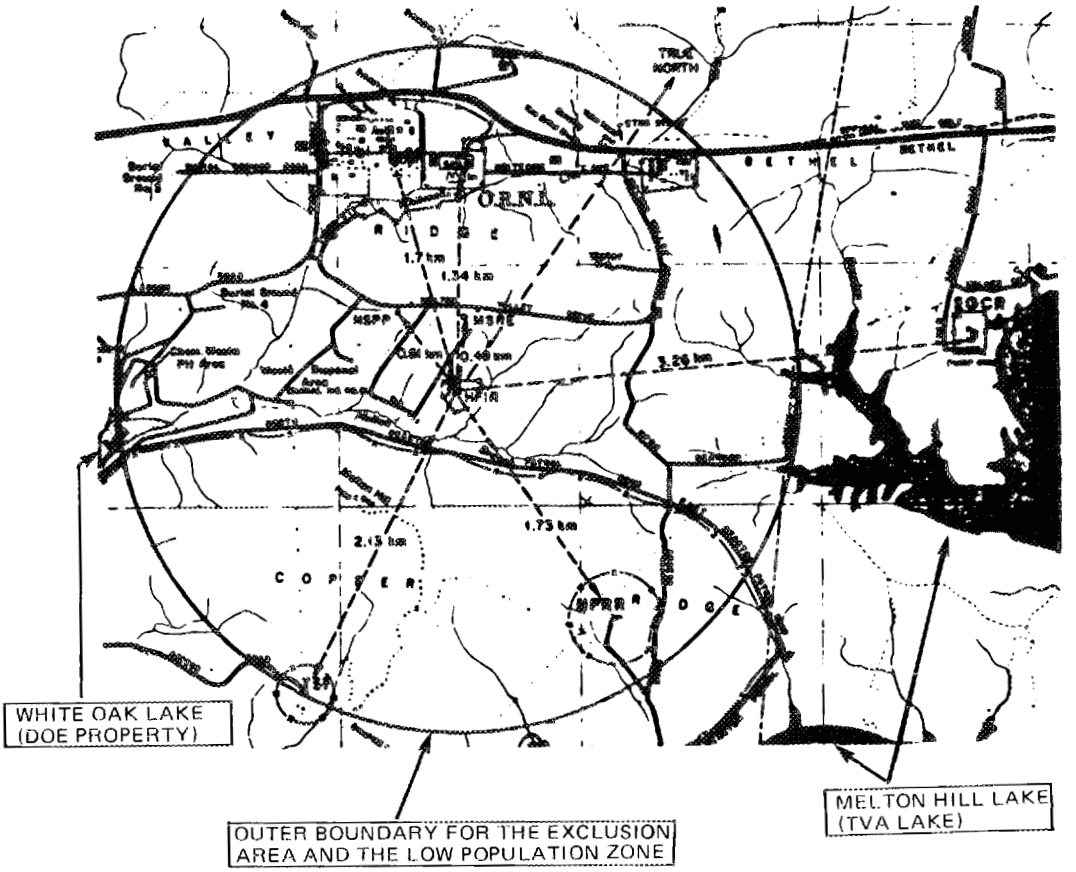

Fig. 25. Site boundaries for ANS reactor

To determine off-site exposures for the maximum hypothetical accident, each of the following calculations or determinations must be performed: (1) how much of each fission product escapes from the damaged fuel to the containment atmosphere; (2) how much of each nuclide in the containment atmosphere subsequently escapes from the containment to the environment; (3) based on meteorological conditions and the rate of release to the environment, what nuclide air concentrations exist at the receptor sites of interest; and (4) what radiation exposures would be incurred by an individual at the receptor site. Each of these four areas presents a formidable challenge. A computer code was written that calculates each of the four quantities to determine

the off-site radiation exposures. The computer code is described in the following section.

Simplifying assumptions have been used where justified and desirable, and in general the approach is a conservative one. The single, most significant simplifying assumption is provided by the suggestion in 10 CFR 100 to use the TID-14844 numbers[12] for the fractional release of each nuclide from damaged fuel to containment atmosphere: 100% of the core inventory of noble gases, 25% of the iodines, and 1% of all other radioactive fission products. This is, in effect, a definition of the maximum hypothetical accident. As explained in TID-14844, it is based on a postulated large-break loss-of-coolant accident with the assumed simultaneous failure of all reactor vessel injection systems and therefore involves the meltdown in air of the reactor core. Because the ANS reactor will have a pool of water around the reactor vessel, with a valving arrangement to admit water in the event of a loss-of-coolant from the vessel, the assumption of a dry meltdown is conservative.

The most important containment functions for off-site dose reduction are containment leak rate, removal of fission products from containment atmosphere before escape to the environment, and the efficiency with which fission products are filtered from the effluent that escapes from the containment. Because the ANS project is still at the preconceptual stage, precise containment system features have not been determined. Therefore, it was necessary to survey the parameter space by making many computer runs. As discussed in the results section, it was found that there are many practical combinations of these parameters that would lead to acceptable off-site doses. The acceptable combinations require a degree of containment leaktightness that has long been routinely achieved at other reactors.

3.4.2 Calculation model

This section describes the computer model and corresponding input data used to generate the results presented in this report.

The starting point for any calculation of off-site radiation exposures is the amount of fission product nuclides held within the fuel before the accident. The number of curies of each of the many fission products was obtained from an ORIGEN run.[13] The total list of nuclides was shortened by eliminating those present in relatively small quantity and those with a half life < 30 min. The short-lived radionuclides cannot contribute significantly to the total dose accumulation because only a fraction of the containment atmosphere escapes each day and radioactive decay removes the nuclides before they escape. Containment would have to fail catastrophically early in the accident if short-lived nuclides were to have a significant effect on total doses. The shortened list of 58 nuclides appears in Table 6, along with the half-life and number of curies of each immediately after shutdown from full power at the end of a complete operating cycle. This is the worst case for fission product accumulation and represents a conservative assumption of this analysis. Also indicated in Table 6 is whether each nuclide is part of a decay chain with parent or grandparent nuclides, with fractional branching ratios given where necessary. Information on the decay chain of each nuclide was taken from Kocher's handbook.[14] Utilization of the end-of-cycle fission product inventories is another conservative assumption.

The calculation is initialized by the assumption that the appropriate fraction of each nuclide escapes from the fuel at the beginning of the accident and is immediately dispersed uniformly into the atmosphere of the containment; a delay in dispersion would of course, reduce the total release because of radioactive decay. As mentioned in the introduction, the TID-14844 escape fractions were chosen for this analysis: 100% for noble gases, 25% for iodines, and 1% for all others.

Once a nuclide is dispersed into the containment atmosphere, it is assumed to remain there until either it undergoes radioactive decay, is removed from the containment atmosphere by an inherent fall-out process or by an installed in-containment air treatment system, or escapes by containment leakage. In addition,

Table 6. Nuclides considered in the calculation of off-site radiation exposures

NUCLIDE	HALF LIFE (H)	ACTIVITY (CI)	P	SP
BR82	35.300	0.650E+05	0.00	0.00
KR85M	4.480	0.267E+07	0.00	0.00
KR87	1.272	0.583E+07	0.00	0.00
KR88	2.840	0.819E+07	0.00	0.00
SR89	1213.200	0.194E+07	0.00	0.00
SR90	250500.000	0.118E+05	0.00	0.00
Y90	64.100	0.107E+05	1.00	0.00
SR91	9.500	0.132E+08	0.00	0.00
Y91	1404.200	0.200E+07	1.00	0.00
SR92	2.710	0.134E+08	0.00	0.00
Y92	3.540	0.133E+08	1.00	0.00
Y93	10.100	0.146E+08	0.00	0.00
ZR95	1536.500	0.205E+07	0.00	0.00
NB95	841.400	0.266E+06	1.00	0.00
ZR97	16.900	0.135E+08	0.00	0.00
MO99	66.020	0.138E+08	0.00	0.00
TC99M	6.020	0.121E+08	1.00	0.00
RU103	944.400	0.163E+07	0.00	0.00
RH103M	0.935	0.147E+07	1.00	0.00
RU105	4.440	0.254E+07	0.00	0.00
RH105	35.360	0.116E+07	1.00	0.00
RU106	8836.801	0.250E+05	0.00	0.00
CD115	1070.400	0.240E+05	0.00	0.00
SN125	231.400	0.200E+05	0.00	0.00
SB126	297.500	0.115E+04	0.00	0.00
SB127	92.400	0.283E+06	0.00	0.00
TE127M	2616.000	0.233E+04	0.17	0.00
TE127	9.350	0.244E+06	0.98	0.33
SB129	4.400	0.147E+07	0.00	0.00
TE129M	806.400	0.544E+05	0.17	0.00
TE129	1.160	0.137E+07	0.64	0.33
TE131M	30.000	0.834E+06	0.00	0.00
I131	192.960	0.447E+07	1.00	0.00
TE132	78.200	0.920E+07	0.00	0.00
I132	2.300	0.957E+07	1.00	0.00
TE133M	0.923	0.685E+07	0.00	0.00
I133	20.800	0.153E+08	1.00	0.00
XE133	125.900	0.107E+08	1.00	0.00
TE134	0.697	0.152E+08	0.00	0.00
I134	0.875	0.172E+08	1.00	0.00
CS134M	2.900	0.193E+06	0.00	0.00
CS134	18063.000	0.960E+04	1.00	0.00
I135	6.610	0.144E+08	0.00	0.00
XE135	9.110	0.154E+07	1.00	0.00
CS137	264300.000	0.123E+05	0.00	0.00
BA139	1.385	0.145E+08	0.00	0.00
BA140	306.900	0.760E+07	0.00	0.00
LA140	40.220	0.687E+07	1.00	0.00
LA141	3.940	0.133E+08	0.00	0.00
CE141	780.000	0.344E+07	1.00	0.00
LA142	1.590	0.138E+08	0.00	0.00
CE143	33.000	0.135E+08	0.00	0.00
PR143	325.400	0.546E+07	1.00	0.00
CE144	6823.000	0.418E+06	0.00	0.00
ND147	263.500	0.232E+07	0.00	0.00
PM148M	991.200	0.170E+04	0.00	0.00
PM148	128.900	0.697E+05	1.00	0.00

atoms of a given nuclide may be created even after the accident by radioactive decay of a parent nuclide suspended in the containment atmosphere. A simple, first-order differential equation is solved to calculate the number of atoms of each nuclide in the containment atmosphere as a function of time.

The rate at which each nuclide (except noble gas nuclides) escapes to the environment is taken to be proportional to the product of the number of nuclide atoms, the containment leak rate, and the fractional filtration inefficiency (i.e., one minus the efficiency). The noble gas nuclides are assumed to be unaffected by filtration, a conservative assumption because in fact some would be held up on the activated charcoal filters.

The three parameters that were varied to obtain the results of this study are the containment leak rate, the in-containment removal rate (removal of nuclides from the containment atmosphere while still inside the containment), and the effluent filtration efficiency. For analysis purposes, each parameter was assumed to remain constant throughout the accident, with the exception of several runs that were made to test the effect of a Grenoble-style containment that prevents any release at all until several hours have passed. For those few runs, the containment leak rate was held at zero for an initial period and then set at the applicable nonzero value for the remainder of the accident.

Having calculated the source term, in curies per unit time escaping from the containment into the environment, two steps remain in the calculation of radiation exposures: (1) the calculation of the radioactivity concentration in air at the receptor sites of interest and (2) the resultant radiation exposures. The transport of airborne radioactivity in the atmosphere depends on many factors, including the height of release, the period of time over which the accidental release occurs, the distances of travel to the receptor sites, and the degree of conservatism desired in the result. The height of release is conservatively assumed to be zero (ground level); that is, no credit is taken for the stack that will in fact be

installed. If the ANS reactor facility stack were similar to the HFIR/TRU stack, the off-site doses would be reduced by a factor of 2 or more.

For a release that occurs over a long period of time, there is more of a chance for wind shifts that tend to spread the plume over a broader scope of territory, resulting in lower concentrations at any particular receptor site. The effect of greater distance (i.e., a larger EAB and LPZ) would also be to reduce doses. Conservatism is built in, as desired, by choosing suitably pessimistic weather conditions to be in effect at the time of the accident. Generally, slower wind speeds and more stable atmospheric conditions lead to higher downwind concentrations.

The approach used for the atmospheric diffusion coefficients was to divide the time scale of the accident into five segments: 0 to 2 h, 2 to 8 h, 8 to 24 h, 1 to 3 d, and 3 to 30 d. The most pessimistic coefficient is used for the first 2 h, followed by a slightly less pessimistic coefficient for the 2- to 8-h time segment, and so on out to 30 days. This progression from worse to better values could mirror reality because the atmospheric conditions are typically worse early in the day but generally improve as the wind picks up later in the day and perhaps even shifts direction significantly. It is generally unnecessary to carry the calculation past 30 days because by that time almost all of the radioactivity has decayed, settled out in containment, or escaped and been dispersed past the point of interest.

The intended degree of conservatism for the present evaluation is to use atmospheric diffusion coefficients that would be exceeded in only a small fraction (~5%) of randomly selected initiation times. The help of ORNL Energy Division meteorologist F.C. Kornegay was enlisted to select the diffusion coefficients for each time segment. The technique he and Computing & Telecommunications programmer R.D. Sharp used was to search through a year's worth of data taken at the 30-m HFIR

meteorological observation tower to find the single 1, 8, 24-h and 30-d periods with the worst atmospheric dispersion conditions. The following dispersion coefficients were selected from Kornegay's results[15] for the proposed 2.2-km ANS Facility LPZ outer boundary radius (the use of these coefficients for calculating downwind concentration is explained below):

2.1×10^{-4} s/m^3 for the first 2 h,

0.9×10^{-4} s/m^3 for the 2- to 8-h period,

4.6×10^{-5} s/m^3 for the 8- to 24-h period,

1.8×10^{-5} s/m^3 for the 1- to 3-d period, and

3.9×10^{-6} s/m^3 for the 3- to 30-d period.

These values, based on actual measurements, are in substantial agreement with the dispersion coefficients that one can calculate from the cookbook approach of NRC Regulatory Guide 1.3 or 1.4.[16]

The concentration of a given nuclide at a receptor site is calculated from the diffusion coefficient as follows:

$$C(i,j) = S(i)\ ADF(j,k),$$

where

$C(i)$ = concentration of the *i*-th nuclide (ci/m^3)

$S(i)$ = source term (ci/s) for the *i*-th nuclide, and

$ADF(j,k)$ = atmospheric dispersion coefficient (s/m^3) for the *j*-th receptor during the *k*-th time segment.

Having calculated the concentration of each nuclide at each of the receptor locations, the corresponding dose rates can be calculated. Because the present study is primarily aimed at the criteria of 10 CFR 100, only the whole-body (external exposure due to absorption of gamma rays) and the thyroid doses (due to inhalation of the radioiodine isotopes and subsequent absorption into the blood stream and concentration in the thyroid gland) are calculated. These two exposures, one external and one internal, form an index of how well the reactor containment systems are able to control the consequences to individuals at the receptor sites. More sophisticated analyses planned for the future will include other critical organs such as the lungs and bone marrow.

The whole-body exposure rate at the *j*-th off-site receptor is given by the following formula:

WBE(j) = :sum over all i of: C(i,j) DCFWB(i),

where

DCFWB(i) = dose conversion factor (rem per hour/ curie per cubic meter) for the *i*-th nuclide.

Dose conversion factors for whole body exposure were taken from the compilation by Kocher.[17] The whole-body doses off-site are usually dominated by the noble gases; however, all 58 nuclides of interest are included in the calculation.

The calculation of thyroid exposure is a little more complicated than the whole-body exposures, because proper consideration must be given to the breathing rate. The highest breathing rate is specified for the first 2 h of the accident, when activity levels must be assumed to be elevated. The dose conversion factors used for this study are 40-year dose commitments for the inhalation of a given amount of iodine nuclide (only the iodines were considered because the relative contribution of other nuclides is orders of magnitude smaller). The thyroid exposure rates are calculated as follows:

THY(j) = :sum over all i of: C(i,j) BR(k) DCFTHY(i),

where

THY(j) = thyroid exposure rate for the *j*-th receptor site,

C(i,j) = concentration of the *i*-th nuclide at the *j*-th site,

BR(k) = breathing rate for the *k*-th time segment,

DCFTHY(i) = 40-year dose commitment (rem) per inhaled curie of the *i*-th nuclide.

The breathing rates were taken from the American Nuclear Society standard for site evaluation for research reactors:[18]

for 0 to 2 h: BR(1)= 3.33×10^{-2} m^3/s

2 to 24 h: BR(2)= 2.58×10^{-2} m^3/s

>24 h: BR(3)= 2.64×10^{-2} m^3/s.

The dose commitment factors for the radioiodines were taken from the compilation of Dunning et al.[19]

3.4.3 Analysis results

An early finding of the calculations was that even a very tight containment would not, without iodine removal, provide sufficient thyroid dose reduction at the proposed 2.2-km LPZ distance following the maximum hypothetical accident. For example, a containment with a 0.25%/d leak rate but without any iodine filtration or removal would limit the whole-body dose on the LPZ to a desirably low 0.62 rem, but it would allow a thyroid dose of 158 rem, which would be uncomfortably close to the 300-rem limit specified by 10 CFR 100. Therefore, most of the calculations reported in this section include effluent filtration and/or in-containment removal for containments of various degrees of leaktightness.

Containment leak rates of between 0.25%/d and 22.5%/d were examined. Leak rates higher than 22.5%/d would not, in any case, be permissible because the escape of noble gases (assumed to be unaffected by filtration or sprays) would lead to excessive whole-body exposures along the 2.2-km radius LPZ outer boundary. The lower limit of 0.25%/d extends the calculation to the lower limit of practicality for large containments, as exemplified by the 0.25%/d containment building described in the Final Safety Analysis Report (FSAR) for the Calvert Cliffs 2560-MW pressurized-water reactor[20]. Several other reactors have been approved with containment leak rates about one order of magnitude higher: the primary containment of the Browns Ferry 3200-MW boiling water reactor meets a 2%/d maximum leak rate specification, and the containment building of the 40-MW High Flux Beam Reactor (HFBR) at BNL meets a 5%/d specification.

Effluent filtration efficiencies between about 0.50 and 1.00 were considered. As defined in this report, a filtration efficiency is the fraction of the nuclides in the effluent that remains in the filter and thus does <u>not</u> escape to the environment. The lower end of the range (efficiency near 0.5) represents an unrealistically low filter system efficiency system -- 0.95 or

better would be more typical. An overall effluent efficiency of 0.5 could, however, be realized if part of the effluent bypassed the filters. The HFIR reactor air treatment system (charcoal and absolute filters) meets a technical specification of 0.995 efficiency; the in-house ORNL procedures actually applied at the HFIR require that filters be changed when the measured efficiency slips below 0.9985. In this investigation it was assumed that the same efficiency applies to the radioiodines and all other nuclides, except the noble gases, which are assumed to be totally unaffected by filtration (even though a small amount of the noble gases would in fact be retained on the charcoal).

In-containment removal rates of between 100%/d and 1600%/h were investigated in the parameter study. The lower rate might be representative of the natural settling out from containment atmosphere onto walls and floors that a fission-product-bearing aerosol would undergo, and the upper removal rate would represent a well-designed, high-volume, in-containment air treatment or spray system. The same removal rate is applied to all nuclides, except the noble gases, which are again assumed to be totally unaffected by the removal process. As used in the model, these rates are a measure of the rate of removal from containment atmosphere in terms of percent per unit time of the nuclide inventory in the atmosphere at any given instant.

The results of the parameter study show in general that the whole-body exposures (absorption of gamma radiation due to the immersion of the body in a semi-infinite cloud of gamma emitter) are dominated by the gamma radiation from the noble gases. This is primarily because of the basic assumption that the accident causes the escape from the fuel of <u>all</u> of the noble gases, but only 25% of the iodines and 1% of all other nuclides.

Most of the whole-body dose accumulation occurs over the first 24 h of the accident, because the noble gas nuclides that have the highest energy gammas also have the shortest half-lives. For example, Krypton-88 emits a 1.95-MeV gamma but has a 2.84-h half-life and is therefore essentially gone after 24 h. The thyroid

doses accumulate at a more sustained rate over the whole 30-d period covered by the calculations because of the longer half-lives of the dominant iodine isotopes (e.g., Iodine-131 has an 8-d half-life).

Figures 26 and 27 illustrate the accumulation of whole-body and thyroid doses over the 30-d accident period for 1, 5, and 20%/d containment leak rates. The accumulated doses are shown at

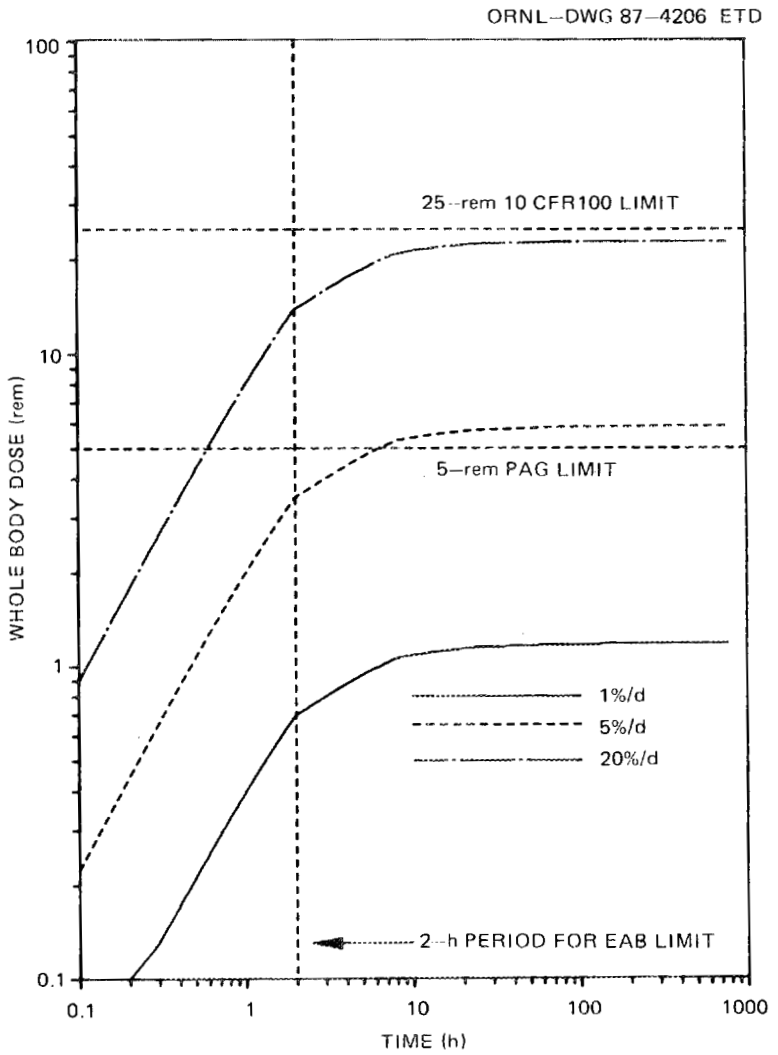

Fig. 26. Maximum hypothetical accident whole-body dose accumulation at 2.2-km LPZ distance (containment leak rate = as indicated; fractional effluent filtration efficiency = 0.99)

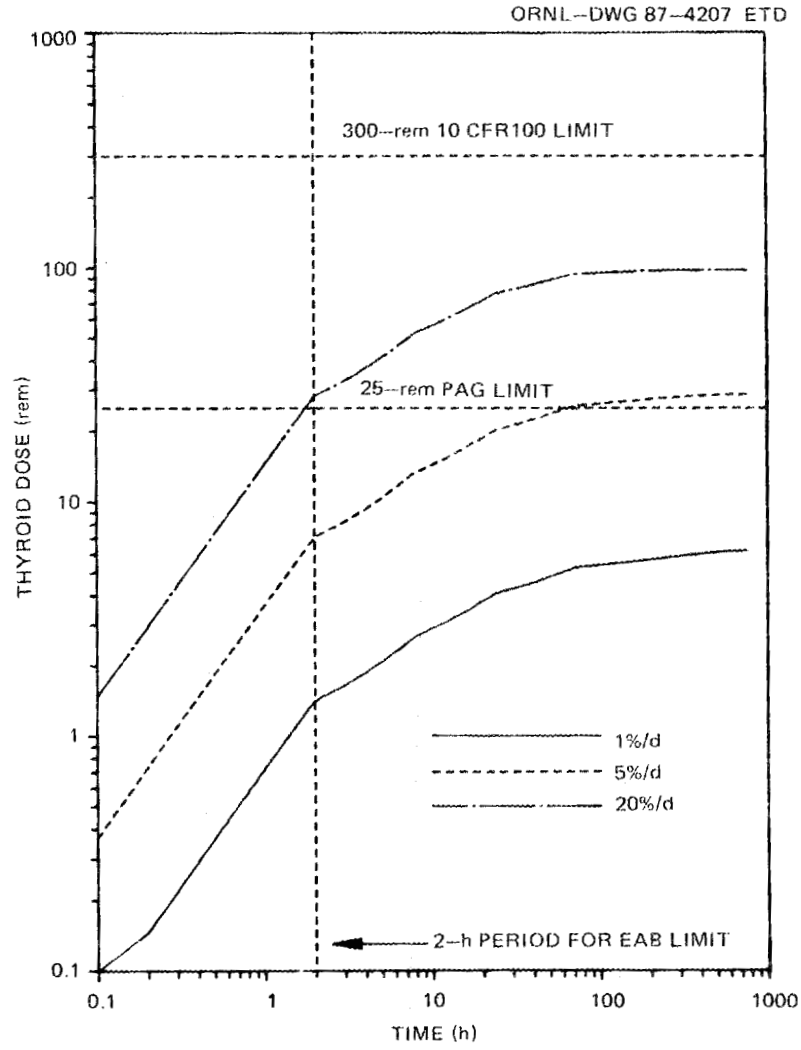

Fig. 27. Maximum hypothetical accident thyroid dose accumulation at 2.2-km LPZ distance (containment leak rate = as indicated; fractional effluent filtration efficiency = 0.99)

the 2.2-km radius of the LPZ outer boundary proposed for the ANS reactor. For these calculations, the efficiency of effluent filtration is taken at 99%, and there is no in-containment nuclide removal.

3.4.3.1 Filtration Only (no in-containment removal). Figure 28 summarizes the results of a series of calculations with various degrees of effluent filtration efficiency and containment leak rate. The top curve on Fig. 28 is the locus of combinations of

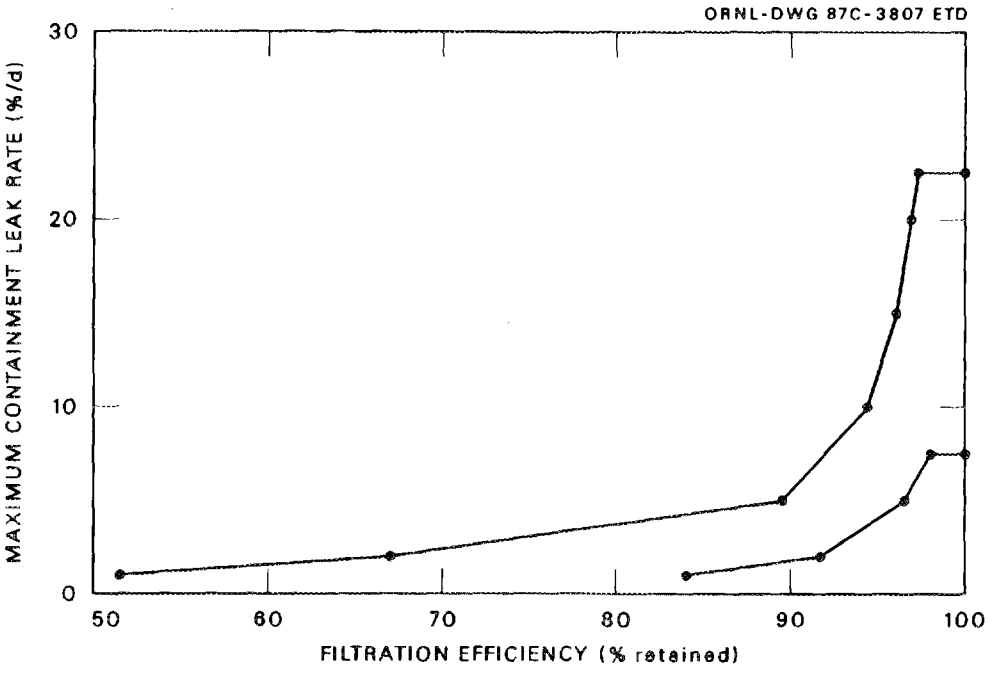

Fig. 28. Combinations of containment leak rate and effluent filtration efficiency that exactly meet 100% (upper curve) or 33 1/3% (lower curve) of 10 CFR 100 limits for maximum hypothetical accident radiation exposures

containment leak rate and effluent filtration that exactly meet but do not exceed either the 25-rem whole body limit or the 300-rem thyroid dose limit of 10 CFR 100. Most of the points along this curve were actually determined by the thyroid limit. However, the whole-body exposure is limiting in some cases because even with perfect filtration (efficiency = 1.0) the containment leak rate must not exceed 22.5%/d in order to satisfy the whole-body exposure limits. All combinations below the top curve would meet the nominal requirements of 10 CFR 100.

Because past regulatory positions have demanded that site suitability studies show doses substantially below the 10 CFR 100 limits, another curve is shown on Fig. 28. The lower curve is the locus of leak rate and efficiency combinations that meet but do not exceed one-third of the 10 CFR 100 limits--i.e., 0.33 x 25 or 8.33-rem for whole-body dose and 0.33 x 300 or 100-rem for thyroid

dose. The shape of this lower curve is similar to the upper one, but the maximum allowable containment leak rate is 7.5%/d with perfect filtration. No combinations below the lower curve would exceed one-third of the nominal 10 CFR 100 limits. One example point on the lower curve is a case with a containment leak rate of 5%/d and a filtration efficiency of 0.965. In this example, the corresponding 30-d whole-body dose at the 2.2-km LPZ distance is 6 rem and the thyroid dose is 100 rem. Thus, the thyroid dose, at 100 rem, is controlling because the whole-body dose of 6 rem is well below the target dose of 0.33 x 25 or 8.33 rem.

3.4.3.2 In-containment removal (no filtration). Figure 29 summarizes the results of a series of calculations with various degrees of (unfiltered) containment leak rate and in-containment removal. Combinations along the upper curve exactly meet the nominal 10 CFR 100 limits and those along the lower curve exactly

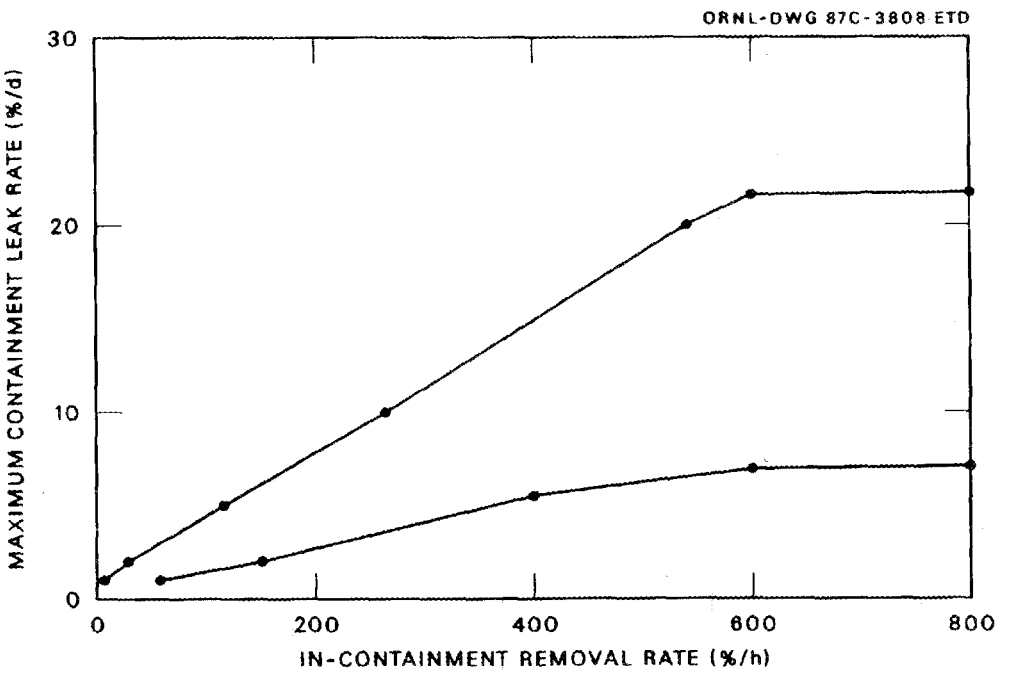

Fig. 29. Combinations of containment leak rate and in-containment removal rate exactly meet 100% (upper curve) or 33 1/3% (lower curve) of the 10 CFR 100 limits for maximum hypothetical accident radiation exposures

meet one-third of the limits. For the upper curve the 300-rem thyroid dose is controlling for containment leak rates below 22.5%/d and the 25-rem whole-body dose limit makes leak rates above 22.5%/d unacceptable regardless of in-containment removal. The region of acceptable performance is found below the curve for each case.

3.4.3.3 Removal and filtration. Calculations were performed over a range of containment leak rates to determine the usefulness of a 100%/d in-containment removal rate in conjunction with an effluent filtration efficiency of 0.99. The results, plotted on Fig. 30, demonstrate a substantial potential reduction in thyroid dose compared with the same cases without in-containment removal; the reduction of whole-body doses is minimal and therefore not

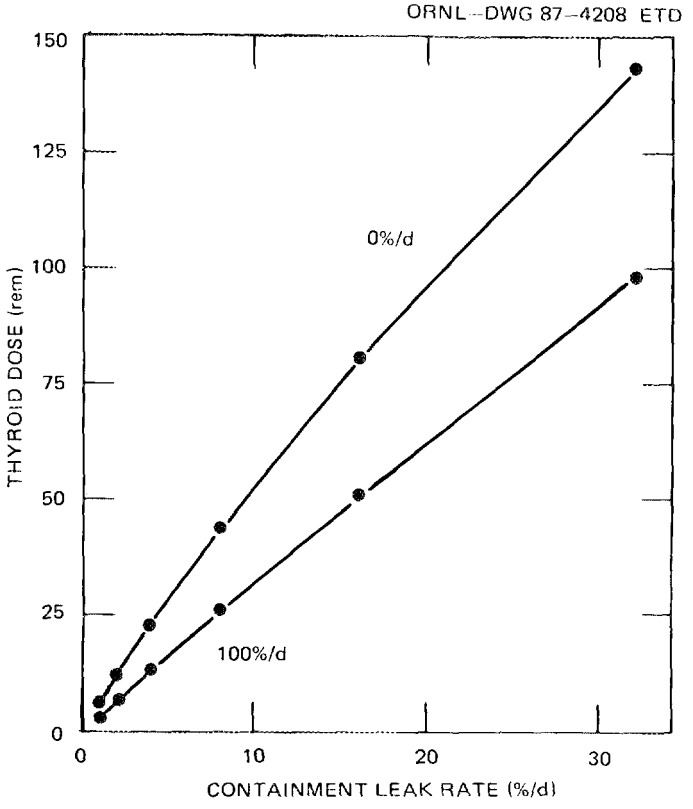

Fig. 30. Effect of 0%/d and 100%/d in-containment removal rates on 30-d thyroid dose accumulation received at 2.2-km LPZ distance following the ANS maximum

included on Fig. 30. The assumed 100%/d in-containment removal rate could be representative of either a low-capacity installed system (e.g., a low-volume containment spray system) or simply of natural settling-out processes.

3.4.3.4 Delayed release. The containment concept of the 57-MW ILL reactor at Grenoble, France, inspired another series of runs. In that series, the code input simulates the double-containment system at Grenoble, with the outer containment pressurized with respect to the inner containment by blowing ambient air into the space between the inner and outer containments. According to the assistant reactor department chief at ILL, Dr. E. Bauer,[21] the ILL safety analysis demonstrates that following the maximum hypothetical accident, there would be a slow increase in inner-containment pressure, but the outer-containment pressure would remain above inner-containment pressure; therefore, significant releases would not begin until after 12 h: even those releases would be filtered effluent.

A series of calculations was made in which the containment was assumed not to leak until 4, 8, and 12 h after the beginning of the accident. In-containment removal was taken to be zero, effluent filtration at 99%, and two containment leak rates were examined, 2 and 10%/d.

The results (Fig. 31) show that delaying the onset of the release has the potential to reduce the whole-body exposures by almost an order of magnitude. This advantage is gained because of decay of the dominant radioactive noble gas nuclides. Figure 31 shows reductions by a factor of about 2 for the thyroid exposures, but this is solely because the computer code applies less pessimistic atmospheric dispersion factors and individual breathing rates at longer times after accident initiation. In actuality, the delay would reduce off-site thyroid exposures because of natural in-containment settling-out processes not included in these calculations.

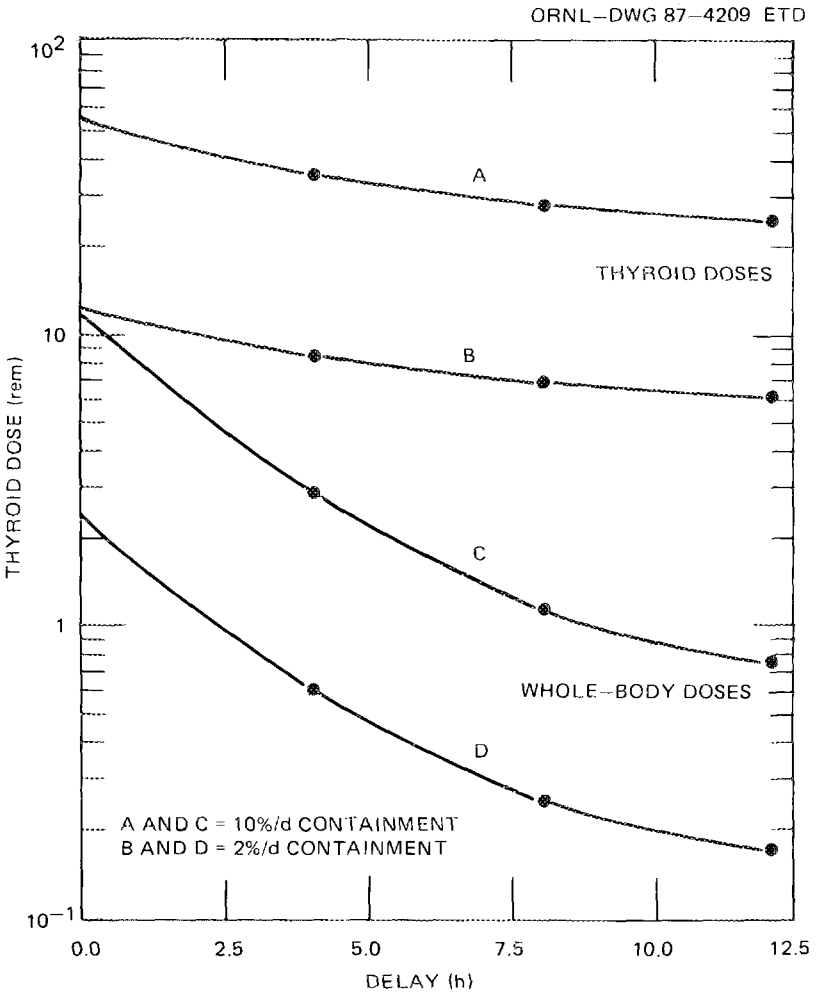

Fig. 31. Effect of delay in onset of release on 30-d thyroid and whole-body dose accumulations received at 2.2-km LPZ distance following the ANS maximum hypothetical accident

Even if the ILL style containment is not selected for the ANS reactor, a more mechanistic analysis of the pressure build-up within containment would show that it takes some time, perhaps hours, to reach the peak release rates. This gradual buildup in release rate would approximate the delay considered here and would result in lower off-site radiation exposures.

3.4.4 Implications for design

The specification of a low (less than ~ 5%/d) containment leak rate has some obvious implications for containment design. For

example, all cracks will have to be eliminated or sealed by tight gaskets, because even a short length of open crack would cause such a low leakage specification to be exceeded even for low internal pressures. The specification of a high effluent filtration efficiency implies that the effluent air treatment include at least one stage of a special iodine treatment, such as the activated charcoal filters incorporated in the HFIR ventilation system.

The specification of a maximum leak rate cannot, at present, be directly translated into a containment design pressure specification, because the rate of gas generation during hypothetical severe accidents has not yet been reliably estimated for the ANS reactor. If an assumption is made that the 4%/d maximum leak rate is to be applied, for example, at an internal gauge pressure of 0.014 MPa (2.0 psig), containment design could proceed; but then a later analysis might show that the accident gas generation and expansion could pressurize the containment to above the 2.0-psig reference pressure and thus cause the resultant leak rate to exceed the rate assumed for the site suitability analysis. On the other hand, it would be possible to specify that the maximum leak rate applies at <u>any</u> containment pressure. But this would leave unknown and unspecified the containment internal design pressure. Until a good estimate of severe accident gas generation and expansion rate is available, the containment design pressure cannot be set with any certainty. Future investigations are planned to develop this much needed information.

3.4.5 Implications for emergency planning

The Environmental Protection Agency (EPA) Protective Action Guidelines (PAGs) for emergency planning[22] specify that emergency personnel should strongly consider evacuation if doses to members of the general public are likely to exceed 5 rem to the whole body or 25 rem to the thyroid. Sheltering is to be considered if doses are likely to exceed 1 rem to the whole body and 5 rem to the thyroid. Because these dose limits are much lower than the

nominal 10 CFR 100 limits, they may be considered the limiting factor for containment design consideration. The containment functional performance specifications of 5%/d and 97% filtration efficiency suggested by these calculations were based on the higher limiting doses of 8.33-rem whole-body dose and 100-rem thyroid dose (i.e., one-third of the nominal 10 CFR 100 limits). Therefore, a prudent step would be to improve the functional containment performance requirements from 5%/d to 4%/d maximum leak rate and from 0.97 to 0.99 effluent filtration efficiency. This would bring the presently estimated maximum hypothetical accident doses to below the upper PAGs for evacuation.

Further reduction in estimated doses may follow improvement in the calculation and knowledge of the probable severe accident response of this reactor; this work will be undertaken at an appropriate, but later, time. Specification of leakage and filtration requirements to meet the lower (sheltering) PAG limits is not recommended until more is known about the severe accident response and about containment design options. However, it will be recalled that the calculational results reported in Sect. 3.4.3.4 for the ILL double containment (for which there would be a 12-h delay after initiation of the maximum hypothetical accident before the beginning of release to the environment) show promise for reduction of whole-body doses to below the lower PAG limits. Similar containment designs should be investigated for the ANS reactor.

Specification of containment leaktightness of 0.25%/d along with highly efficient iodine removal would practically guarantee that the LPZ exposures for the maximum hypothetical accident would not exceed the lower PAGs, but the need for such stringent specifications cannot be fully evaluated at present.

3.4.6 Containment analysis conclusions

The major conclusion for this study is that the containment for the ANS reactor should have a leak rate of 5%/d or less and that it should be provided with an effluent filtration system with

an efficiency factor of 0.97 or better to meet the requirements of 10 CFR 100. An in-containment removal system of 400%/h capability would be roughly equivalent to the 0.97 filtration efficiency and could be substituted for the effluent filtration. The adoption of these functional performance specifications would meet by a comfortable two-thirds margin the requirements of 10 CFR 100 with the EAB and the LPZ entirely on the DOE reservation and ensure one very major aspect of the suitability of the present HFIR site for the 270-MW ANS reactor.

It is further concluded that because of emergency planning considerations we may choose to adopt containment requirements even more stringent than would be required for compliance with 10 CFR 100. How much more stringent cannot presently be stated with certainty, but a 4%/d maximum leak rate and a 0.99 minimum filtration efficiency (or equivalent in-containment iodine removal) would represent the least restrictive requirements that should be adopted for emergency planning purposes.

3.4.7 Recommendations

The design goal for containment for the ANS should be to have as tight a containment as practicable and one that is provided with a highly effective means for iodine removal. As discussed above, a design goal for maximum containment leak rate of 4 %/d can presently be justified. The corresponding goal for iodine removal would be an efficiency of 0.99 if implemented as an effluent (or containment leakage) treatment or 1300%/h removal rate if implemented as an in-containment removal system.

The calculations described in this report need to be strengthened with more mechanistic treatments of all phases of the hypothetical severe accidents of interest, including the cooling of the core debris from postulated severe accidents; the generation of steam and/or noncondensibles including hydrogen; the heat-up and pressurization of the containment atmosphere; fission product plate-out and removal from the containment atmosphere; and the leakage of fission products from the containment to the

environment. Concurrently, actual containment designs should be selected and evaluated as the improved calculational models become available.

4. CONCEPTUAL DESIGN TASKS

Preparation for the conceptual design falls into two categories: planning for the architect-engineer (AE) to generate the conceptual design for the major construction packages and planning for ORNL teams to generate the conceptual design for key reactor and experiment hardware.

Several tasks must be completed prior to initiation of the facility conceptual design by an AE firm: site selection, generation of conceptual design criteria, and the AE selection process. Although these tasks were originally planned for FY 1987, funding limitations and priorities given to execution of the R&D plan have deferred them until early in FY 1988. Thus, there will be no significant progress on activities directly supporting the AE conceptual design effort this year. Much of the planning conducted under project support, as well as the BOP activities under the R&D plan, will contribute to the timely execution of those activities next year.

4.1 Main Construction Contracts

This activity is not scheduled to begin until FY 1988.

4.2 ORNL Retained Reactor

At this time no significant planning for the reactor conceptual design activities assigned to ORNL has taken place. Again, however, work currently under the R&D plan will support development of teams and criteria for the ORNL conceptual design tasks.

4.3 ORNL Retained Experiments

No significant planning for the conceptual design of scattering, irradiation, and other experiment hardware assigned to ORNL has taken place. Work currently under the R&D plan will support development of teams and criteria for the ORNL conceptual design tasks.

4.4 Systems Integration

Attention was given to identifying tasks and milestones for safety, environmental, and other assessment activities as part of

the overall scheduling and cost compilation effort. However, early work in these areas has been considered under safety rather than systems integration and is reported in Sects. 3.1, 3.2, and 3.4. Thus, there is no significant work to report under the category of systems integration.

5. PROJECT SUPPORT

Project support covers the managerial and administrative activities necessary for planning and executing the ANS project. The material covered in this section falls into a single task in the preconceptual plan. Several key activities have been initiated during the last 6 months and are reported as sections below. These activities include development of an initial version of the project work breakdown structure (WBS), and development of project schedules and cost estimate data.

5.1 Work Breakdown Structure

The WBS to be used for managing the design and construction of the ANS was revised during this reporting period. The top level of the WBS is shown in Fig. 32, and further breakdowns are shown in the Appendix B. The initial box in the WBS covers the entire ANS project, including capital and expense-funded activities, and all activities from design and construction to assessments and project administration. The second level is composed of seven elements. Technology development includes the list of items appearing in the current R&D plan. Project support covers the ANS Project Office itself. All activities presently under way fall into one of these two categories. Elements 1.3, 1.4, and 1.5, which have not yet begun, cover the actual conceptual and detailed designs and the construction of the ANS. Element 1.3 is broken into three major design and construction contracts, with design and construction management by AE firms. Elements 1.4 and 1.5 cover those reactor and experiment design and procurement activities under ORNL control because of their unusual nature and their high importance to safety. Element 1.6 includes safety, assessment, and integration activities that will continue for the duration of the project (current safety studies are considered a part of R&D, as element 1.1.9.) Element 1.7 will include operations up to placing the facility into routine operation.

This WBS will be considered a "living document" and will be revised as the need arises. Although generally oriented toward managing funding throughout the project the WBS is particularly

ORNL–DWG 87–4226 ETD

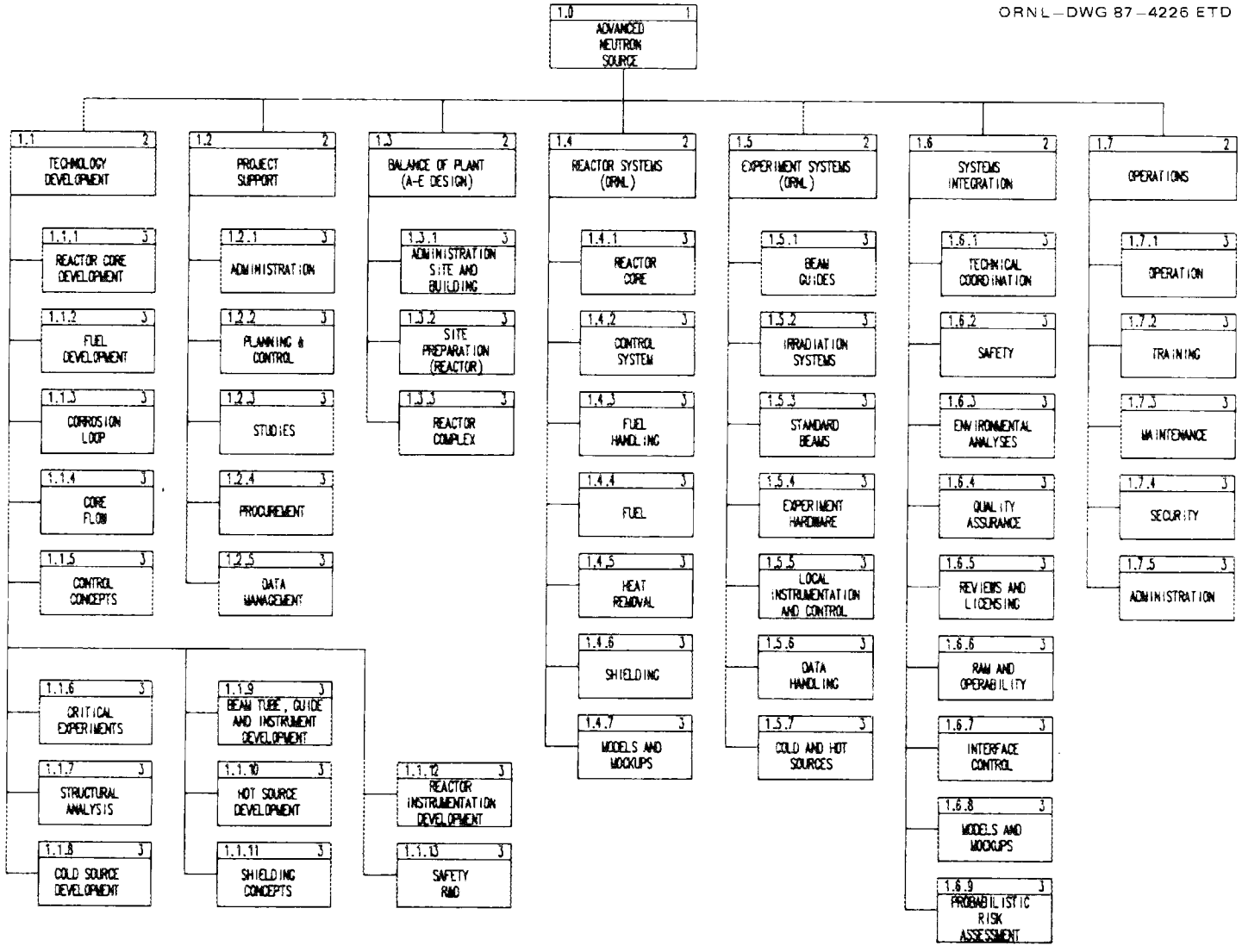

Fig. 32. Top level of WBS

oriented toward the design and construction of buildings and hardware. Other types of breakdown, such as by functional system, will be developed as needed for activities such as safety studies and risk assessments.

5.2 Schedule

A major review of the schedule assumptions for the overall ANS project was made during this reporting period. Major milestones for each main phase of the project were reviewed against the standard DOE line-item sequence, NRC-type licensing requirements, and experience with other major projects. A revised overall schedule was generated as shown in Fig. 33. The early years are driven by funding availability, execution of the R&D plan to provide a reasonable basis for design, and the steps needed to bring an AE firm on board for the facility conceptual design.

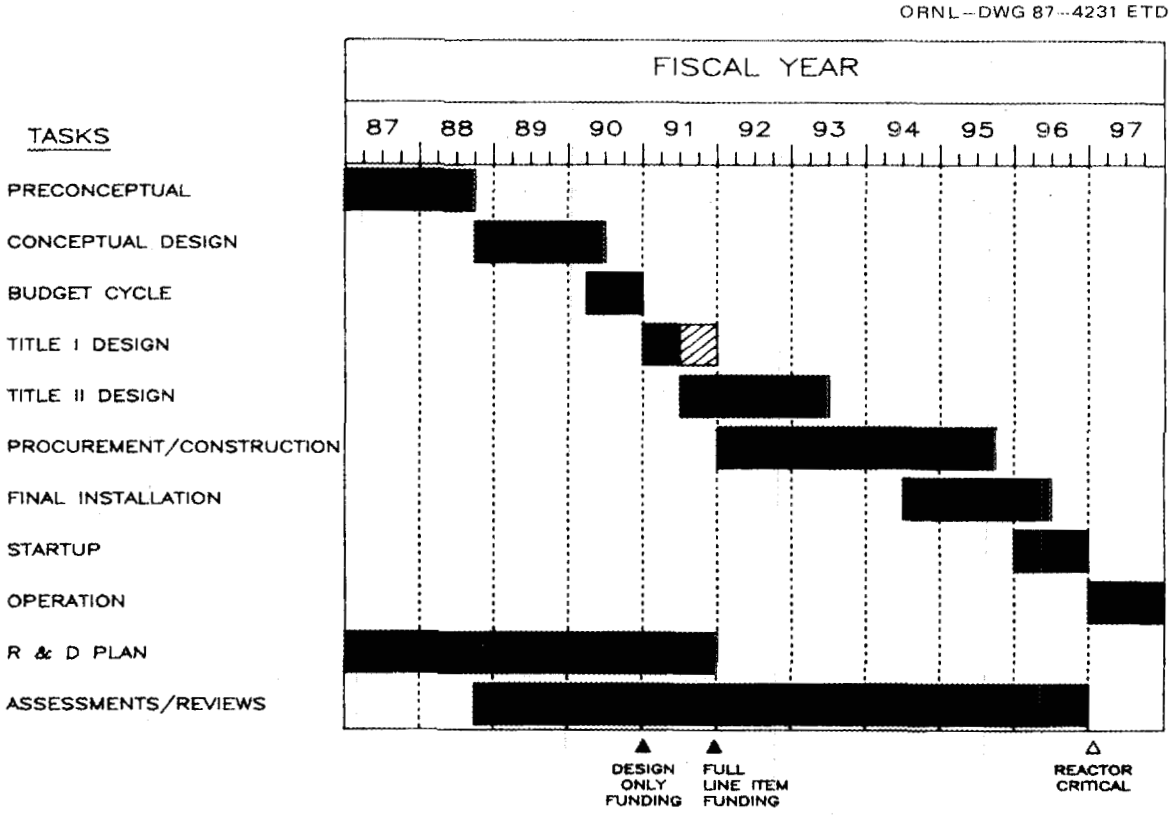

Fig. 33. Summary schedule for the ANS Project

Because the drafting of AE design criteria and the AE selection process will not begin until FY 1988, the earliest the facility conceptual design by an AE can now begin is the last quarter of FY 1988. The conceptual design could then be completed and the construction data sheet submitted in second quarter FY 1990, as required for a FY 1992 line item. A "design-only" line-item request will be used to fund Title I and some initial Title II design work in FY 1991, avoiding a 1-year delay resulting from the budget cycle between conceptual design and the FY 1992 line-item authorization for design and construction of the facility.

Although formal licensing by the NRC is not presently required for DOE-operated reactors, all documentation required of NRC licensees will be generated for the ANS, as required by DOE Order 5480.6 (see Sect. 3.0). This provides major milestones in the schedule for generation of construction permit documentation and the documentation used to apply for DOE permission to operate the reactor. Integrating these documents into the DOE project cycle places a milestone for the construction permit documentation at the end of the Title I design phase. At that time, an NRC-style Preliminary Safety Analysis Report (PSAR) and other documentation will also be required. The schedule shown in Fig. 33 allows for a 6-month review period between completion of the construction permit documentation and start of site work. Title II design, procurement and facility construction begins with line-item authorization in FY 1992 (with initial Title II design, particularly on site preparation, beginning 6 months earlier under design-only, line-item funding) and runs through FY 1994. At the end of FY 1994, the operating permit documentation will be submitted to DOE for the necessary reviews. A 1-year period, during which final installation of reactor equipment will take place, is allowed for review of this submission. The FSAR and final environmental documentation is required at the end of FY 1994 as part of the final package submitted to DOE. Permission for low-power testing would be needed at the beginning of FY 1995,

with startup and testing extending through that year. This schedule assumes sufficient progress in startup to close the construction phase and enter the operations phase by the end of FY 1995. Specific criteria for project completion remain to be identified.

Further breakdown of the baseline project schedule according to the top-level WBS was entered into a PC-based scheduling program. Output from this program is included in the appendices. Use of the computer-aided scheduling package allows ready tracking and revision to the schedule and also allows input and tracking of cost estimates as they become available.

5.3 Costs

Along with the schedule review discussed above, an effort was made to compile and escalate the most current known estimates for all activities associated with the ANS project. Estimates were entered into the computer-aided scheduling package, and a table of costs in current-year dollars by fiscal-year quarter was generated. The DOE escalation factors given in the Oak Ridge Operations Office (ORO) Estimating and Cost Control Manual[23] were then used to escalate the estimate to the year of expenditure. Both the current-year dollar and escalated versions of the overall estimate were then tabulated by fiscal year.

In the case of the design and construction of the facility, the primary basis for the estimate was the feasibility study generated in FY 1984. Cost-vs-power curves generated early in FY 1985 were used to bring the feasibility study estimate, which was for a 200-MW reactor, up to an estimate for the current baseline of a 270-MW reactor. Costs were then escalated to second quarter, FY 1987 for "current-dollar" estimates. Costs for activities covered by the R&D plan were covered by entering the R&D plan data directly into the current-dollar estimate base. Costs for the ANS Project Office and for manpower during startup were obtained by estimating staff size and using current rates in the unescalated version. Heavy-water costs for the reactor were based on the

recent purchase price of heavy water for the corrosion test loop. Costs for the various assessments were based on discussions with persons experienced in similar activities, although the cost for NRC-type reviews is difficult to predict. Some of the weakest points in the existing estimates are in the areas of hardware to be designed and procured by ORNL, such as the reactor control system.

This estimate review was done as an independent activity and was not directly factored to take budget documents currently in preparation into account. Work on bringing the estimates into agreement with the current project planning base is continuing. Until revised estimates are available from future design and planning work, the only method for bringing this estimate and official budgets into agreement is to adjust schedules. This task provides a tool for explaining the schedule loss that will be encountered if requested funding is not provided. Since a computerized system is being used, revised estimates and schedules can readily be incorporated in a timely manner.

REFERENCES

1. C. D. West et al., "Center for Neutron Research Project Status Report", ORNL/TM-10065, Oak Ridge National Laboratory, September 1986.

2. TK Solver Plus, Universal Technical Systems, Inc., Copyright 1987.

3. P. Ageron, R. Ewald, H. D. Harig, and J. Verdier, "The Cold Neutron Source for the High-Flux Franco-German Reactor at Grenoble", ORNL-tr-5085, [Translated from the French, ENERGIE NUCLEAIRE, vol. 13, no. 1 (Jan-Feb. 1971), pp. 1-7]

4. "Feasibility Study for the High Flux Isotope Reactor II", X-OE-265 (an internal ORNL document), Oak Ridge National Laboratory, September 1984.

5. C. A. Flanagan, "Report of Foreign Travel to Grenoble, France", ORNL/FTR-2475, Oak Ridge National Laboratory, December 1986.

6. U.S. Department of Energy Administrative Order No. 5480.6, Safety of Department of Energy-Owned Nuclear Reactors, Assistant Secretary for Environment, Safety, and Health, (September 1986).

7. Code of Federal Regulations, Title 10, Part 100.

8. Code of Federal Regulations, Title 10, Part 50.

9. U.S. Federal Register, Volume 51, page 30028.

10. C. A. Flanagan and R. M. Harrington, "Advanced Neutron Source (ANS) Safety Related Functional Requirements", (To be published).

11. C.F. Obenchaih, PARET--A Program for the Analysis of Reactor Transients, IDO-17282 (1969).

12. Technical Information Document 14844, March 23, 1962.

13. R.T. Primm, III, ORIGIN code calculation dated November 25, 1986.

14. D.C. Kocher, "Radioactive Decay Data Tables", DOE/TIC-11026, 1981.

15. Internal memos, F.C. Kornegay (ORNL) to R.M. Harrington (ORNL): "Preliminary CNR Results", December 16, 1986 and January 20, 1987.

16. USNRC Regulatory Guide 1.3, "Assumptions Used for Evaluating the Potential Radiological Consequences of a Loss of Coolant Accident for Boiling Water Reactors", June 1974 (Rev. 2).

17. D.C. Kocher, "Dose-Rate Conversion Factors for External Exposure to Photon and Electron Radiation from Radionuclides Occurring in Routine Releases from Nuclear Fuel Cycle Facilities", Health Physics 38 543-621 April.

18. American Nuclear Society, "American National Standard for Research Reactor Site Evaluation", ANS/ANSI-15.7-1977.

19. D.E. Dunning, Jr. et al, Estimates of Internal Dose Equivalent to 22 Target Organs for Radionuclides Occurring in Routine Releases from Nuclear Fuel-Cycle Facilities, Vol. 3, NUREG/CR-0150 (ORNL/NUREG/TM-190/V3), Union Carbide Corp. Nuclear Div., Oak Ridge Natl. Lab., October 1981.

20. Calvert Cliffs Nuclear Power Plant Units 1 and 2 Updated Final Safety Analysis Report, Section 1.2.5, pp. 1-4.

21. Personal communication between R.M. Harrington (ORNL) and Dr. Ekkehardt Bauer Institut Laue-Langevin, March 19, 1987.

22. Environmental Protection Agency, Protective Action Guidelines for Emergency Planning, EPA-520/1-75-001.

23. Department of Energy Oak Ridge Operations Office, Estimating and Cost Control Manual for Construction Projects, April 1981.

Appendix A:

Ground Rules For Core Design Studies

FACTOR OR ISSUE	GROUND RULE
1. Coolant inlet temperature	49°C
2. Maximum fuel temperature	The maximum hot spot centerline temperature should not at any time during the cycle exceed 385°C. This includes all allowances for the nuclear power peaking and also for engineering factors (such as channel-to-channel variations in coolant gap and hot streaks) or statistical margins affecting the fuel temperature.
3. Minimum margin to CHF:	
a. CHF correlation	ORNL will use the updated Gambill (superposition) correlation. INEL will use the Modified Bernath correlation. Based on INEL evaluations the results produced by the two correlations are quite close.
b. Uncertainties	3σ
4. Minimum margin to hydraulic instability	3σ
5. Maximum core delta P	We do not feel that the maximum core pressure drop should be specified by a ground rule, because any reasonable value would not appear to be limiting. However, the pressure you choose should be used to determine the necessary pressure vessel thickness.
6. Oxide buildup issues:	
a. Correlation	We agree with INEL to use a Griess correlation biased by the factor of 0.5 developed from experimental data from ATR.
b. Prefilm	Assume a 0.002 mm boehmite prefilm.
c. D2O vs H2O differences	Essentially none
d. Sloughing	Sloughing at 0.05mm is acceptable. However, in each case, INEL and ORNL should indicate whether the 0.05mm was

	reached and if the limit was reached, the time in the cycle at which the limit was reached should be indicated. (This is because the alloys that slough most readily also suffer the most from pitting corrosion.)
e. Hot spot treatment	Direct tracking of movement
7. Heat transfer correlation	Petukhov Correlation
8. Incipient nucleate boiling	Although ORNL will continue to avoid bubble formation on our own design, we concede that small bubbles, smaller than the thermal boundary layer, can be allowed.
9. Friction factor	ORNL will use the Filonenko correlation. If as indicated by INEL the locally preferred data base is not much different, we have no problem with the substitution.
10. Thermal conductivity of materials (assumes 45% Vol of U in Fuel Meat at 90% TD)	
a. Fuel	60 W/mK
b. Clad	180 W/mK
c. Oxide	2.25 W/mK
11. Critical velocity methodology	For flat or uniformly curved plates, use Miller correlation.
12. Fuel burnup limit	Data indicate a permissible burnup limit of 2.6×10^{21} fissions/mL of meat at 45 vol%.
13. Fuel density issues:	
a. Maximum volume fraction of uranium in fuel Meat	0.45
b. Maximum void fraction	0.10
c. Maximum uranium density	4.8 g/mL of fuel meat

14. Peak thermal neutron Flux	> $5x10^{19}$ neutrons/m^2-s is the minimum project goal.
15. Operational requirements	There is no established requirement for operation at constant flux, and from BOP considerations, it is much more reasonable to require constant power. However, we will not insist on this as a design requirement.
16. Minimum cycle length	14 day core life plus 3 day average shutdown. Evaluation of the refueling process indicates that at least 3 days will be required for the refueling process (averaged over a year). This coupled with our desire for a minimum 14 day core life leads to a minimum cycle length of 17 days.
17. Pool temperature/ pressure	Room/atmospheric
18. Bias for beams/ sources/targets	The 2% in k value proposed by INEL may be a little low. However, at this point the most important factor is that we both use the same value. Therefore, we will use the 2% bias in k as the ground rule.
19. Maximum k excess	We do not see a need at this time for identifying a specific maximum k excess.
20. Pressure vessel	Al-6061 or Zircaloy 4 should be used as the pressure vessel material. The maximum operating temperatures for these materials are 149°C for the Al-6061 and 371°C for the Zircaloy 4. The maximum temperature in the vessel wall material under the chosen conditions should be calculated and included in the results. Other material properties, (allowable stress, corrosion allowance, creep, etc.), are available if needed.
21. Maximum allowable core outlet D_2O bulk temperature	$<t_{nbp}$, 99°C. Although this temperature will not preclude steam generation for all LOCA events, it will preclude steam generation for the most probable small break LOCAs.

22. Maximum fuel concentration ratio	Although we have requested information from B&W on this issue, it will be a while before they can fully evaluate it. Therefore, we will not include a maximum concentration ratio at this time.
23. In-core irradiations	Provisions must be made for in-core irradiations of material samples at or near high energy flux peak. At this time, k bias or target types are not known. The ground rule at this time only indicates that space be made available in the core configuration.
24. MeV/fission	202 MeV/fission based on ENDF/B-V
25. Fission power to thermal power conversion factor	Based on INEL data, the value of 0.91 will be used for conversion purposes. This value may, however, be revised in the future if more detailed nuclear heating calculations indicate that a change is needed.
26. Efficiency factor	To avoid confusion about scaling factors, it is convenient to intercompare efficiency factors where the efficiency factor is defined as the peak flux per unit power; it can be computed very easily by dividing the peak flux by the total fission power.
27. Cross sections	ENDF/B-V
28. Energy boundaries for flux reporting	For various reasons it is important that the flux be reported as a function of specific energy levels. As a result the following definitions should be used: fast flux > .183 MeV thermal flux < .625 eV epithermal flux .414 eV to 101 eV These levels correspond to user needs and do not correspond to our cross section energy boundaries. Therefore, we as well as INEL will have to perform interpolations/ extrapolations in order to report the fluxes in this manner.

29. End Caps

The fuel meat does not and cannot extend to the very edge of the fuel plate. Therefore, sections of unfueled aluminum plates are required. A realistic minimum length for the unfueled region entrance(s) and exit(s) to the core(s) would be 20 times the coolant gap. The effect of these unfueled aluminum regions must be included in the calculations of flux and core life.

Appendix B:

Further Definition of Work Breakdown Structure

ORNL–DWG 87–4226 ETD

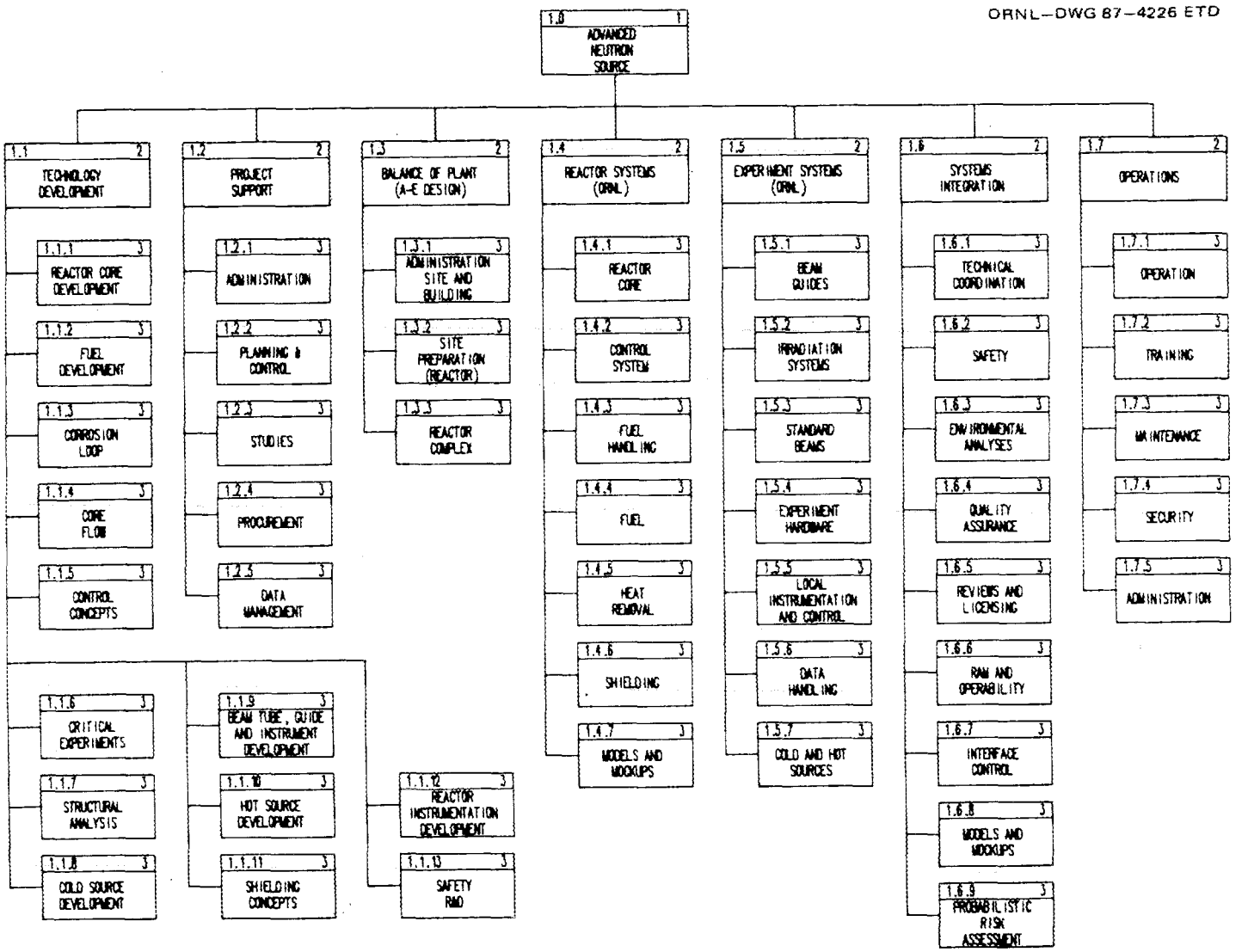

ORNL-DWG 87-4227 ETD

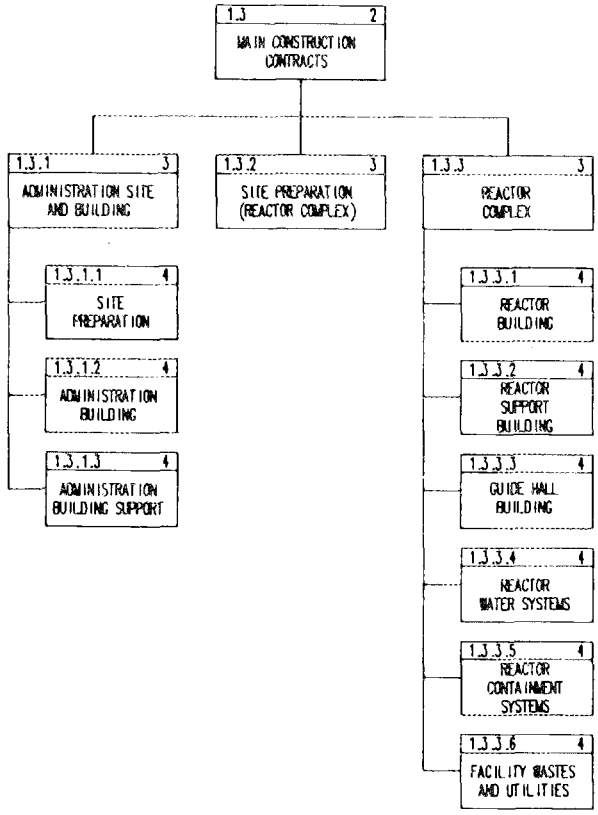

ORNL-DWG 87-4228 ETD

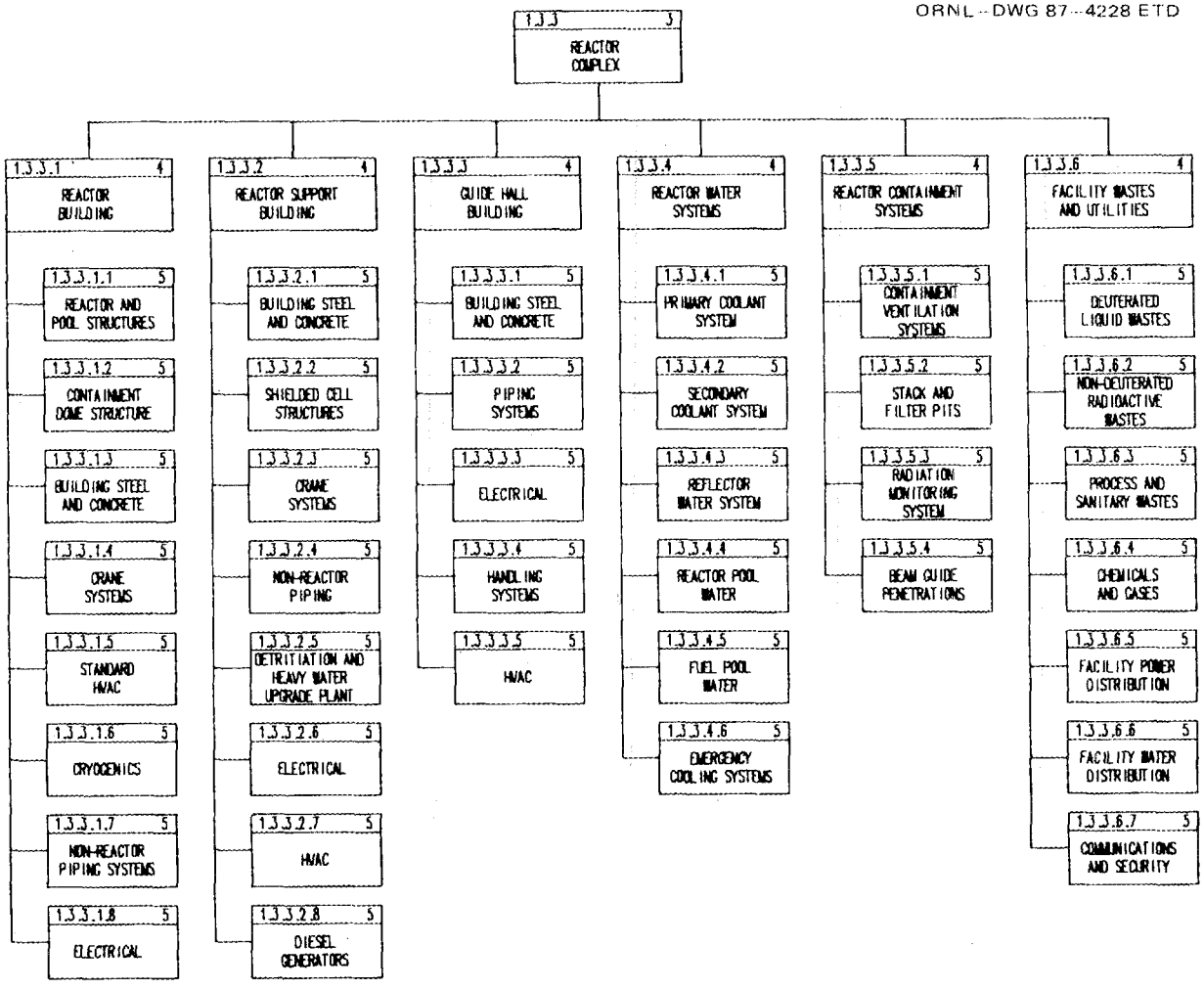

ORNL-DWG 87-4229 ETD

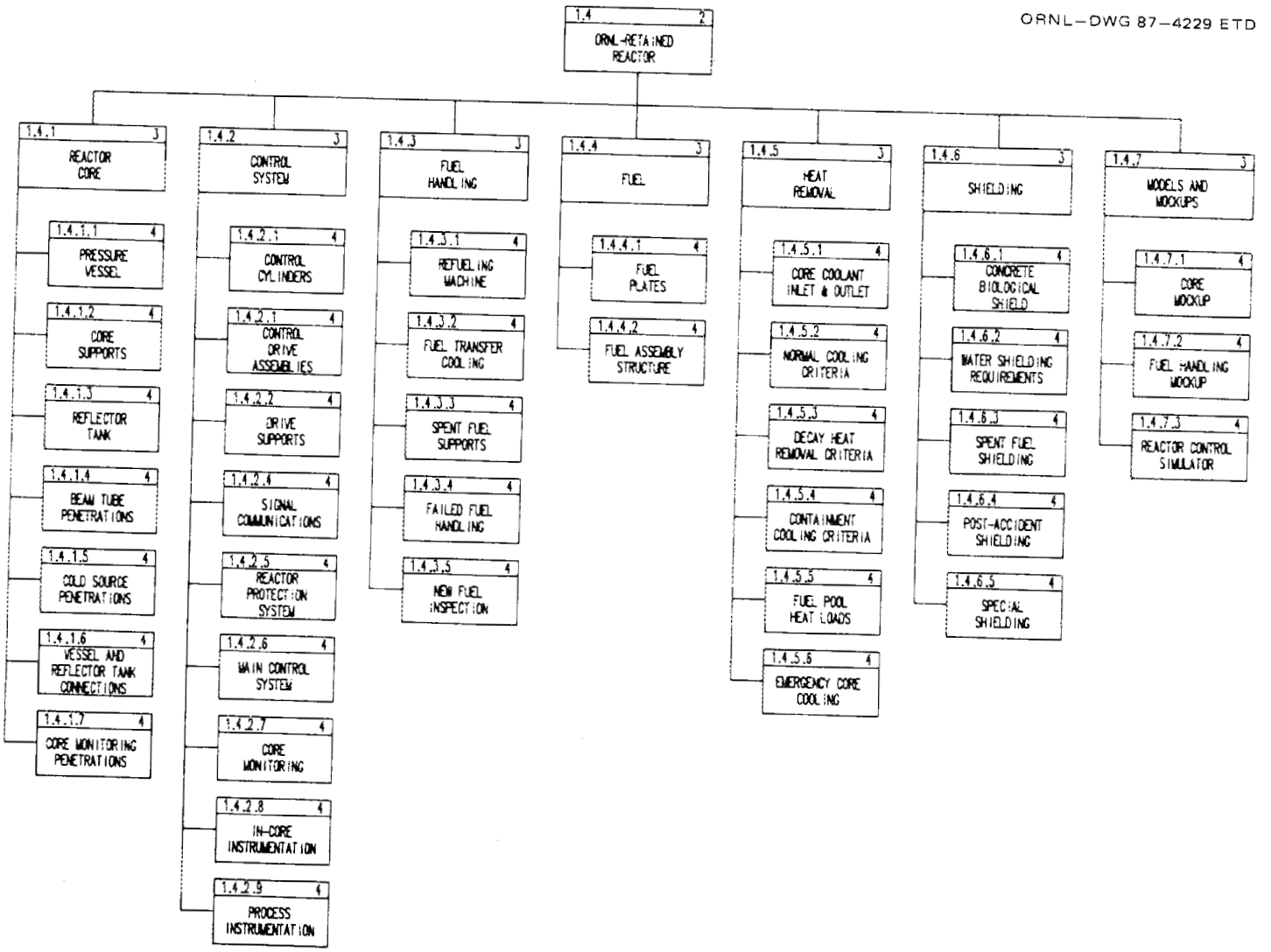

ORNL–DWG 87–4230 ETD

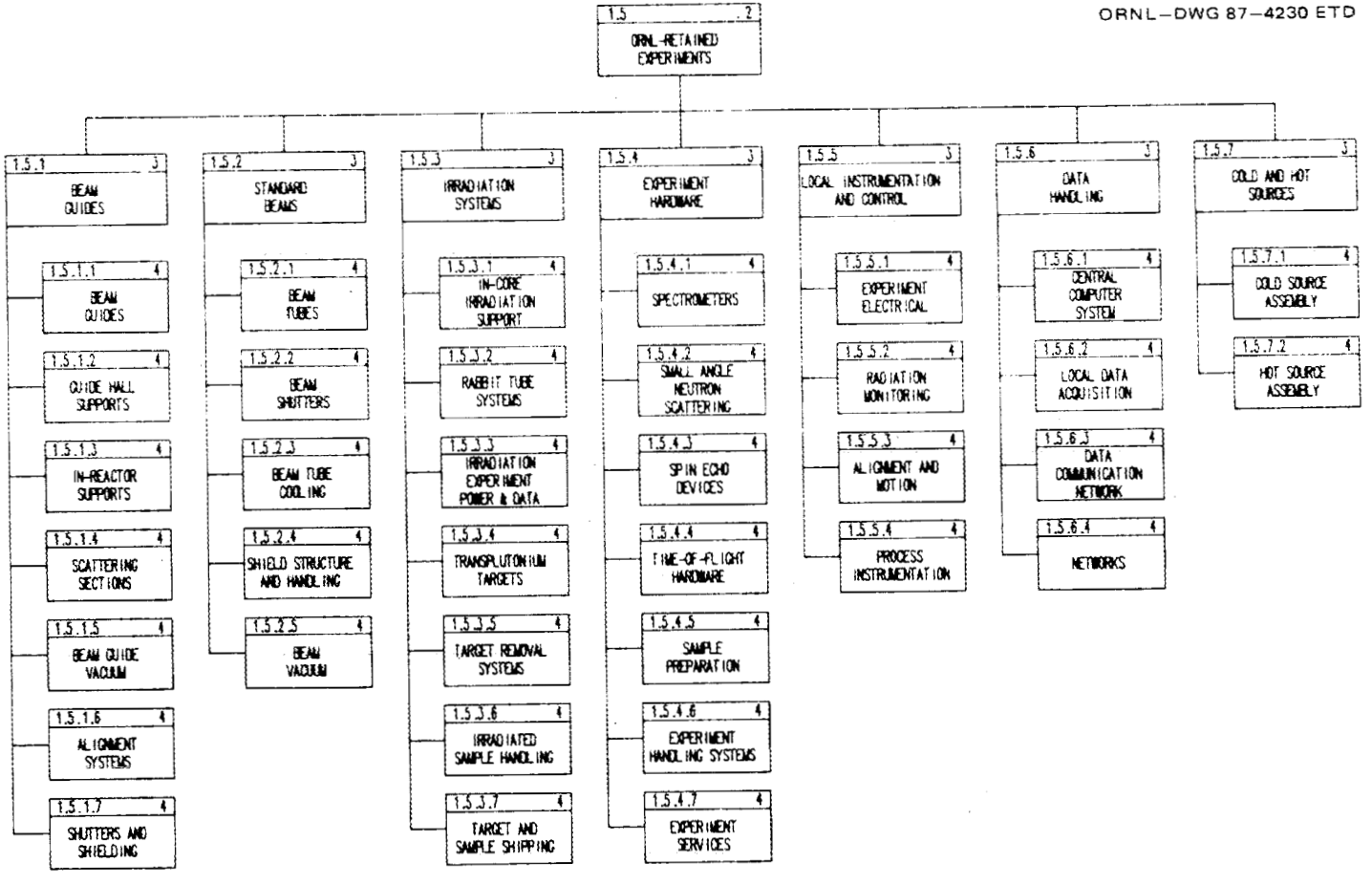

Appendix C:

Detailed Schedule for the ANS Project

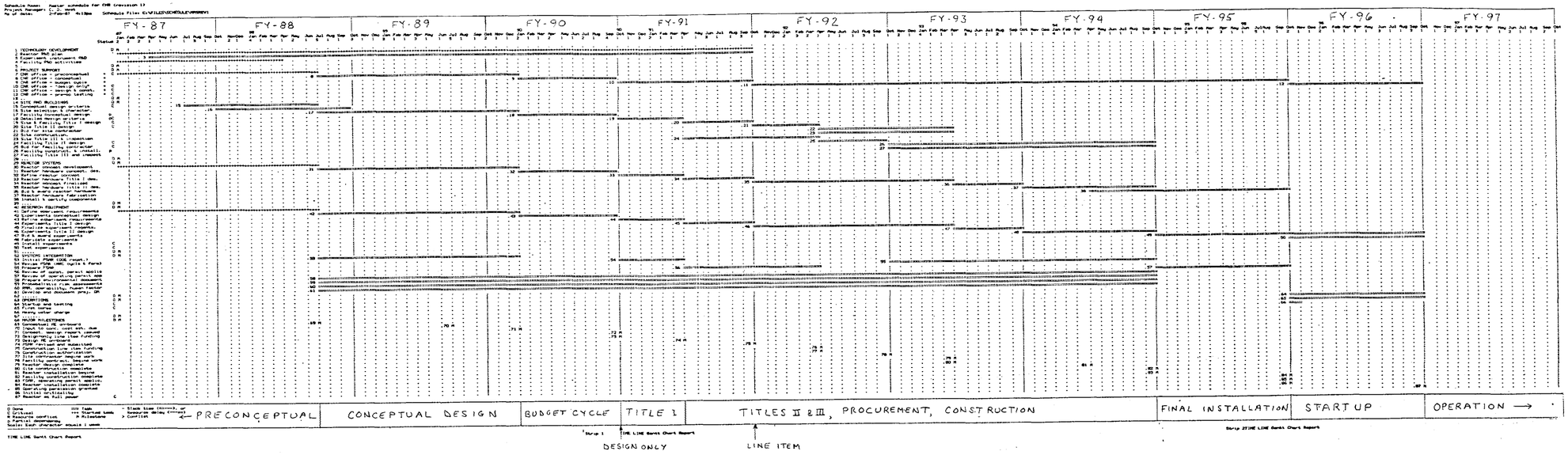
FY-87
FY-88
FY-89
FY-90
FY-91
FY-92
FY-93
FY-94
FY-95
FY-96
FY-97
PRECONCEPTUAL
CONCEPTUAL DESIGN
BUDGET CYCLE
TITLE I
TITLES II & III, PROCUREMENT, CONSTRUCTION
FINAL INSTALLATION
START UP
OPERATION →
DESIGN ONLY
LINE ITEM

Internal Distribution

1. R. G. Alsmiller
2. J. L. Anderson
3. T. D. Anderson
4. Y. Y. Azmy
5. S. J. Ball
6. E. E. Bloom
7. G. H. Burger
8. D. G. Cacuci
9. R. M. Canon
10. R. D. Cheverton
11. G. L. Copeland
12. W. G. Craddick
13. F. C. Difilippo
14. C. A. Flanagan
15. C. P. Frew
16. W. R. Gambill
17. J. A. Getsi
18. R. W. Glass
19. J. C. Griess
20-21. R. M. Harrington
22. D. L. Henderson
23. L. L. Horton
24. S. S. Kalsi
25. O. L. Keller
26. D. B. Lloyd
27. A. L. Lotts
28. D. C. Lousteau
29. M. F. Marchbanks
30. G. S. McNeilly
31. P. E. Melroy
32-33. B. H. Montgomery
34. R. M. Moon
35. J. A. Murray
36. F. R. Mynatt
37. F. S. Patton
38. R. E. Pawel
39. F. J. Peretz
40. H. B. Piper
41. K. H. Poteet
42. R. T. Primm, III
43. C. E. Pugh
44. T. L. Ryan
45-46. D. L. Selby
47. H. B. Shapira
48. J. H. Swanks
49-50. P. B. Thompson
51. H. E. Trammell
52. D. B. Trauger
53. R. E. Uhrig
54-78. C. D. West
79-93. M. K. Wilkinson
94. R. G. Wymer
95. G. T. Yahr
96. A. Zucker
97. ORNL Patent Office
98. Central Research Library
99. Document Reference Section
100-101. Laboratory Records Dept.
102. Laboratory Records (RC)

External Distribution

103. P. Ageron, Institute Laue Langevin, 156X 38042, Grenoble Cedex, France
104. Takumi Asaoka, Deputy Director General, Tokai Research Establishment, Japan Atomic Energy Research Institute, Tokai-mura, Naka-gun, Ibaraki-ken, Tokyo 319-11, Japan
105. W. P. Barthold, Barthold & Associates, Inc., P.O. Box 11730, Albuquerque, NM 87192
106. G. Bauer, KFA Julich, SNQ, P.O. Box 1913, D15170 Julich, West Germany
107. H. A. Capote, Burns & Roe, 800 Kinderkamack Rd., Oradell, NJ
07649

108. H. L. Dodds, Jr., Nuclear Engineering Department, University of Tennessee, Knoxville, TN 37996
109. J. Dorning, University of Virginia, Department of Nuclear Engineering and Engineering Physics, Charlottesville, VA 22901
110. Dr. B. Chalmers Frazer, U.S. Department of Energy, Office of Basic Energy Sciences, ER-132, Germantown, MD 20545
111. R. Fullwood, Brookhaven National Laboratory, Upton, NY 11973
112. W. Glaser, Fakultat fur Physik, Technische Universitat Munchen, D-8046 Garching, West Germany
113. K. J. Henry, Head, Research Reactors Division, AERE Harwell, Oxfordshire, OX11 ORA, England
114. Dr. L. C. Ianniello, U. S. Department of Energy, Director of Materials Sciences, Office of Basic Energy Sciences, ER-13, Germantown, MD 20545
115. Masashi Iizumi, Japan Atomic Energy Research Institute, 222, Uchisaiwai-cho; Chiyoda-ku, Tokyo, Japan
116. J. Kallfelz, Georgia Institute of Technology, Nuclear Engineering Department, Atlanta, GA 30332
117. Professor K. Kanda, Research Reactor Institute, Kyoto University, Kumatori, Osaka 590-04, Japan
118. Nobuhiki Kunitomi, Osaka University, 1-1 Yamadaoka, Fuita-Shi, Osaka 565 Japan
119. J. A. Lake, Nuclear Engineering, Idaho National Engineering Laboratory, P.O. Box 1625, Idaho Falls, ID 83415
120. L. LeSage, Argonne National Laboratory, 9700 South Cass Ave., Argonne, IL 60439
121. W. Nash, Program Manager, Research and Test Reactor Fuel Elements, Babcock & Wilcox, P.O. Box 785, Lynchburg, VA 24505
122. A. Olsen, Argonne National Laboratory, 9700 South Cass Ave., Argonne, IL 60439
123. J. R. Powell, Brookhaven National Laboratory, Upton, NY 11973
124. John J. Rush, National Bureau of Standards, Washington, D.C. 20234
125. Professor T. Shibata, Kinki University, Kowakae, Hogashiosaka, Osaka 577, Japan
126. J. L. Snelgrove, Coordinator, Engineering Applications, RERTR Program, Argonne National Laboratory, 9700 South Cass Ave., Argonne, IL 60439
127. Dr. D. K. Stevens, Associate Director for Basic Energy Sciences, Office of Energy Research, Department of Energy, Washington, D.C. 20545
128. Dr. Ivan Thomas, Department of Energy, Office of Basic Energy Sciences, ER-132, Germantown, MD 20545
129. D. C. Wade, Argonne National Laboratory, Applied Physics Division, Building 208, 9700 South Cass Ave., Argonne, IL 60439
130. D. K. Wilfert, Department of Energy, Oak Ridge Operations, Federal Building, Oak Ridge, TN 37830

131. Office of Assistant Manager for Energy Research and Development, Department of Energy, ORO, Oak Ridge, TN 37831

132-161. Technical Information Center, Department of Energy, Oak Ridge, TN 37831

☆U.S. GOVERNMENT PRINTING OFFICE:1987 -548-118/ 60115